NONLINEAR VIBRATION OF BEAM AND MULTIBEAM SYSTEMS

by

Mahmood M. Tabaddor

Dissertation submitted to the Faculty of the
Virginia Polytechnic Institute and State University
in partial fulfillment of the requirements for degree of

DOCTOR OF PHILOSOPHY

in

Engineering Mechanics

APPROVED:

Ali H. Nayfeh, Chairman

Odis H. Griffin

Rakesh K. Kapania

Liviu Librescu

Dean T. Mook

September 24. 1996
Blacksburg, Virginia

Keywords: Nonlinear. Vibration. Cantilever Beam. Frame, Parameter Identification

NONLINEAR VIBRATION OF BEAM AND MULTIBEAM SYSTEMS

by
Mahmood M. Tabaddor

Chairman: Dr. Ali H. Nayfeh
Department of Engineering Science and Mechanics

(ABSTRACT)

In this dissertation, an experimental and theoretical investigation into the nonlinear vibration of beam and beam-like structures with rectangular cross sections is presented. Two structures, a cantilever beam subject to a harmonic external excitation and a portal frame subject to a harmonic base motion, are the objects of study.

For the cantilever beam, we present experimental results regarding multimode behavior. The beam was tested in both a vertical and horizontal configuration. Our experiments show that, for a forcing frequency near the fourth natural frequency of the beam, a low-frequency mode can be activated through a nonlinear mechanism. The nonlinear mechanism responsible for the transfer of energy to a low-frequency mode of the beam in the horizontal configuration was a subcombination internal resonance. However, for the same beam in the vertical configuration, both a subcombination internal resonance and a nonresonant modal interaction were observed to transfer energy to a low-frequency mode. The subcombination internal resonance consisted of contributions from the directly excited fourth mode, the fifth mode, and the low-frequency second mode. The response due to the nonresonant modal interaction consisted of contributions from the directly excited fourth mode and the indirectly excited low-frequency first mode. Both of these interactions are the result of a system with a dominant cubic nonlinearity.

The single-mode response of the cantilever beam in the horizontal configuration was the subject of study. A comparison between the theoretically and experimentally obtained frequency-response curves revealed a discrepancy for an assumed ideal clamp. The model was

brought into agreement by incorporating a quadratic damping term modeling the effect of air damping and a nonlinear rotational spring to model the flexibility of the clamp.

The portal frame is a structure with a dominant quadratic nonlinearity. Experimental results are presented for the cases of a single combination resonance and multiple combination resonances. For the multiple combination resonances, excitation of a single mode was found to eventually activate contributions from six other modes, most of them possessing lower frequencies. The amplitudes of these lower-frequency modes were at times larger than that of the directly excited mode.

The final topic is parameter identification for nonlinear systems. A scheme of experiments is designed that in conjunction with a multiple scales analysis can accurately estimate the nonlinear coefficients of a single-degree-of-freedom model. Parameters for a portal frame were ascertained by activating a subharmonic resonance of order one-half.

DEDICATION

This work is dedicated to my father, Dr. Farhad Tabaddor, and my friend, Nathan Ross, who have taught me that intellect and integrity need not be strangers.

ACKNOWLEDGMENTS

In the course of our lives, no achievement can be considered to be truly the effort of an individual. In modern society, it is often forgotten that the efforts of the many insure that we can go about our so-called individual lives. Nevertheless, one can point out certain persons whose influence have been significant on the path taken in life. In this brief moment, I can only acknowledge a few of those, and a few they are, that have been such an influence and whose efforts have been known to me.

First and foremost, I must thank my friend Dr. Kyoyul Oh who initiated me into the vast world of experimental techniques. His genuine friendship has been a source of strength and wisdom.

I would like to thank my advisor Dr. Ali Nayfeh who was the reason for my choosing Virginia Tech. His book, *Nonlinear Oscillations*, was an added inspiration to the decision to devote my academic pursuits to the study of vibration.

As a graduate student one quickly learns the importance of learning from others, mostly other graduate students. I would like to thank Jon Pratt, Wayne Kreider, Dr. Char-Ming Chin, Dr. Tony Anderson, Shafic Oueini, and Dr. Balakumar Balachandran for their insights and knowledge.

I would like to thank the members of my committee - Dr. Rakesh Kapania (AOE), Dr. Odis Griffin (ESM), Dr. Liviu Librescu (ESM), and Dr. Dean Mook (ESM) - for the time and efforts they have devoted to overseeing my doctoral work. I would also like to thank Dr. Eric Johnson (AOE) for his help. I would like to extend a special thanks to Dr. Muhammad R. Hajj (ESM). I would like to thank Sally Shrader for all her help and friendship.

I must also thank my friends who filled my sojourn in Blacksburg with kindness and memories: Dr. Nirmal Iyengar, Idine Ghoreshian, Marc Krieder, Dr. Char-Ming Chin, Wayne Kreider, Eva Cruz, and Jon Pratt.

I would like to thank my parents Zahra Tabaddor and Dr. Farhad Tabaddor for all they love and encouragement. I would like to thank my uncle Dr. Kamran Tabaddor for his love and humor.

I would like to thank Bahman Dariush and Behzad Dariush for their enduring friendship.

And, most of all, I would like to thank my wife Dr. Priya L. Tabaddor for her love, support, and companionship.

TABLE OF CONTENTS

LIST OF FIGURES

LIST OF TABLES

CHAPTER ONE

Literature Review

'wherefore all remained confused, understanding what he meant: that after the deed is done, everybody knows how to do it' G. Benzoni

1.1 INTRODUCTION

Within the world of nonlinear dynamics, we are only beginning to grasp the possibilities of complexity that exist in our humanly created objects let alone nature. However, the beginning of all this immense richness is contained in the deceptively simple relations known as Newton's laws of motion. From these empirical laws, the equations describing the past, present, and future dynamics of a system can be approximated (Goldstein, 1981). The qualifier, linear or nonlinear, is actually a *reflection* of the mathematical formalism and does not necessarily characterize any natural process. Nature may not know that it is behaving in a nonlinear or linear manner. However, linear dynamical studies (Genta, 1993; Meirovitch, 1975; Thomson, 1981; Harris, 1988; Blevins,1979), though rich in content, are limited in the type of phenomena they can predict. Chaos, multiple solutions, limit cycles, saturation, intermittency, jumps and hysteresis, and modal interactions (Nayfeh and Mook, 1979; Moon, 1987; Cartmell, 1990; Schmidt and Tondl, 1986; Szemplinska-Stupnicka, 1990; Guckenheimer and Holmes, 1983) are but a few of the phenomena revealed only by the insights of a nonlinear approach with many more assuredly yet to be uncovered.

1.2 NONLINEARITY IN ENGINEERING

The inclusion of nonlinearity in the modeling of engineering structures allows for more sophistication and realism in the design, analysis, and control of engineering structures (Thompson and Bishop, 1994; Skowronski, 1991; Ditto and Pecora, 1993). For dynamic systems, several general categories of nonlinearities are defined:

(1) Geometric Nonlinearity

For structural mechanics problems, sources of geometric nonlinearity include large deformations which necessitate a nonlinear strain-displacement relation and the case of a nonlinear curvature-displacement relation (Sathyamoorthy, 1982).

(2) Material Nonlinearity

For some fabricated materials, the generalized Hooke's law is no longer an adequate approximation and a nonlinear stress-strain relationship provides a more realistic model. Rubber is the classic example. Another source is a dissipative process inherent in the material that can only be modeled by a nonlinear damping mechanism. The field of *biomimetics* finds that nature works exclusively with materially nonlinear biological structures (Jeronimidis and Atkins. 1995).

(3) Inertial Nonlinearity

In dynamics, nonlinear inertia (Bolotin, 1964) or kinematic nonlinearities (Moon. 1987) derive from terms associated with velocities and accelerations in the equations of motion. In particle dynamics, Coriolis forces could be responsible for nonlinear terms in the acceleration.

(4) Topological Nonlinearity

This last category describes a system where the differential equation experiences a discrete finite change. A system reaching a physical stop that impedes its motion is one such example (Ibrahim, 1991).

Now despite the greater generality of nonlinear studies, the usual starting point is the proper identification of the *linear* natural frequencies and mode shapes of a structure. A nonlinear analysis, based on the assumption of *weak* (small) nonlinearity, assumes that the dynamic response

is still describable in terms of the natural frequencies and mode shapes of the *linearized* structure. In what follows, a brief review of references in the English technical literature relevant to the dynamics of beams, mostly cantilever, and multibeam systems is presented.

1.3 BEAM STUDIES

One of the fundamental elements of an engineering structure is the beam. This basic structural component provides an adequate model for many objects, such as antennas, helicopter blades, robot arms, bridges, airplane wings, and subunits of more complex structures, such as space trusses and buildings, just to mention a few.

1.3.1 LINEAR VIBRATION

As noted above, the beginning of any weakly nonlinear analysis is an accurate determination of the linear natural frequencies and mode shapes of the structure under investigation. This can be done both theoretically and experimentally. The experimental procedure of determining natural frequencies is multidisciplinary, integrating linear vibration theory with digital signal processing (Randall, 1987), experimental techniques (Kobayashi, 1993), and numerical and optimization methods. The collective effort is known as *experimental modal analysis* (Ewins, 1991). Even here, research is under way to expand the scope of modal analysis for purposes of nonlinear parameter identification (Busby, Nopporn, and Singh, 1986; Zavodney, 1991).

The earliest model of a beam is the Euler-Bernoulli beam (Shames and Dym, 1985). The use of this elementary beam model in linear vibration theory leads to a transcendental characteristic equation in terms of the natural frequencies of a cantilever beam. The solution of this equation can be found numerically with the help of modern mathematical software (Wilson and Gupta, 1992). Early improvements to the Euler-Bernoulli model were the inclusion of rotary inertia (Lord Rayleigh, 1877) and shear deformation (Timoshenko, 1921; Laura, Maurizi, and Rossi, 1989). Further variations on this theme include variable cross section, tip mass, support flexibility, static

deflection, composite materials, and effect of gravity (Wagner and Ramamurti, 1977; Farghaly and Shebl, 1995; Leissa and Sonalla, 1991; Low and Ng, 1992; Abramovich and Hamburger, 1991; To, 1982; Bhat and Wagner, 1976; Liu and Huang, 1988; Laura, Pombo and Susemihl, 1974; Blevins, 1979; Kapania and Raciti, 1989; Narita and Leissa, 1992). Once the linear natural frequencies and mode shapes are determined, the next step in a nonlinear analysis is to examine the relationship amongst the various natural frequencies of the structure.

1.3.2 NONLINEAR VIBRATION

For the forced vibration of weakly nonlinear systems, interesting phenomena occur when energy is transferred amongst the *linear* modes of the system. That is, the linear natural frequencies and mode shapes still provide an adequate description of the weakly nonlinear response of the system. Depending on the order of the nonlinearity (the two most common are quadratic and cubic), when certain relationships amongst some of the natural frequencies of the system and the frequency of excitation are satisfied, modal interactions may occur (Nayfeh and Mook, 1979; Evan-Iwanowski, 1976). This phenomenon is not predictable by a linear analysis. Most of the research in nonlinear dynamics has focused on these resonant modal interactions (Nayfeh and Balachandran, 1989) where the natural frequencies are commensurate. On the other hand, recent research (Nayfeh and Mook, 1995) has also documented nonresonant modal interactions. For this type of modal interaction, the frequencies of the interacting modes are non-commensurate. For either case, the implication is that for a structure that is behaving in a nonlinear manner, a linear analysis will fail to detect the additional modes that were excited through the modal interaction mechanism. This could have adverse effects on the design, performance, and control of engineering structures.

Despite numerous experimental and analytical studies into the nonlinear vibrations of cantilever beams, much about the dynamics of such simple structures remains to be unveiled. Also knowledge of the dynamical behavior of cantilever beams may, in turn, shed light on the

dynamical behavior of more complicated structures. With this said, we move onto a survey of contemporary research starting with the modeling of beam dynamics, then looking at single-mode nonlinear vibration of beams, and followed by looking at the multimode vibration of beams. Then we present a survey of work done on multibeam systems and end with a brief mention of additional topics current in the study of beam and multibeam systems.

Theoretical Modeling

Bypassing the complexity of a full three-dimensional elasticity analysis, Crespo da Silva and Glynn (1978a, b) derived nonlinear integro-partial-differential equations governing the nonplanar dynamics of an isotropic, inextensional beam. The resulting equations, developed through the extended Hamilton's principle, retain all nonlinearities up to third order. Therefore, contributions from both nonlinear curvature and nonlinear inertia were kept. The form of these equations allows for a solution based on perturbation analyses (Nayfeh, 1973, 1981). Pai and Nayfeh (1992) developed a more comprehensive beam theory which fully accounts for geometric nonlinearities, including large rotations and displacements and shear deformation. Hodges (1984, 1987a, 1987b), Pai and Nayfeh (1990), and Nayfeh and Pai (1996) discussed the development of concepts in nonlinear beam kinematics. Hodges, Crespo da Silva, and Peters (1988) discussed some of the common mistakes in the nonlinear modeling of a cantilever beam. Specifically, they addressed the issues of the proper physical interpretation of the Euler angles and the failure to obtain equations consistent to the order of approximation being considered.

Simplifying assumptions are common in engineering theories of beams (Donnell, 1976; Love, 1944). They make the world easier to understand or, at least, solve mathematically. Efforts to develop equations of motion describing the behavior of a beam in a manner that lends itself to a viable solution have resulted in numerous modeling techniques (Boutaghou and Erdman, 1989; Haering, Ryan and Scott, 1992; Nayfeh and Pai, 1996; Crespo da Silva, 1991). Each researcher attempts to improve the comprehensiveness of a model over previous models by accounting for

various complicating effects, such as torsion, rotary inertia, shear center eccentricity, warping, axial stretching, and general deformations. The challenge is to include enough complexity so that the problem is meaningful and, yet, apply simplifying assumptions that make the problem tractable (Suleman, Modi, and Venkayya, 1995).

The advent of the digital computer has no doubt played a hand in the progress of dynamic modeling. However, the use of numerical algorithms in the area of computational mechanics is not without its dangers and blind faith in numerical answers should be avoided (Oden and Bathe, 1978). Nevertheless, since for most nonlinear systems a closed-form solution is unattainable, recourse is made to perturbation methods (Nayfeh, 1973, 1981) and hybrid perturbation-numerical methods (Nayfeh, Mook and Lobitz, 1974; Nayfeh and Balachandran, 1995) for qualitative information about the solution space. A combined qualitative and quantitative analysis is the most reassuring strategy in the tackling of nonlinear problems.

Single-Mode Response

Nonlinear motions of beams vibrating in a manner essentially captured by a single mode were the focus of early works cited in Nayfeh and Mook (1979). The characteristics of bending of the frequency-response curve, amplitude jumps, limit cycles, and hysteresis are well documented for the case of a single mode under the influence of nonlinearity.

Dowell, Traybar, and Hodges (1977) compared linear and nonlinear theories with experiments for large deformations of a cantilever, metallic beam due to a tip load. They concluded that the experimental results for various frequency measurements were in close agreement with linear and nonlinear theories only for tip deflections that are not a significant fraction of the beam span.

Zavodney and Nayfeh (1989) compared experimental and analytical results for a parametrically excited cantilever, metallic beam with a lumped mass. Their theoretical model contained nonlinear terms up to third order. The sources of the nonlinearities were the inertia, curvature, and axial displacement (produced by a large transverse deflection). They concentrated

on single-mode planar motions. They experimentally documented jumps in the frequency-response curves for metallic and composite beams. The jump points varied with increasing acceleration levels. For the theoretical results, they relied on a discretization of the governing equation by Galerkin's method followed by the application of the method of multiple scales (Nayfeh, 1981) to obtain the time variation of the amplitude and phase of the motion as a function of the system and forcing parameters.

Anderson, Nayfeh, and Balachandran (1996b) experimentally observed that, for a primary excitation of the first mode of a cantilever, metallic beam, the curvature nonlinearity dominates the inertia nonlinearity. The resulting frequency-response curve is bent to the right, revealing a hardening-type nonlinearity. For a primary excitation of the second mode, they found that the inertia nonlinearity dominates. In this case, the frequency-response curve is bent to the left and the nonlinearity is of a softening type.

Berdichevsky and Ozbek (1995) analytically studied the nonlinear vibrations of a cantilever, isotropic beam excited at the free end. They found that, for a one-degree-of-freedom model, the dynamical response can be explained in terms of a dynamical potential.

Experimental studies by Moon and Holmes (1985) on the vibration of a buckled elastic beam found the existence of chaotic motions as the beam alternates between the two static equilibrium positions.

For a single-mode response, complicated motions are possible but difficult to achieve without high excitation levels. However, the inclusion of more than one mode of a structure allows for more realistic modeling and prediction of complicated motions, some unique to multimode systems.

Multimode Response

The phenomenon of modal interaction is a source of complexity in nonlinear systems. The activation of a nonlinear mechanism that is responsible for energy transfer from a directly excited

mode to other modes of the structure increases the potential for all sorts of unusual and complicated behavior, such as chaos, saturation, and torus breakdown, just to mention a few. For beams, the coupling could involve planar and nonplanar modes or torsional modes, depending on the order of the nonlinearity and the frequency relationships. In addition, the transfer of energy can occur amongst modes that are non-commensurate but widely spaced. Very few published experiments have borne witness to this latter phenomenon.

Amongst the earliest investigations, Haight and King (1971) focused on the excitation of nonplanar motions of a slender, elastic rod subject to a planar excitation. They mapped out the regions of instability for the case of a one-to-one internal resonance between the first planar and first nonplanar modes. Qualitative agreement was found between theory and experiment. They conjectured that an improved quantitative agreement may be achieved by incorporating a more complex [nonlinear] damping model. Their results also showed that the nonplanar instability need not require a large amplitude of excitation for its onset. Nonlinearities can be activated for low forcing levels. Hyer (1979) developed a model for a base excited beam whose principal moments of inertia of the cross section were nearly equal. He found that for an external forcing frequency slightly below a bending natural frequency, out-of-plane motions were realizable. The resulting whirling motion was due to the nonlinear coupling provided by the axial inertia and the one-to-one frequency ratio. Crespo da Silva and Zaretzky (1990) developed a theoretical model to study modal coupling in an inextensional cantilever, isotropic beam subject to a periodic excitation. Zaretzky and Crespo da Silva (1994) performed experiments on cantilever aluminum beams with rectangular and square cross sections. They observed, for square cross sections, a one-to-one modal coupling between a planar mode and a nonplanar mode.

Shyu (1991) numerically studied the coupled planar and nonplanar motions of a cantilever, isotropic beam including a static deflection. The two governing equations of motion contained quadratic and cubic terms. He was interested in the onset of whirling motions. His results

showed that out-of-plane motions were realizable for nearly equal principal moments of inertia of the beam cross-section when a resonance is activated. He considered primary resonance, subharmonic resonance of order one-half, subharmonic resonance of order one-third, superharmonic resonance of order three, and superharmonic resonance of order two of the first and second modes. He found that the appearance of nonplanar motions was dependent on the level of damping and forcing in the system. He also noted that a larger excitation amplitude is necessary for exciting a subharmonic resonance as compared to a superharmonic resonance.

Pai and Nayfeh (1990a) investigated the response of a cantilever, isotropic beam subject to a lateral base excitation. The two integro-differential equations of motion (Crespo da Silva and Glynn, 1978a) were solved by a combination of the Galerkin procedure and the method of multiple scales. They found that, depending on the thickness-to-width ratio, nonplanar motions were realizable. They studied two cases: one-to-one internal resonance between the first inplane and the first out-of-plane modes, and one-to-one internal resonance between the second inplane and the first out-of-plane modes. Quantitative results showed that these whirling motions could be steady, beating type, or chaotic, depending upon certain parameter values. Nayfeh and Pai (1989) studied the response of a cantilever, isotropic beam to a principal parametric excitation. The same two cases as in Pai and Nayfeh (1990a) were considered. Without the inclusion of the nonlinear curvature terms, they found that the onset of nonplanar motions would not be predicted. Again, for certain parameter values, the whirling motions were found to be steady, nonperiodic, or chaotic.

Haddow and Hasan (1988) parametrically excited a cantilever, metallic beam near twice the natural frequency of its fourth mode. Initially, they observed a planar periodic motion involving the fourth mode, resulting from a principal parametric resonance. Increasing the excitation frequency, they observed that the planar periodic motion lost stability and gave way to a nonplanar chaotic motion. As a consequence, the energy in the beam seemed to cascade down

through the modes, resulting eventually in a very low-frequency high-amplitude steady-state response. Burton and Kolowith (1988) conducted an experiment similar to that of Haddow and Hasan. For some excitation amplitudes and frequencies, they observed chaotic motions where the first seven bending modes as well as the first torsional mode were present in the response. For some excitation amplitudes and frequencies, they observed a cascading of energy into low-frequency components in the response associated with chaotic nonplanar motions. Cusumano and Moon (1989) performed an experiment with an externally excited cantilever, metallic beam. They observed a cascading of energy into low-frequency components in the response associated with chaotic nonplanar motions. Also, Cusumano and Moon (1995a) varied the forcing frequency and amplitude to develop stability boundaries for planar motions of a cantilever beam. Within the instability wedges, they observed 'energy cascading', 'intermittent side-to-side trapping', and chaotic motions. They developed a two-mode model that predicted much of the behavior observed during the physical experiments (Cusumano and Moon, 1995b).

Dugundji and Mukhopadhyay (1973) conducted experiments on a cantilever beam subjected to a transverse base excitation with a frequency close to the sum of the natural frequencies of the first bending and first torsional modes. They found that a low-amplitude high-frequency external excitation could produce a high-amplitude low-frequency motion through a combination external resonance of the additive type. In this case, the excitation frequency is not near a natural frequency of the system but, instead, nearly equals the sum of two natural frequencies of the system. Anderson, Balachandran, and Nayfeh (1994) parametrically excited a cantilever, metallic beam with a frequency close to the sum of the natural frequencies of the first and fourth modes. They found that a combination parametric resonance of the additive type resulted in energy transfer to the first and fourth modes.

In two experiments with cantilever, metallic beams, Anderson et al. (1992, 1994) and Nayfeh and Nayfeh (1994) uncovered a new mechanism by which modal interactions can channel energy

from a low-amplitude high-frequency excitation into high-amplitude low-frequency vibrations. Anderson et al. (1992, 1996a) conducted an experiment with a beam that is parametrically excited near twice the natural frequency of its third mode. For certain excitation amplitudes and frequencies, they observed a large-amplitude planar motion consisting of the fourth, third, and first modes accompanied by amplitude and phase modulations of the third and fourth modes. The mechanism for the excitation of the first mode (whose frequency was approximately 1/50 of the excitation frequency) is neither a classical internal resonance nor an external or parametric combination resonance involving the first mode, as in the experiments of Dugundji and Mukhopadhyay (1973) and Anderson et al. (1994). Rather it is an example of a nonresonant modal interaction. The signature of this type of modal interaction appears to be the presence of asymmetric sidebands around the higher-frequency component in a spectral plot. The sideband spacing is approximately equal to the frequency of the lower mode. The sidebands and their asymmetry point to phase and amplitude modulations of the contributions of the higher frequency mode.

Nayfeh and Nayfeh (1994) conducted an experiment with a circular, metallic rod that is transversely excited near the natural frequency of its fifth mode. Because of the axial symmetry, one-to-one internal resonances occur at each natural frequency of the beam and the mode in the plane of the excitation interacts with the out-of-plane mode at the same excitation frequency, resulting in nonplanar motions. For a certain range of excitation parameters, they observed a large-amplitude first-mode response. As in the experiment of Anderson et al. (1992, 1994), the appearance of the first mode was accompanied by a modulation of the amplitude and phase of the fifth mode, with the modulation frequency being approximately equal to the natural frequency of the first mode.

More general reviews on beam vibrations can be found in Wagner and Ramamurti (1977), Sathyamoorthy (1982), and Sathyamoorthy (1985).

1.4 MULTIBEAM SYSTEMS

The natural extension of the study of the dynamic behavior of a single beam is a system of beams. Haddow, Barr, and Mook (1984) conducted an experimental and theoretical study of an L-shaped structure consisting of two beams. Their mathematical model consisted of only the two lowest planar degrees of freedom. The frequency ratio of these two modes was approximately two-to-one. They observed the physical phenomenon of saturation along with jump conditions and non-steady responses. Using a simplified mathematical model, they qualitatively matched the experimental results. Balachandran and Nayfeh (1990) and Nayfeh, Balachandran, Colbert, and Nayfeh (1989) also performed experiments on a system of two beams and two masses. The natural frequencies of the L-shaped structure were tuned such that, for the two lowest modes, the frequency ratio was nearly two-to-one. When either mode was directly excited, periodic, periodically modulated, and chaotically modulated motions were observed.

Nayfeh, Nayfeh, and Mook (1994) investigated theoretically and experimentally the dynamics of a T-shaped structure. The structure was tuned so that the sum of the first and second natural frequencies were close to that of the third natural frequency. The excitation was near the third natural frequency. This is known as a combination internal resonance. Documented phenomena included two-period quasi-periodic motions, periodic motions, and saturation.

Barr and McWhannell (1971) briefly considered the nonlinear vibration of a portal frame by considering a model with only two independent coordinates. They found that under certain frequency relationships, for a. frame under support motion, a multimode response may exist. Specifically, they mention the case where the forcing frequency was twice the second natural frequency and, in turn, the second natural frequency was twice the first natural frequency. Forys and Niziol (1984) performed an analysis of internal resonances in a system of three rods. They included nonlinear inertia and nonlinear damping. Popovic, Nayfeh, Oh, and Nayfeh (1995)

considered a three-beam structure with corner masses. They experimentally observed subharmonic resonance of order one-half, combination resonance of the additive type. and interaction between widely spaced modes. Mazzilli and Brasil (1995) and Andre (1996) discussed the importance of including the static equilibrium configuration in an analytical model of frame structures. Andre (1996) showed that the inclusion of the static equilibrium configuration in the nonlinear dynamic modeling of L-shaped and portal frame structures could produce qualitative and quantitative differences in the amplitude- and frequency-response curves in comparison to an analysis based on the undeformed configuration.

Bux and Roberts (1986) studied theoretically and experimentally the forced vibration of a system of two coupled beams. The experimental results revealed a response consisting of three modes and, in another case, four modes of the structure. The three modes were activated through a combination internal resonance of the additive type. For the four-mode case, the simultaneous activation of two resonance conditions. a combination resonance of the additive type and a two-to-one internal resonance. were responsible for the observed behavior. Ashworth and Barr (1987) modeled the fuselage and tail of an aircraft with a system of beams. Their experiments also focused on the simultaneous satisfaction of two resonance conditions. Cartmell and Roberts (1988) investigated the case of a system of two coupled beams under the condition where two combination resonances were slightly detuned from each other. Small changes in the internal tuning were found to affect the modal responses.

1.5 ADVANCED TOPICS

Advanced topics include cantilever beams consisting of composite material (Kapania and Raciti, 1989, Kapania and Raciti, 1989a, and Pai and Nayfeh, 1992), rotating beams (Kim and Dugundji, 1993), beams subject to random excitations (Ibrahim, 1991), and calculation of the non-

linear normal modes (Hsieh, Shaw, and Pierre, 1994, and Nayfeh, Chin, and Nayfeh, 1994). Also for multibeam systems, similar complications have been considered, such as a system of beams consisting of composite material (Balachandran and Nayfeh, 1990a), a system of beams subject to a random excitation (Roberts, 1980), and the calculation of nonlinear normal modes for a discretized system, representing a portal frame (Balthazar and Brasil, 1995).

1.6 PARAMETER IDENTIFICATION

The recognition of the prevalence of nonlinear phenomena in the dynamics of complex structures leads to the need for more improved modeling and parameter estimation methods (Tailor, Kirkman, Hershfeld, and Wojnar, 1994; Marlowe and Buehrle, 1993). As mentioned earlier, the field of modal analysis is moving toward the identification of parameters of nonlinear systems (Slater and Inman, 1994; He and Ewins, 1987). The approaches are varied and each is successful under specific circumstances.

One approach takes advantage of perturbation methods to set up the modulation equations. The parameters in the modulation equations are then identified by carrying out a set of experiments where, in one case, both the amplitude and phase are monitored as a function of a control parameter (Hajj, Nayfeh, and Popovic, 1995). The bispectrum and trispectrum provide the necessary phase information, depending upon the type of nonlinearity, to solve for the parameters in the modulation equations (Hajj, Miksad, and Powers, 1993; Balachandran and Khan, 1995; Fackerell, White, and Pinnington, 1993; Pezeshki, Elgar, Krishna and Burton, 1992; Shyu, 1994). For the other case, Nayfeh (1985) showed that, for a two-degree-of-freedom system with quadratic and cubic nonlinearities, experiments can be devised that require only the amplitudes of motion along with the jump points in an excitation-amplitude sweep to obtain numerical values for the parameters.

Some of the other approaches include Hilbert transform methods (Feldman and Braun, 1995; Simon and Tomlinson, 1984; Tomlinson, 1985): describing function method (Benhafsi, Penny, and Friswell, 1995); a non-parametric identification technique relying on a power series expansion (Yang and Ibrahim, 1985); restoring force method (Worden and Wright, 1994); identification of nonlinearities from complex modes (Lin and Lim, 1993; Ozguven and Imregun, 1993); time-frequency techniques (Dippery and Smith, 1995); and a method combining experimental data with an FE model (Lin and Ewins, 1990).

1.7 DAMPING

No vibration model is complete without the inclusion of damping. Compared to the stiffness and inertia properties of a system, the modeling of damping has proven to be very difficult. The most popular representation of damping is the linear viscous model. For most metals, the linear viscous model leads to what is known as lightly damped vibration. Bert (1973) and Crandall (1970) gave early reviews of damping models and mechanisms. A large amount of the literature on damping deals with viscoelastic materials (Nashif, Jones and Henderson, 1985). For thin, flexible cantilever beams, some attempts to measure the effect of air damping have been made. Baker, Woolam, and Young (1967) incorporated the effect of external air damping in addition to internal linear viscous damping in the governing equations. Experiments were conducted with beams in various atmospheric pressure environments. Cusumano and Moon (1995a) briefly compared the nonlinear vibrations of a flexible metallic cantilever beam in both air and helium. They found no significant difference in the beam response in the studied regions. Other researchers have found it necessary to include a quadratic term in velocity to match theoretical and experimental results for cantilever beams (Anderson, Nayfeh, and Balachandran, 1996b; Zaretzky and Crespo da Silva, 1994). The quadratic nature of the damping indicates that for thin

structures, the effect of air damping can be significant. Forys and Niziol (1984) included a quadratic damping term in their analysis of a portal frame.

1.8 DISSERTATION OVERVIEW

The first part of the Dissertation (Chapters 2, 3 and 4) deals with the vibration of a metallic uniform cantilever beam. In Chapter 2, we determine the theoretical and experimental linear natural frequencies of a cantilever beam. We find it necessary to include the effect of gravity to improve agreement for the cantilever beam in a vertical configuration.

In Chapter 3, we present experimental results from excitation amplitude and frequency sweeps around the fourth natural frequency of the cantilever beam. For the vertical configuration, both resonant and nonresonant modal interactions lead to an energy transfer from the fourth mode to a lower-frequency mode. However, for the beam in a horizontal configuration, only a resonant modal interaction was observed.

In Chapter 4, we develop the modulation equations for the single-mode response of a cantilever beam. We find that, to bring the theoretically and experimentally obtained results into agreement, it is necessary to incorporate the effect of air damping as a quadratic term in velocity and the influence of a nonideal clamp as a cubic torsional stiffness term into the analysis.

The second part of the Dissertation (Chapters 5 and 6) focuses on the vibration of a portal frame. In Chapter 5, we model the frame, showing that the dominant nonlinearity is of the quadratic type. Next we calculate the linear natural frequencies and mode shapes. In Chapter 6, we present results for the case of a single resonance condition. This is followed, briefly, with some results where more than one resonance condition was satisfied. The response for the latter involved up to seven modes of the portal frame.

In Chapter 7 we end the Dissertation with an outline of a series of experiments that when coupled with a perturbation analysis can provide estimates of the parameters of a nonlinear system. We show the example of a portal frame.

Chapter 8 provides an overview of all of the results along with a discussion. This is followed by some recommendations for further research in the study of nonlinear vibration of structures.

CHAPTER TWO

Effect of Gravity on the Bending Frequencies of Vertical Cantilever Beams

'We must never theorize without access to data' Sherlock Holmes

2.1 INTRODUCTION

In this chapter, we detail the influence of gravity on the natural frequencies of a cantilever beam in a vertical configuration. Since the first part of this dissertation concentrates on the nonlinear behavior of cantilever beams, it is important to obtain accurate estimates of the linear natural frequencies. This requires proper matching of experimental results, when available, with analytical results. Should discrepancies arise, then the model must be improved or replaced until experimental results can be predicted. When we first compared the experimentally obtained natural frequencies with the theoretically obtained natural frequencies of an Euler-Bernoulli analysis, we found a large discrepancy for the first natural frequency. This discrepancy was found to be due to the effect of gravity on the stiffness of the very flexible beam and so the beam model was improved to include the gravity effect (Blevins, 1979; Dym and Shames, 1973). In what follows, we investigate in detail theoretically and experimentally the influence of gravity on the natural frequencies of a uniform cantilever beam in either an upward or downward position. The theoretical formulation is based on an initially straight configuration and, therefore, the effect of static deflections is not considered.

2.2 ANALYSIS

The linear natural frequencies of an Euler-Bernoulli cantilever beam are well known. The transcendental characteristic equation governing the frequencies can be solved numerically. Essentially, the first few natural frequencies are considered to be accurate. Beyond that, as the number of nodes increases with increasing frequency, the *wrinkling* or rotation is no longer negligible, violating a major assumption of the Euler-Bernoulli beam theory (Meirovitch. 1967).

The linear undamped free vibrations of a cantilever beam with uniform properties are described by

$$m\frac{\partial^2\bar{v}}{\partial\bar{t}^2} + EI\frac{\partial^4\bar{v}}{\partial\bar{s}^4} = \pm mg\left[\frac{\partial^2\bar{v}}{\partial\bar{s}^2}(\bar{s}-l) + \frac{\partial\bar{v}}{\partial\bar{s}}\right], \tag{2.1}$$

where the term on the right hand side captures the effect of gravity. This term is a result of gravity acting through the *shortening* of the beam due to the transverse deflection. The accompanying boundary conditions are

$$\bar{v}(0,\bar{t}) = 0\,,\ \frac{\partial\bar{v}}{\partial\bar{s}}(0,\bar{t}) = 0\,,\ \frac{\partial^2\bar{v}}{\partial\bar{s}^2}(l,\bar{t}) = 0\,,\ \frac{\partial^3\bar{v}}{\partial\bar{s}^3}(l,\bar{t}) = 0. \tag{2.2}$$

The variable $\bar{v}$ describes the deflection of the beam. $\bar{s}$ is the arclength, l is the length of the beam, m is the mass per unit length, g is the local gravitational acceleration. E is Young's modulus, and I is the moment of inertia of the beam cross section. The minus sign corresponds to a beam pointing downward in the direction of gravity and the plus sign corresponds to a beam pointing upward against gravity.

The first step is to nondimensionalize the equation of motion and its associated boundary conditions. To this end, we set

$$v = \frac{\bar{v}}{l},\ s = \frac{\bar{s}}{l},\ t = \bar{t}\sqrt{\frac{EI}{ml^4}},\ \text{and}\ G = \frac{gml^3}{EI}. \tag{2.3}$$

In nondimensional quantities, the equation of motion becomes

$$\ddot{v} + v^{iv} = \pm G\left[\,(s-1)\,v'' + v'\,\right], \tag{2.4}$$

and the boundary conditions become

$$v(0,t) = 0\ ,\ v'(0,t) = 0\ ,\ v''(1,t) = 0\ ,\ v'''(1,t) = 0, \tag{2.5}$$

where the overdot denotes the time derivative and the prime denotes the spatial derivative.

To determine the natural frequencies, we let

$$v(s,t) = e^{i\omega t}\varphi(s) \tag{2.6}$$

in Eqs. (2.4) and (2.5) and obtain

$$\varphi^{iv} - \omega^2\varphi = \pm\ G\,[\ (s-1)\,\varphi'' + \varphi'\ ] \tag{2.7}$$

and

$$\varphi(0) = 0,\ \varphi'(0) = 0,\ \varphi''(1) = 0,\ \varphi'''(1) = 0. \tag{2.8}$$

We note that ω is the nondimensional natural frequency.

Next, we approximate the solution of Eqs. (2.7) and (2.8) using the Bubnov-Galerkin method (Washizu, 1982). As trial functions, we employ the eigenfunctions for the classical case: they satisfy all of the boundary conditions, Eq. (2.8), but not the equation of motion. Eq. (2.7). Thus, we approximate $\varphi(s)$ as

$$\varphi(s) = \sum_{i=1}^{n} a_i\varphi_i(s) \tag{2.9}$$

where

$$\varphi_i(s) = \cosh(\sqrt{\omega_i}s) - \cos(\sqrt{\omega_i}s) - k_i[\ \sinh(\sqrt{\omega_i}s) - \sin(\sqrt{\omega_i}s)\ ], \tag{2.10}$$

and

$$k_i = \frac{\cosh(\sqrt{\omega_i}) + \cos(\sqrt{\omega_i})}{\sinh(\sqrt{\omega_i}) + \sin(\sqrt{\omega_i})} \tag{2.11}$$

and the ω_i are the roots of the transcendental equation

$$\cos(\sqrt{\omega})\cosh(\sqrt{\omega}) + 1 = 0 \tag{2.12}$$

Substituting Eq. (2.9) into Eq. (2.7), multiplying the outcome with $\varphi_j(s)$, and integrating the resulting equation from $s = 0$ to $s = 1$, we obtain

$$\sum_{i=1}^{n}(\omega^2 - \omega_i^2)\, a_i \int_0^1 \varphi_i \varphi_j ds \mp G \sum_{i=1}^{n} a_i \left[\int_0^1 \varphi_i'' \varphi_j (s-1) ds + \int_0^1 \varphi_i' \varphi_j ds \right] = 0 \qquad (2.13)$$

Setting the determinant of the coefficient matrix in Eq. (2.13) equal to zero yields a polynomial equation for the nondimensional natural frequency ω.

2.3 RESULTS

2.3.1 EXPERIMENTALLY OBTAINED NATURAL FREQUENCIES

As a point of comparison, the natural frequencies of a flexible cantilever beam consisting of SAE 1095 steel were studied. The properties of the beam are listed in Table 2.1. The cantilever beam was mounted vertically using a clamping fixture attached to an exciter. A dynamic signal analyzer provides both the excitation, a random signal, and a means to calculate the frequency-response function. Data were fed to the signal analyzer and processed. Each peak in the frequency-response display was then associated with a natural frequency. The natural frequencies were obtained for the beam both in the upward and downward directions. The first four natural

Table 2.1: Properties of SAE 1095 beam

Properties	Values
Density	0.28 *lb/in*^{3}
Width	0.62 *in.*
Length	33.0 *in.*
Thickness	0.032 *in.*
Young's Modulus	30.0 x 10^6 *psi*

frequencies are shown in Table 2.2 side by side with those found from the Euler-Bernoulli model, with no gravity influence. Also, results from a finite element analysis of the cantilever beam using the commercial code ABAQUS are shown. The finite element code also fails to account for the effect of gravity. We note that the difference is most pronounced for the first natural frequency and significantly less for the higher natural frequencies.

2.3.2 ANALYTICALLY OBTAINED NATURAL FREQUENCIES

Because of the nature of the eigenfunctions, the integrations in Eq. (2.13) were performed numerically. Taking $n = 4$ in Eq. (2.13) yields

$$\left[\omega^2\begin{vmatrix}1&0&0&0\\0&1&0&0\\0&0&1&0\\0&0&0&1\end{vmatrix}-\begin{vmatrix}12.36&0&0&0\\0&485&0&0\\0&0&3806&0\\0&0&0&14616\end{vmatrix}\pm G\begin{vmatrix}1.57&-0.42&-1.07&-.087\\-0.42&8.64&1.89&-3.64\\-1.07&1.89&24.9&8.34\\-0.87&-3.64&8.34&51.45\end{vmatrix}\right]\begin{Bmatrix}a_1\\a_2\\a_3\\a_4\end{Bmatrix}=\begin{Bmatrix}0\\0\\0\\0\end{Bmatrix} \tag{2.14}$$

Table 2.2: Natural frequencies of a cantilever beam, Hz

Mode No.	Finite Element	Euler-Bernoulli	Experimental		
			Up	Down	Horizon.
1	0.95	0.96	0.70	1.15	0.94
2	5.95	6.03	5.85	6.20	5.86
3	16.67	16.87	16.65	17.10	16.78
4	32.67	33.07	32.95	33.35	32.56

The diagonal terms in the second matrix represent the squares of the nondimensional natural frequencies of the beam in the absence of gravity, $\omega_{Bi}{}^2$, while the third matrix provides the adjustment of these frequencies due to gravity. Neglecting the off-diagonal terms in Eq. (2.14) yields four uncoupled equations, each of which generates a natural frequency. This is a one-term

Bubnov-Galerkin approximation to the natural frequencies. For a four-term approximation, we set the determinant of the coefficient matrix in Eq. (2.14) equal to zero and obtain a fourth-order polynomial equation for the squares of the nondimensional natural frequencies. The obtained natural frequencies are listed in Table 2.3. Clearly, the convergence is fast. It follows from Table 2.3 that the analytically predicted natural frequencies are in excellent agreement with those found experimentally. The largest error is about 3% for the first natural frequency.

Table 2.3: Analytically and experimentally obtained natural frequencies with gravity. Hz

Up			Down		
1-term	4-term	Expt.	1-term	4-term	Expt.
0.677	0.677	0.70	1.17	1.18	1.15
5.81	5.81	5.85	6.23	6.23	6.20
16.65	16.65	16.65	17.09	17.09	17.10
32.80	32.83	33.35	33.29	33.29	33.35

We note that, for a beam pointing upward, gravity lowers the natural frequencies, while for a beam pointing downward, gravity increases the natural frequencies. This is explained physically by the fact that for a beam pointing downward, gravity provides a compressive force that decreases the stiffness and, therefore, the natural frequencies. Similarly, when the beam is pointing downward, gravity exerts a tensile force, thereby increasing the stiffness. As a consequence, the natural frequencies increase.

2.3.3 PARAMETRIC STUDY

Nondimensional Natural Frequencies

Figures 2.1-2.4 show variation of the first four nondimensional natural frequencies of a vertical cantilever beam with G. The increasing values of the natural frequency with G correspond to a

beam pointing downward while the decreasing values of the natural frequency with G correspond to a beam pointing upward. Figures 2.1-2.4 were generated by taking $n = 7$ in Eq. (2.13). Comparing these results with those obtained when $n = 4$ shows an excellent convergence in the range of considered values of G. The analysis is valid only for values of G for which $\omega^2 \geq 0$. Thus, for beams pointing downward, the analysis is valid for all values of G. However, for beams pointing upward, the analysis is valid only for values of $G \leq 7.8$. It follows from Fig. 2.1 that the first natural frequency is zero when $G \approx 7.8$, indicating a buckling of the beam due to its own weight (Genta, 1993). For $G > 7.8$, the analysis is not valid because the beam buckles under its own weight and Eq. (2.1), derived based on an initially straight configuration, is no longer applicable.

Dimensional Natural Frequencies

To gain some insight into the influence of various parameters, we investigate the dimensional natural frequencies, which are given by

$$\overline{\omega}_i^2 = \left(\frac{EI}{ml^4}\right) \omega_{Bi}^2 \mp (g/l)\ \alpha_i^n \tag{2.15}$$

or

$$\overline{\omega}_i^2 = \left(\frac{EI}{ml^4}\right) \omega_{Bi}^2 \left[1 \mp \left(\frac{gml^3 \alpha_i^n}{EI\, \omega_{Bi}^2}\right) \right] \tag{2.16}$$

where $\overline{\omega}_i$ is the i th natural frequency, the first term on the right-hand side of Eq. (2.15) is the square of the i th Euler-Bernoulli natural frequency, and ω_{Bi}^2 is the i th nondimensional natural frequency, where n is the number of terms in the expansion, Eq. (2.9). We note that α_i^1 is the i th diagonal term of the third matrix in Eq. (2.14) for one-term expansion. In Eq. (2.15), the minus sign corresponds to a beam pointing downward and the plus sign corresponds to a beam pointing upward.

It follows from Eq. (2.16) that increasing the beam length results in an increase in the influence of gravity on the natural frequencies. For example, for a beam pointing upward, increasing the length of the beam will eventually lead to its buckling under its own weight. Again, it follows from Eq. (2.16) that increasing the beam stiffness *EI* results in a decrease in the influence of gravity, whereas increasing *m*, the mass per unit length, leads to an increase in the influence of gravity. Because $(\alpha_i^n / \omega_{Bi}^2)$ decreases with increasing mode number, the effect of gravity decreases with increasing mode number according to Eq. (2.16).

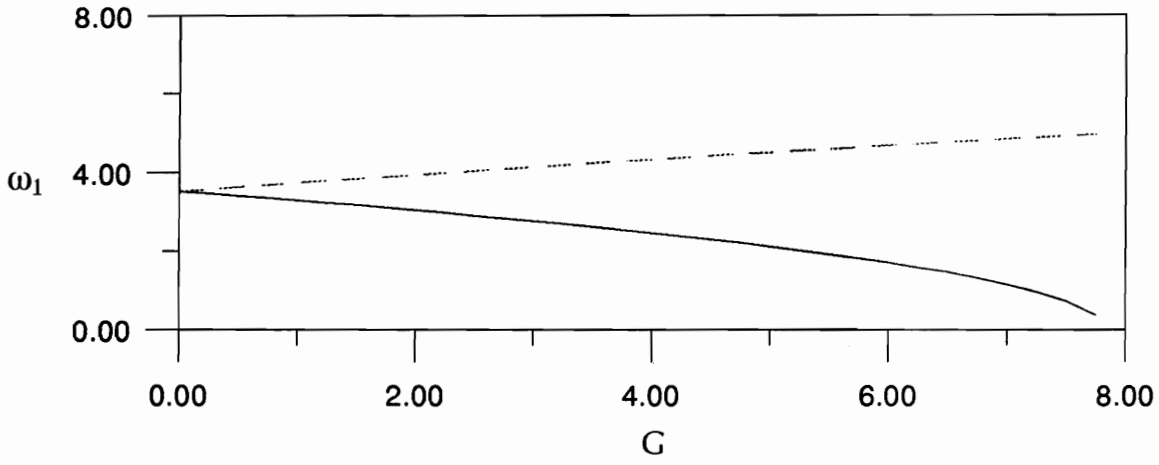

Figure 2.1 Variation of the first nondimensional natural frequency of a cantilever beam with G
- beam pointing up; - - beam pointing down.

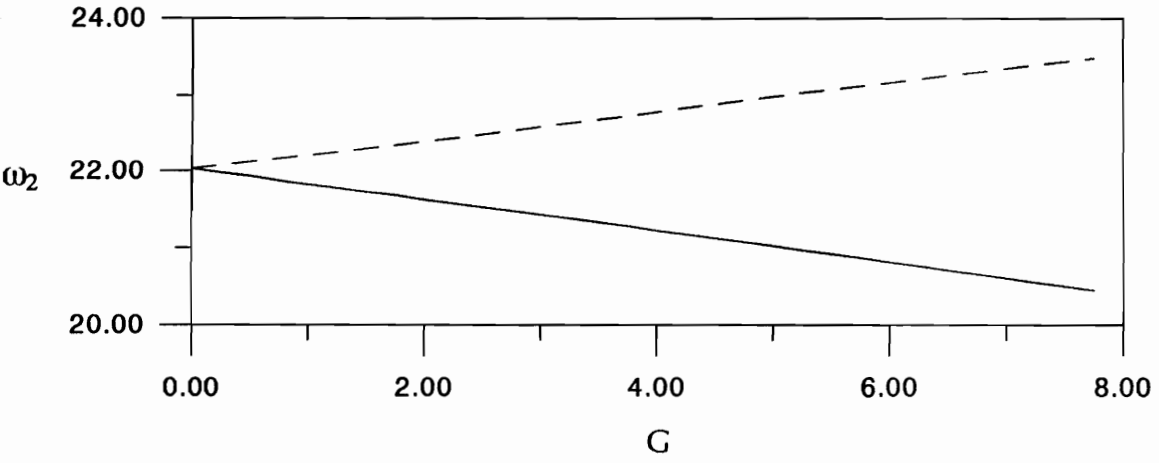

Figure 2.2 Variation of the second nondimensional frequency of a cantilever beam with G
- beam pointing up, - - beam pointing down.

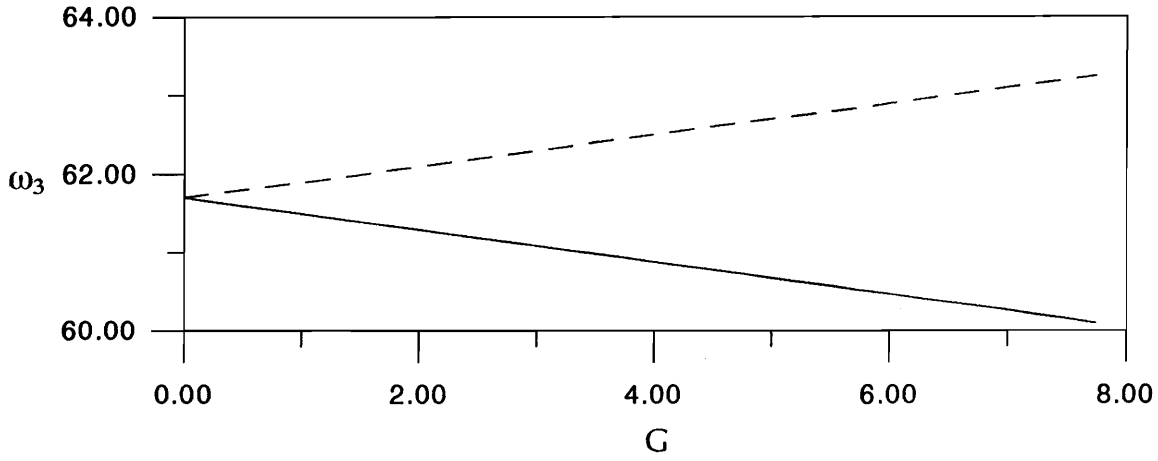

Figure 2.3 Variation of the third nondimensional natural frequency of a cantilever beam with G
- beam pointing up, - - beam pointing down.

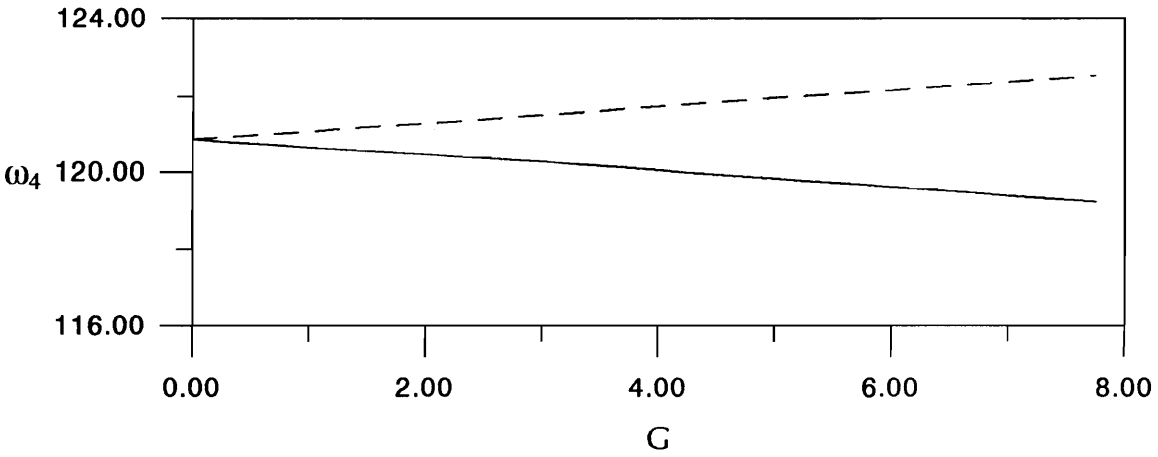

Figure 2.4 Variation of the fourth nondimensional frequency of a cantilever beam with G
- beam pointing up. - - beam pointing down.

2.4 CHAPTER REMARKS

In this chapter, an analytical and experimental study into the effect of gravity on the natural frequencies of a vertical cantilever beam is presented. The first four natural frequencies obtained analytically are in excellent agreement with those found experimentally. For a beam pointing upward, gravity decreases its natural frequencies, whereas for a beam pointing downward, gravity increases its natural frequencies. The largest effect of gravity occurs for the first natural frequency. The effect of gravity diminishes for each successively higher natural frequency. For a beam pointing upward, increasing the value of $G = \frac{gml^3}{EI}$ leads to a vanishing of the first natural frequency. This corresponds to a buckling of the beam under the influence of its own weight. Once buckling occurs, the analytically obtained natural frequencies are no longer valid as the assumption under which Eq. (2.1) was derived, an initially straight configuration, is violated. For a beam pointing downward, the natural frequencies increase with increasing values of G and hence the analysis is valid for all values of G.

The results for the beam can be extended to other structures, such as plates and shells. As these and other structures become lighter and more flexible, the influence of gravity on the natural frequencies may become more pronounced.

CHAPTER THREE

An Experimental Investigation of Multimode Responses in a Cantilever Beam

'ill-conceived applications of linear theory to essentially nonlinear problems can hardly be expected to agree with the results of badly controlled experiments no matter how much money is spent on both' W.T. Koiter

In this chapter, an experimental investigation into the planar, multimode response of a cantilever, metallic beam to a transverse harmonic excitation is presented. The cantilever beam was tested in both the horizontal and vertical directions. In the vertical configuration, the beam was excited near its fourth natural frequency and energy was transferred from the directly excited fourth mode to a low-frequency mode through both resonant and nonresonant modal interactions. In the horizontal configuration, the beam was excited first near its fourth and then sixth natural frequencies. Again, energy was transferred to a low-frequency mode, but in this configuration only through a resonant modal interaction.

3.1 INTRODUCTION

Nonlinearities are responsible for many interesting phenomena in the forced response of structures (Nayfeh and Mook, 1979; Nayfeh and Balachandran, 1989; Nayfeh and Mook, 1995). They include primary, subharmonic, superharmonic, combination, and subcombination resonances; coexistence of multiple responses; jumps; period-multiplying bifurcations: chaos: and modal interactions. The objective of the present chapter is to describe experimental results on modal

interactions in the planar response of a cantilever, metallic beam to a harmonic transverse excitation.

Modal interactions may be the result of internal resonances, external combination resonances, or nonresonant interactions (Nayfeh and Mook, 1995). An internal (autoparametric) resonance may occur if the natural frequencies, ω_i, of the structure are commensurate or nearly commensurate; that is, if there exists positive or negative integers m_i such that $m_1\omega_1 + m_2\omega_2 + \ldots + m_n\omega_n \sim 0$. The degree of an internal resonance is N where $N = |m_1| + |m_2| + \ldots + |m_n|$. Hence, the type and degree of an internal resonance depend on the nonlinearities in the structure. For example, systems having quadratic nonlinearities may possess, to first order, the following internal resonances: $\omega_k \sim 2\omega_l$ (two-to-one internal resonance) and $\omega_k \sim \omega_i + \omega_l$ (combination resonance). Systems with dominating cubic nonlinearities may possess the following internal resonances: $\omega_l \sim \omega_j$ (one-to-one internal resonance); $\omega_l \sim 3\omega_j$ (three-to-one resonance); $\omega_j \sim \omega_k + \omega_l + \omega_m$ and $\omega_j \sim 2\omega_k \pm \omega_l$ (combination internal resonances); and $\omega_j \sim \frac{1}{2}(\omega_m \pm \omega_l)$ (subcombination internal resonances). The subcombination resonance is an alternate form of the combination resonance.

Combination external resonances may occur if the external excitation Ω is commensurate with two or more natural frequencies (Dugundji and Mukopadhyay, 1973; Nayfeh and Mook, 1979). Systems with quadratic nonlinearities may possess a combination resonance of the additive or difference type: $\Omega \sim \omega_i \pm \omega_j$. Systems with cubic nonlinearities may possess one of the combination resonances $\Omega \sim \omega_j \pm \omega_k \pm \omega_l$ and $\Omega \sim \omega_m \pm 2\omega_n$ or the subcombination resonance $\Omega \sim \frac{1}{2}(\omega_k \pm \omega_l)$. Nonresonant interactions may occur in systems with quadratic or cubic nonlinearities between two widely spaced modes (Anderson, Balachandran, and Nayfeh, 1994;

Nayfeh and Nayfeh, 1994; Anderson, Nayfeh, and Balachandran, 1996a). In other words, modes n and m may interact if $\omega_n >> \omega_m$.

For comprehensive reviews of such interactions, we refer the reader to Nayfeh and Mook (1979, 1995) and Nayfeh and Balachandran (1989). In Section 3.2 we describe the experimental setup, in Section 3.3 we discuss calculation of the linear natural frequencies, and in Sections 3.4 and 3.5 we present experimentally observed responses of the cantilever beam in both the horizontal and vertical configurations to a transverse harmonic excitation.

3.2 EXPERIMENTAL SETUP

Figure 3.1 shows a schematic of the experimental setup for the vertically positioned beam. For the horizontally positioned beam, the beam was rotated 90 degrees about the axis of the shaker armature. The beam was made of SAE 1095 steel with the dimensions 84.45 *cm* x 0.81 *mm* x 1.57 *cm*. It was mounted through a steel clamping fixture attached to a 100-*lb* shaker. A signal generator in line with a power amplifier provided a harmonic input signal to the shaker. This allowed for manual control of the excitation frequency and amplitude. The output of the shaker was measured with an accelerometer placed on the clamping fixture, whereas the response of the cantilever beam was measured with a 350 *Ohm* strain gage mounted approximately 2.54 *cm* and 5.0 *cm* from the fixed end of the vertical and horizontal beams, respectively. These signals were subsequently processed through an analog multichannel low-pass filter set to a cut-off frequency of 500 Hz. This filter also allowed for AC coupling of the signals. The power spectra of the transducer signals were calculated in real time over a 40 Hz bandwidth (0.05 Hz frequency resolution) with a Hanning window using a dynamic signal analyzer. At points of interest, the data were converted digitally through an A/D card on a digital computer and stored for further characterization and processing.

For the vertical beam, the investigation concentrated on a frequency range around the fourth natural frequency of the beam. whereas for the horizontal beam, an additional frequency range around the sixth natural frequency was examined. Once the beam was mounted. the only two control parameters were the excitation frequency and amplitude. Sweeps were performed by varying either of these two parameters while keeping the other fixed. These sweeps allowed for characterization of the nonlinear dynamics of the beam by capturing jumps and multiple solutions in a methodical manner. At each increment of the control parameter, we waited for a sufficiently long time, allowing for the transients to die away, before recording the response. The spectrum of the strain gage was the key component in determining whether a stationary state in the dynamics of the beam had been reached. Then, the magnitudes of the peaks in the response spectrum associated with the natural frequencies of the beam were recorded. The collection of such points produced the frequency- and amplitude-response curves that are shown in this chapter. The magnitudes of the strains (in volts) associated with each peak were scaled by the frequency of each peak to obtain a numerical measure that is proportional to the displacement. The calibration constant for the strain gage would be necessary to convert to the actual displacement. All documented motions were observed to be planar.

3.3 LINEAR NATURAL FREQUENCIES

The first step in any vibration study is the determination of the linear natural frequencies. They are then used as a starting point in the investigation of nonlinear phenomena. The natural frequencies of the beam were found experimentally by using the frequency-response function of the analyzer. The inputs processed included the accelerometer signal, measuring the amplitude of a random excitation, and the strain-gage signal, measuring the induced strain. The placement of the strain gage was based on the need for a strong signal-to-noise ratio and the avoidance of being on or near the node of any of the vibration modes of interest. Peaks in the amplitude

portion of the frequency-response function were associated with the linear natural frequencies of the beam. To increase confidence in the experimentally obtained natural frequencies, we measured the frequency-response functions at several low excitation levels. No noticeable shifts in the peaks were observed. Also, a periodic checking of the natural frequencies of the beam were performed to detect any fatigue damage (Ostachowicz and Krawczuk, 1991).

The linear natural frequencies of the cantilever beam in the vertical and horizontal configurations are listed in Table 3.1. Both the Euler-Bernoulli and the finite element values fail to accurately predict the first natural frequency. The agreement improves with each higher frequency for the first eight natural frequencies. The discrepancy is due to the effect of gravity on the stiffness of the cantilever beam as discussed in Chapter 2.

Table 3.1: Natural frequencies of a cantilever beam, Hz

Mode No.	Finite Element	Euler-Bernoulli	Experimental	
			Vertical	Horizon.
1	0.95	0.96	0.70	0.94
2	5.95	6.03	5.85	5.86
3	16.67	16.87	16.65	16.78
4	32.67	33.07	32.95	32.56
5	-	54.0	54.4	53.8
6	-	80.6	81.6	80.5
7	-	112.6	114.05	112.3
8	-	149.9	-	150.6

3.4 NONLINEAR RESPONSE OF THE VERTICAL BEAM

For the vertical beam, we show a typical frequency-response curve in Figure 3.2 (Tabaddor and Nayfeh, 1995). The excitation amplitude was fixed at approximately 1.00 *g*. Starting with an excitation frequency *f* below the fourth natural frequency and incrementally increasing it, we observed a unimodal motion consisting of the fourth mode whose amplitude gradually increased. As *f* was increased past 32.40 Hz, a jump to a large-amplitude fourth-mode motion was observed. Further increases in the forcing frequency resulted in a gradual decrease of the amplitude of the fourth mode. The general shape of the frequency-response curve exhibits a bending to the left, indicating a softening-type behavior. Anderson et al. (1996a) found that the dominance of the inertia nonlinearity in a cantilever beam is the source of this softening effect.

Reversing the sweep direction and slowly decreasing *f*, we found that the response amplitude traced the same path obtained in the forward sweep. As *f* was decreased below 32.40 Hz, the amplitude of the fourth mode continued to increase monotonically and transients associated with the first mode were observed. As *f* was decreased further, a bimodal response consisting of the fourth and first modes was observed for a brief frequency interval. Visually, the beam was vibrating in the fourth mode while swaying back and forth. A spectrum of this behavior is shown in Figure 3.3. The top portion is the spectrum of the excitation while the lower portion is that of the response. All signals 60 dB below the peak signal were assumed to be inconsequential. The input signal is clean in the sense that it consists of a single peak with no apparent feedback. In the response spectrum, we not only see the peaks associated with the fourth and first modes, but we see additional asymmetric sidebands around the peak associated with the fourth mode. The asymmetry of the sidebands indicates that the amplitude and phase of the fourth mode were modulated. It follows from the time trace shown in Figure 3.4a that the amplitude modulation is clear though the phase modulation is not apparent. The spacing of the sidebands in Figure 3.3 is approximately equal to the natural frequency of the first mode. The activation of the first mode and the modulation of the amplitude and phase of the fourth mode occurred

simultaneously without the activation of any intermediate modes. We note that the deflection associated with the directly excited fourth mode is smaller than the deflection associated with the indirectly excited first mode. Furthermore, the ratio of the frequency of the fourth mode to that of the first mode is over 47, which indicates that the activation of the first mode was not the result of a classical internal resonance. Moreover, the presence of the sidebands only around the peak corresponding to the fourth mode (i.e., the amplitude and phase modulations of the contribution of the fourth mode) is an added feature not present in motions caused by internal resonances. This phenomenon has been dubbed *transfer of energy from high-frequency to low-frequency modes* by Anderson et al. (1992). Nayfeh and Nayfeh (1993) showed analytically that the activation of the low-frequency mode is the result of a nonlinear interaction between two widely spaced modes.

Continual decrease in the forcing frequency resulted in what was thought to be a bimodal response, consisting of the fourth and second modes. The spectrum that was initially studied was based on considering the frequency region below 40 Hz (Figure 3.5a). No significant peaks in the spectrum other than those associated with the second and fourth modes had been detected based on the criterion of a 60 dB cutoff. However, no sidebands were observed so nonresonant modal interactions were ruled out and the ratio of the two frequencies were not commensurate, so this behavior was initially unidentified (Tabaddor and Nayfeh, 1995). However, looking at all the possibilities for classical resonances, we later found that a subcombination internal resonance of the additive type, $\omega_4 \approx \frac{1}{2}(\omega_2 + \omega_5)$, was a possibility. However, the fifth mode had not been recognized earlier as a part of the response since its amplitude was significantly smaller than those of the fourth and second modes. Expanding the frequency range of the spectrum of the response (Figure 3.5b) and studying all low-level signals that were previously ignored, we found a peak corresponding to the fifth mode. Indeed, the amplitude of the fifth mode is almost three orders of magnitude smaller than that of the fourth mode and, yet, it is an essential component

of the response. In this case, the usually satisfactory criterion of 60 dB was too restrictive. For this reason, the frequency-response curve shown in Figure 3.3 does not include the amplitude of the fifth mode. To verify that a subcombination internal resonance was indeed the mechanism responsible for the activation of the second and fifth modes, we studied all other peaks in the spectrum for clues to the nature of the response. We found that all other peaks correspond to multiples and sums or differences of the frequencies of the fourth, second, and fifth modes (Figure 3.5b). That is, even though some of the other peaks are much too small, they give an indication of the primary modes that are active in the response. A time trace of the strain response is shown in Figure 3.4b.

The subcombination internal resonance was activated over two separate intervals. In the first interval, the amplitude of the second mode decreased monotonically with decreasing forcing frequency even though the amplitude of the fourth mode increased. In the second interval, the amplitude of the second mode as well as the amplitude of the fourth mode increased with decreasing frequency. Both intervals were brief and, despite several applied disturbances to the beam, the subcombination internal resonance disappeared before the amplitude of the fourth mode reached its peak and the response jumped down to a smaller-amplitude fourth-mode motion.

3.5 NONLINEAR RESPONSE OF THE HORIZONTAL BEAM

Changing the orientation of the beam from vertical to horizontal altered the natural frequencies, with the most significant reduction occurring for the first natural frequency. This changed an additional control variable, namely, the natural frequency of the first mode. This change seems to prevent the activation of the nonresonant modal interaction that excited the first mode for the vertical configuration of the beam. However, the subcombination internal resonance was found to persist.

We investigated two cases: the excitation frequency was near the fourth and sixth natural frequencies. We discuss these two cases separately, starting with the former.

3.5.1 Excitation Frequency Near the Fourth Natural Frequency

In this subsection, we present experimental results where the excitation frequency was swept in a region near the fourth natural frequency of the beam.

The first frequency sweep was performed for a fixed excitation amplitude of 0.7 *g*. Starting at a frequency value below the fourth natural frequency, we slowly increased the excitation frequency and recorded the magnitudes of the peaks in the response spectrum. The resulting frequency-response curve is shown in Figure 3.6. At first the amplitude of the fourth mode increased until 32.20 Hz when there was a jump to a larger-amplitude unimodal motion. The qualitative behavior of the fourth mode resembles that of the response of the fourth mode for the vertical beam. Again, the frequency-response curve is bent to the left. Now further increases in the forcing frequency resulted in a decrease in the amplitude of the fourth mode.

For the reverse sweep, we slowly decreased the excitation frequency to 31.80 Hz, where we observed a strong peak at 5.80 Hz and a much smaller peak at 57.7 Hz in the power spectrum of the response, as shown in Figure 3.7a. These peaks correspond to the second and fifth modes, respectively. This time alert to the possibility of a subcombination internal resonance, we documented the amplitude of the fifth mode. And, indeed, the three aforementioned frequencies once again satisfy the relationship of a subcombination internal resonance of the additive type, namely, $\omega_4 \sim \frac{1}{2}(\omega_2 + \omega_5)$. We note that the amplitude of the second mode, once again, is almost one-half the amplitude of the fourth mode, whereas the amplitude of the fifth mode is almost three orders of magnitude smaller than that of the fourth mode. The displacement values shown are not calibrated to any specific unit of length but reflect relative deflections. As a point of reference, during the experiment, the deflection associated with the fourth mode near the peak of the frequency-response curve was measured to be nearly 2.54 *cm*. To further

validate the nature of the response, we constructed the pseudo-state space and the pseudo Poincare' section for the beam motion at 31.70 Hz. The pseudo-state plane obtained by plotting 9000 points with a time delay of 5 sampling points and the pseudo Poincare' section drawn with 3000 points and a time delay of 5 sampling points. For quasi-periodic behavior, the pseudo-state plane should consist of a non-closed curve while the pseudo Poincare' section should consist of a closed curve (Nayfeh and Balachandran, 1995). However, the low signal-to-noise ratio prevents any reliable conclusion from the aforementioned plots and therefore they are not shown here. The duration of the subcombination internal resonance is short at this excitation level. Only a single interval was observed, and the amplitudes of the second and fifth modes increased monotonically as the excitation frequency was decreased. A time trace of the strain response is shown in Figure 3.7b.

Figure 3.8 shows frequency-response curves for a slightly higher excitation amplitude, namely, 0.9 *g*. They are qualitatively similar to those obtained for the lower excitation level. However, the jump points in the amplitude of the fourth mode are shifted, as expected. The range of the subcombination internal resonance is slightly increased.

Figure 3.9 shows amplitude-response curves for a fixed excitation frequency of 32.00 Hz. The amplitude of the fourth mode jumped to a larger amplitude at nearly 1.0 *g* (The calibration for the accelerometer was 0.1 V/g). Once again, for a limited range, the subcombination internal resonance was activated in both forward and reverse sweeps. There was some hysteresis as the amplitude of the fourth mode jumped down in the reverse sweep at a forcing amplitude below that at which it jumped up in the forward sweep. The curves in Figure 3.9 are typical amplitude-response curves for forcing frequencies below the fourth natural frequency within a certain detuning range. However, for forcing frequencies above the fourth natural frequency, no multi-mode behavior was found up to a forcing level of 5.0 *g*.

3.5.2 Excitation Frequency Near the Sixth Natural Frequency

For structural applications, the conventional practice is that one can avoid low-frequency modes by moving the excitation frequency range to be way above their associated low frequencies. So to test this hypothesis, we decided to excite the beam near the sixth natural frequency (twice the natural frequency of the fourth mode), another place where the subcombination internal resonance of the additive type may be activated. In this case, the directly excited sixth mode transferred energy into the second and eighth modes. Again, we performed many forcing frequency and amplitude sweeps. Here we show a typical plot of each.

In Figure 3.10, we show the frequency-response curves obtained for an excitation amplitude of 0.9 *g*. The difference between the two jump points is very small. Once again, the amplitude of the higher-frequency mode, the eighth mode, is much smaller than that of the directly excited sixth mode. On the other hand, the amplitude of the second mode is two orders of magnitude larger than that of the sixth mode. Also, the subcombination internal resonance was observed in both forward and reverse sweeps.

In Figure 3.11, we show the amplitude-response curves for a fixed forcing frequency of 78.5 Hz. The amplitude of the directly excited sixth mode appears to change gradually with the forcing amplitude, displaying no sudden changes. The resonance is observed for a large range of excitation amplitudes compared to the previous cases. The activation of the subcombination internal resonance occurred after a very long transient (over one-half hour) for both the amplitude and frequency sweeps. As an aside, sometimes a clue to the type of behavior that might arise could be found in the transient. Some of our observations showed that, prior to the onset of the subcombination internal resonance, the transient contained a strong second-mode component.

In Figure 3.12a, we show the power spectrum of the response at the onset of the subcombination internal resonance in the forward sweep direction. We also constructed pseudo-state planes and pseudo Poincare' sections, but the plots were corrupted by the high noise-to-signal ratio. In Figure 3.12b, we show a time trace of the strain response.

3:6 CHAPTER REMARKS

An experimental investigation into the nonlinear planar, response of a transversely excited cantilever, metallic beam to a transverse, harmonic forcing was presented. The beam was tested in both the vertical (opposite to gravity) and horizontal directions. The results indicate that a low-frequency high-amplitude mode can be activated through two different nonlinear modal interactions: a nonresonant modal interaction and a subcombination internal resonance.

The nonresonant modal interaction was observed in the response of the beam in the vertical configuration when excited near the frequency of its fourth mode. In a narrow forcing frequency range, the response consisted of the directly excited fourth mode as well as the first mode. The appearance of the first mode was accompanied by a modulation of the amplitude and phase of the fourth mode with the modulation frequency being approximately equal to the frequency of the first mode. The amplitude of the first mode was larger than that of the fourth mode. This type of interaction occurs between widely spaced modes (the ratio of the natural frequency of the fourth mode to that of the first mode was approximately 47). This modal interaction was not observed for the horizontally positioned beam. Depending upon the orientation of the beam, the influence of gravity on the natural frequencies of the flexible beam was notable. This change in orientation, in turn, acted as an additional control parameter altering the natural frequency of the first mode. The change in orientation of the beam from a vertical to a horizontal position seems to suppress the onset of the nonresonant modal interaction.

Subcombination internal resonances were observed for both beam configurations. When the forcing frequency was swept in a region near the fourth natural frequency, we observed a multi-mode response with contributions from the fourth, second and fifth modes. The amplitude of the second mode was the same order of magnitude as that of the fourth mode. On the other hand, the amplitude of the fifth mode was several orders of magnitude smaller than that of the

fourth mode. Nevertheless, its inclusion was important in identifying the nature of the documented motions.

For the horizontal beam, an additional frequency interval surrounding the sixth natural frequency was tested. A multimode response consisting of the sixth, second, and eighth modes was observed. In this case, however, the amplitude of the second mode was two orders of magnitude larger than that of the directly excited sixth mode. On the other hand, the amplitude of the eighth mode remained very small. The second and eighth modes were also activated through a subcombination internal resonance of the additive type.

Our results show that the importance of the contribution of a particular mode to the response of a structure can not be based solely on its amplitude. When the deflection is not directly measured, then depending on the transducer, one may need a frequency scaling to assess the relative contributions of the various modes to the total response. For the subcombination internal resonance, although the amplitude of the highest-frequency mode was significantly smaller than that of the directly excited intermediate mode, it was necessary for understanding the nonlinear response of the beam.

The present results show that nonlinear resonant and nonresonant mechanisms can channel energy from a high-frequency to a low-frequency mode. Such transfer of energy will necessarily imply large deflections associated with the low-frequency mode relative to those associated with the high-frequency mode. The consequence of any design or control system that excludes the possibility of multimode behavior may be premature failure. Furthermore, exciting a structure at high frequencies does not guarantee that energy would not be transferred to a low-frequency mode by a nonlinear mechanism.

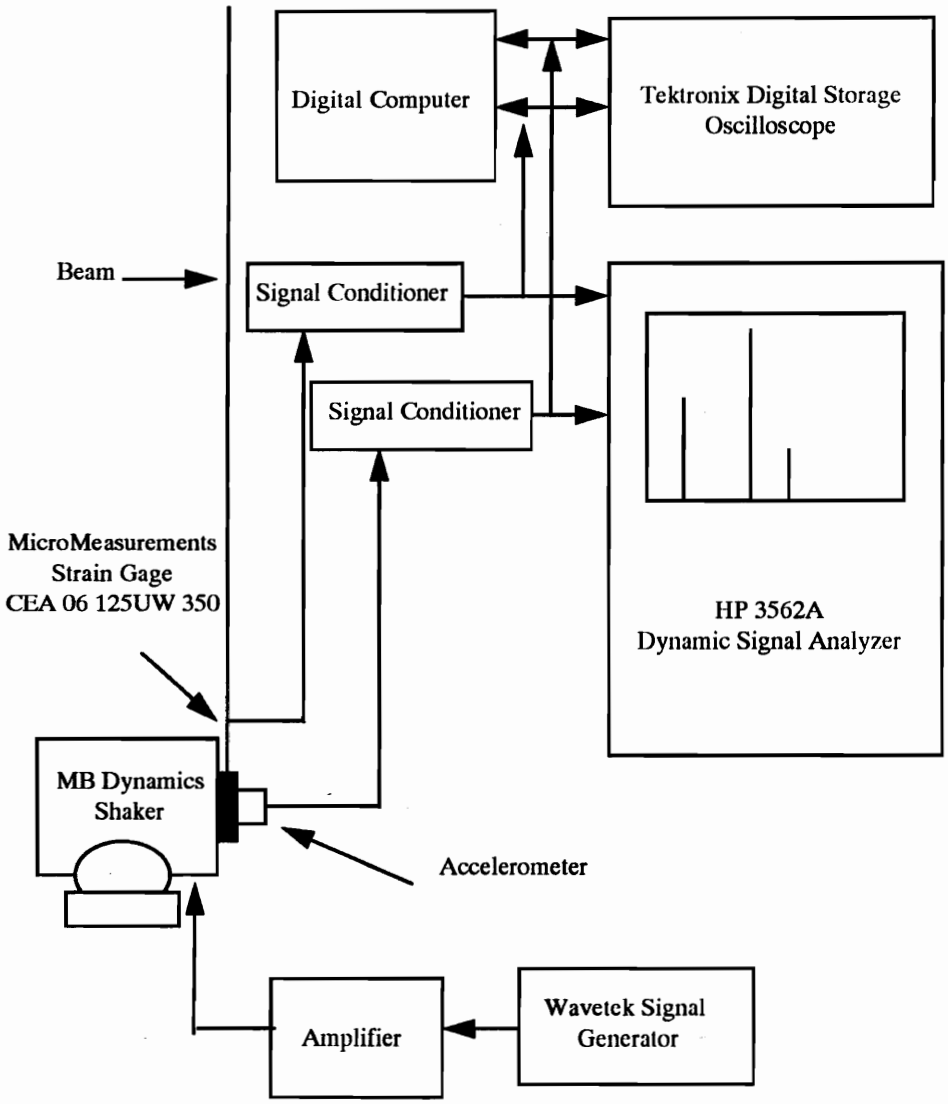

Figure 3.1 A schematic of the experimental setup.

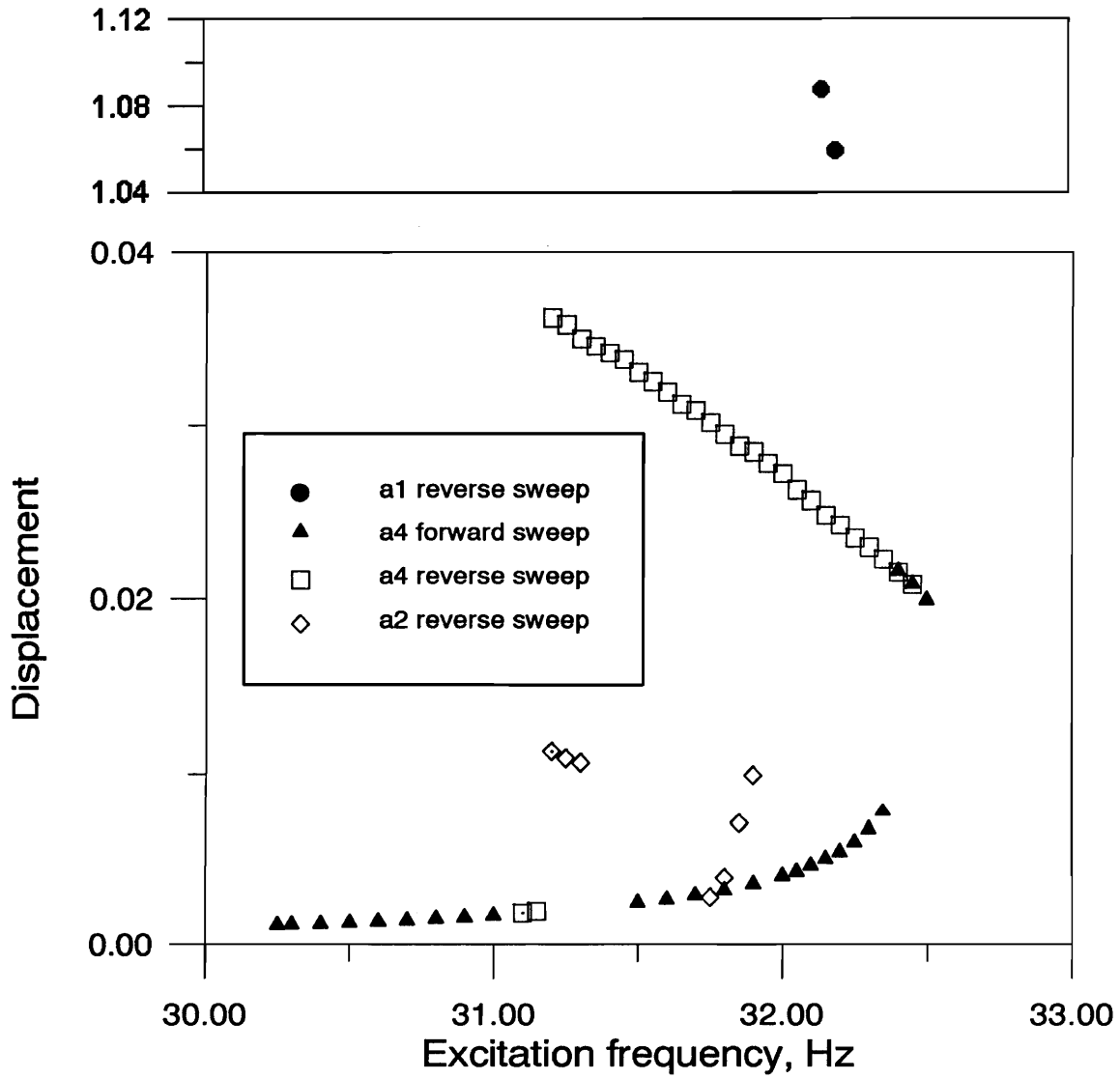

Figure 3.2 Frequency-response curves for an excitation amplitude of 1.00 *g*.

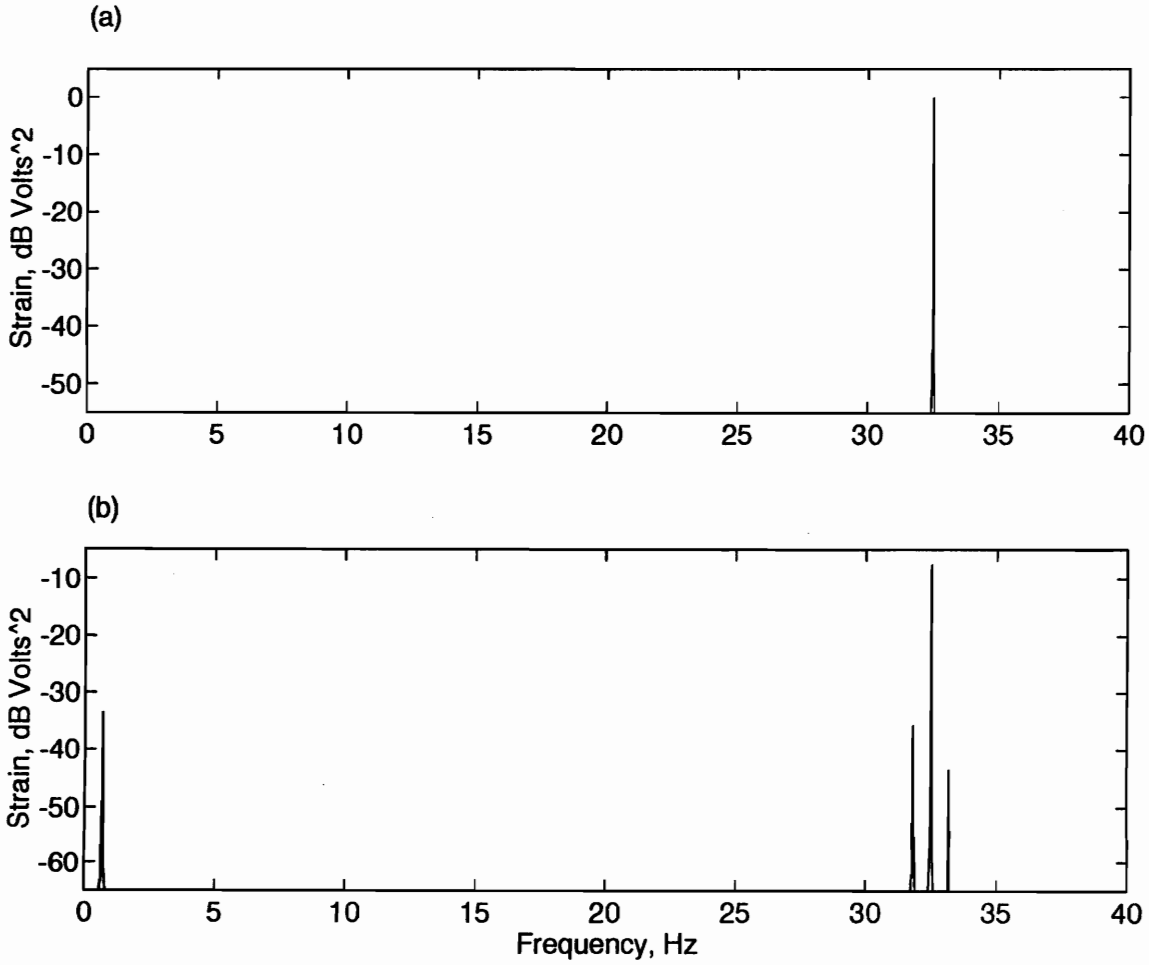

Figure 3.3 Power spectrum of (a) excitation and (b) response at 32.2 Hz for an excitation amplitude of 1.00 *g*.

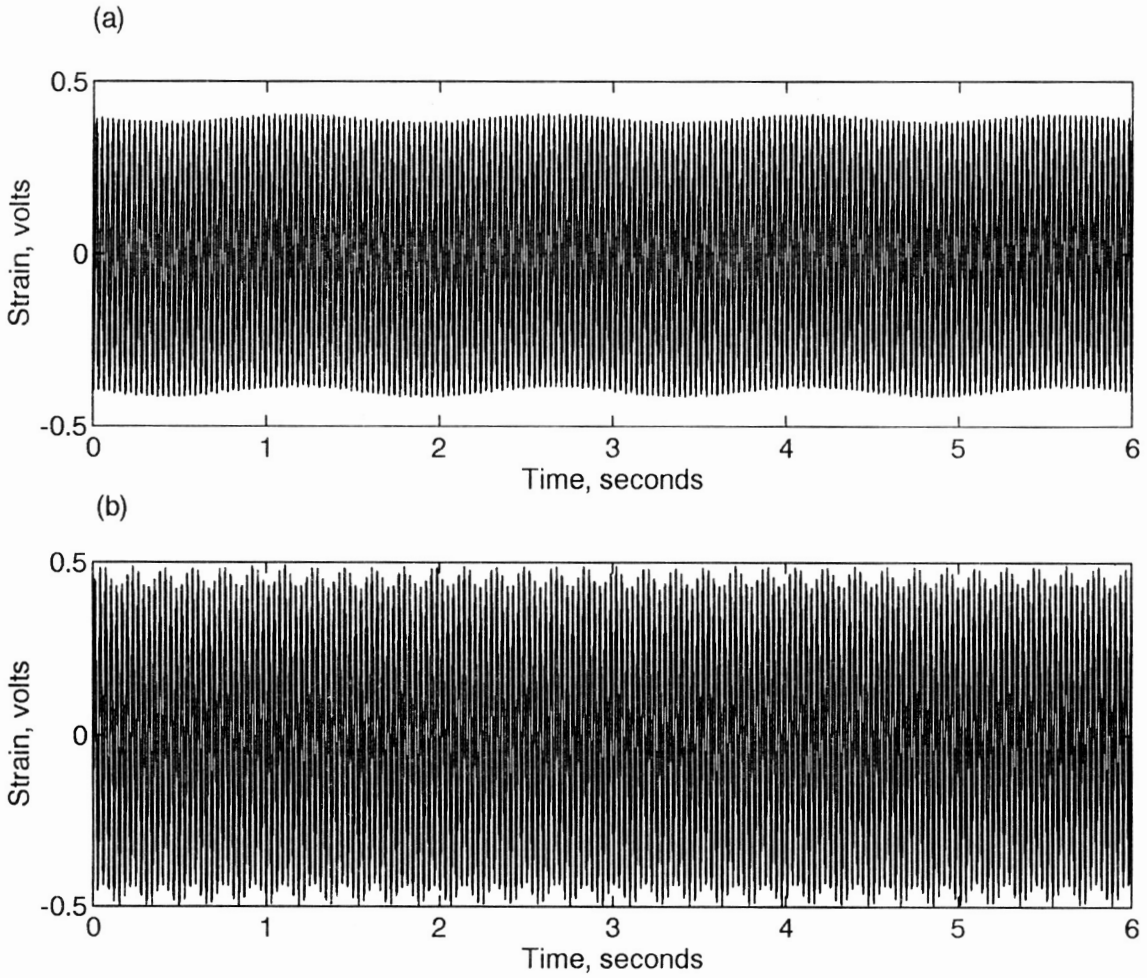

Figure 3.4 Time trace of motion at (a) 32.2 Hz and (b) 31.9 Hz for an excitation amplitude of 1.00 *g*.

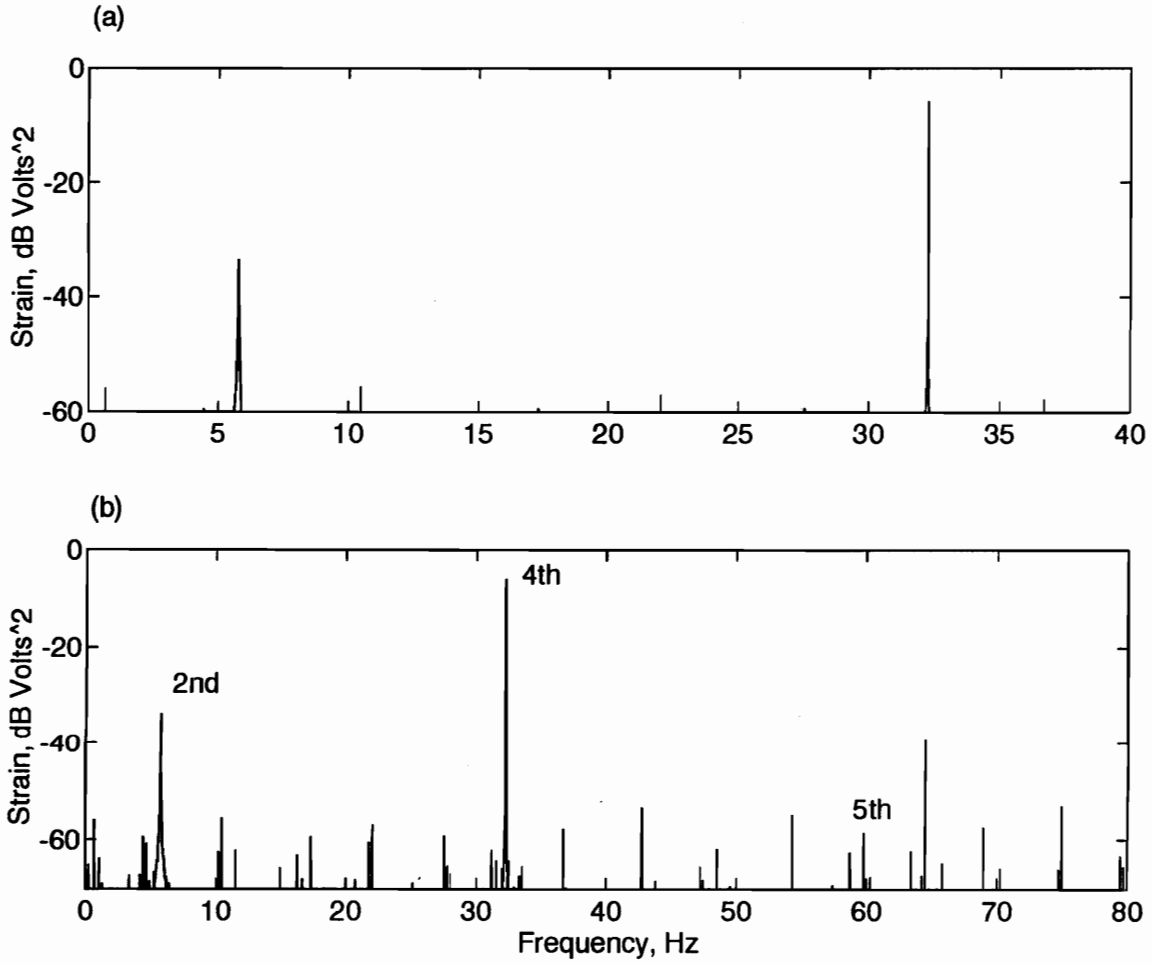

Figure 3.5 Power spectrum of response over (a) a 40 Hz range and (b) an 80 Hz range at 31.9 Hz for an excitation amplitude of 1.00 *g*.

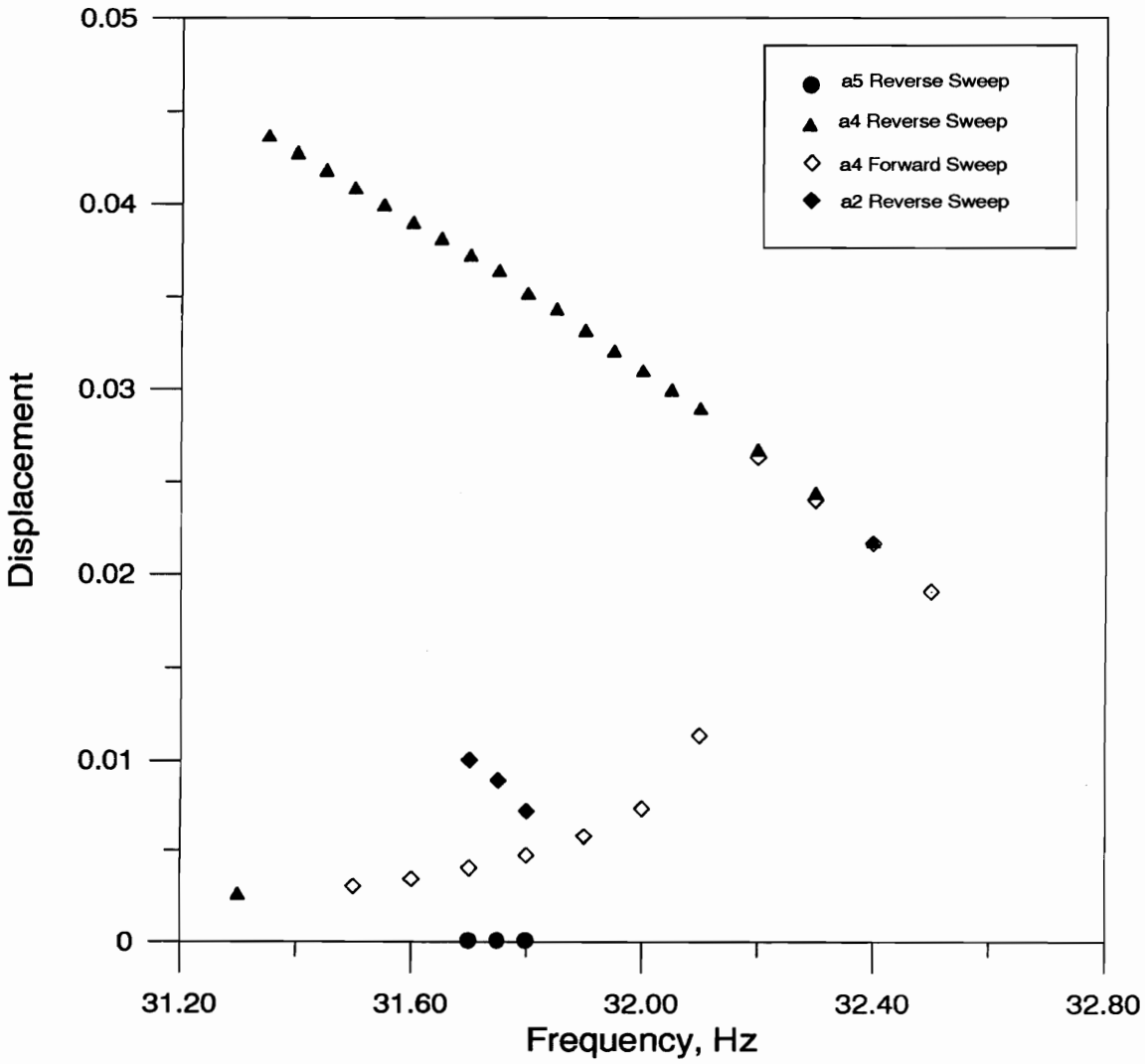

Figure 3.6 Frequency-response curves for an excitation amplitude of 0.7 *g*.

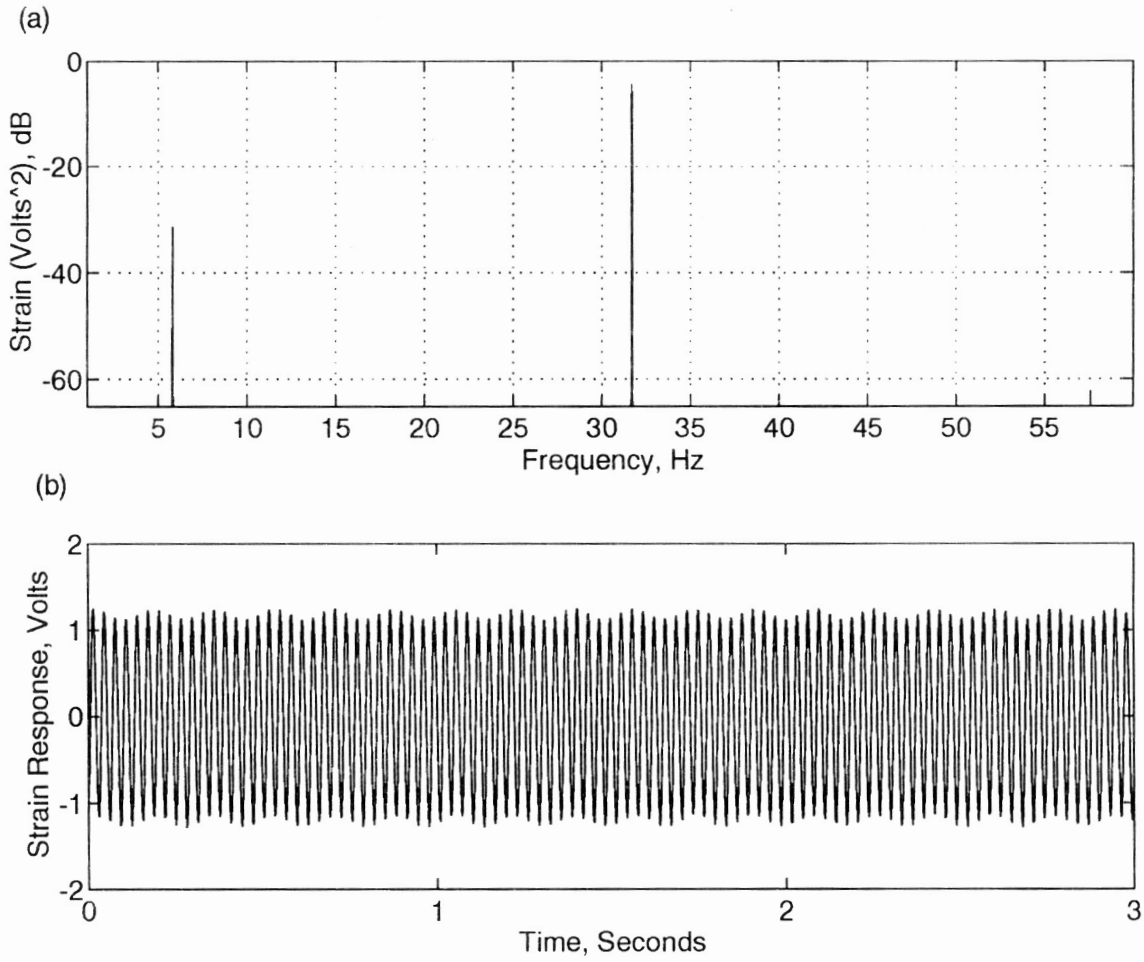

Figure 3.7 Motion at 31.80 Hz for an excitation amplitude of 0.7 g : (a) power spectrum (b) time series.

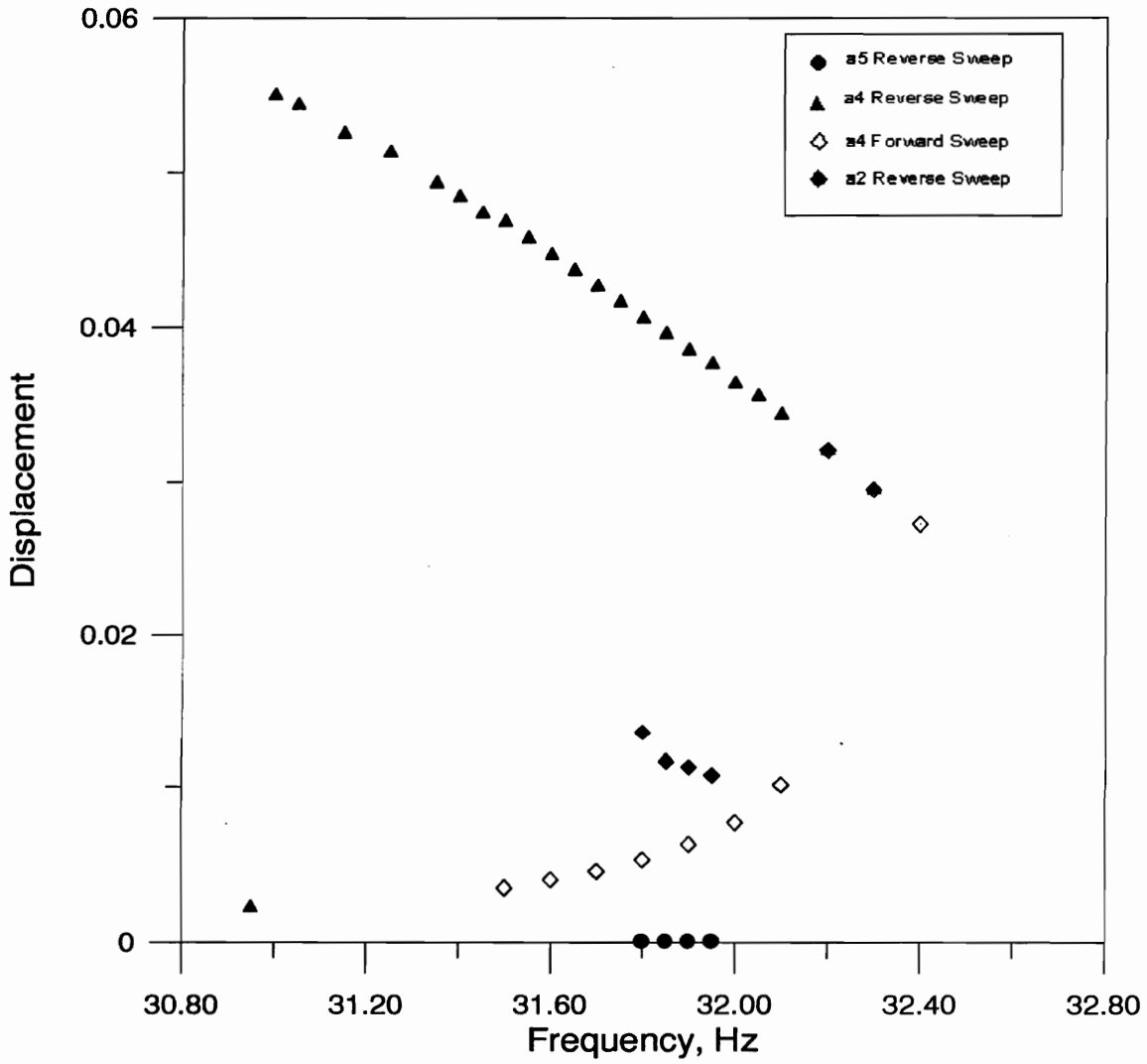

Figure 3.8 Frequency-response curves for an excitation amplitude of 0.9 *g*.

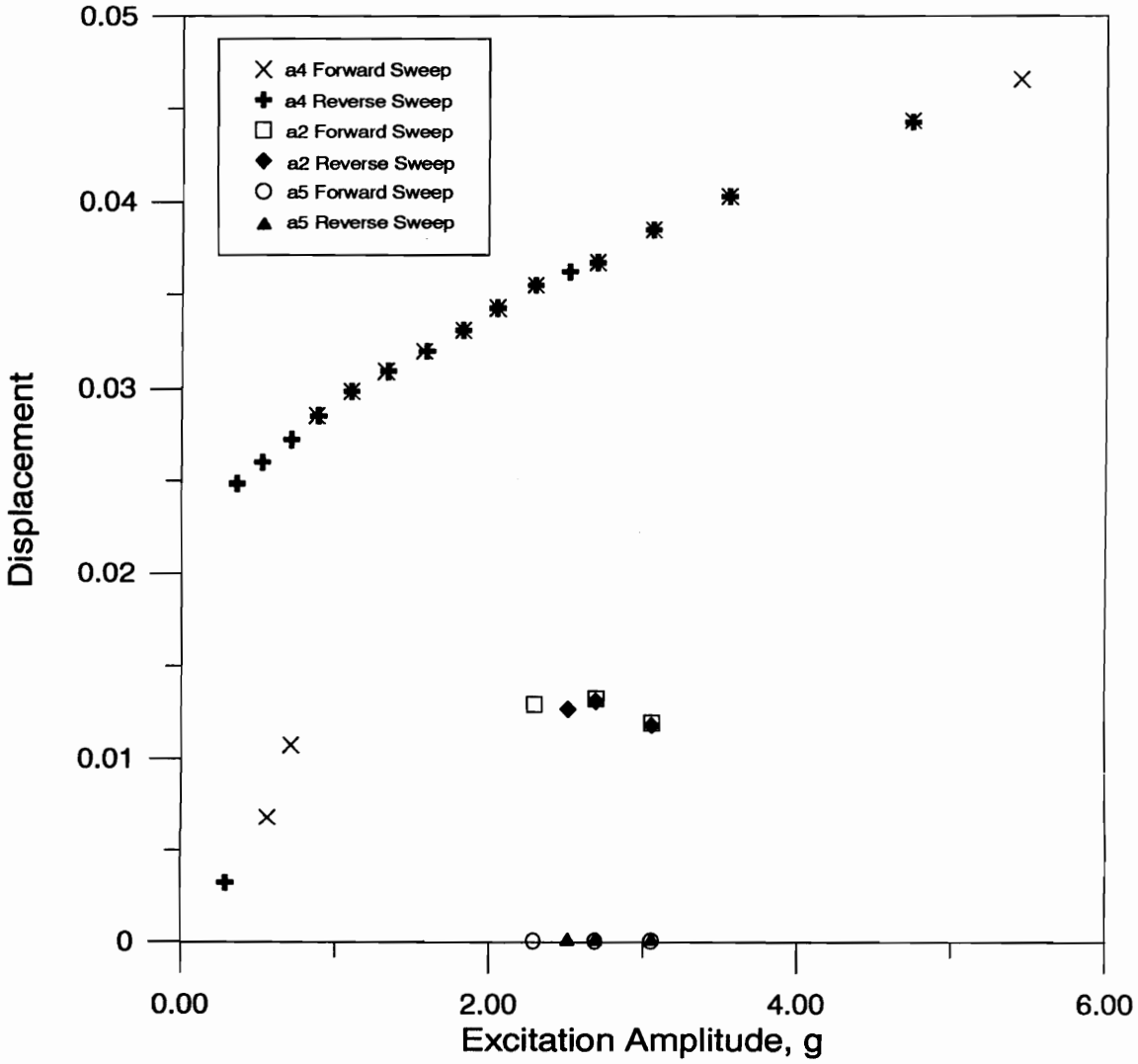

Figure 3.9 Amplitude-response curves for an excitation frequency of 32.00 Hz.

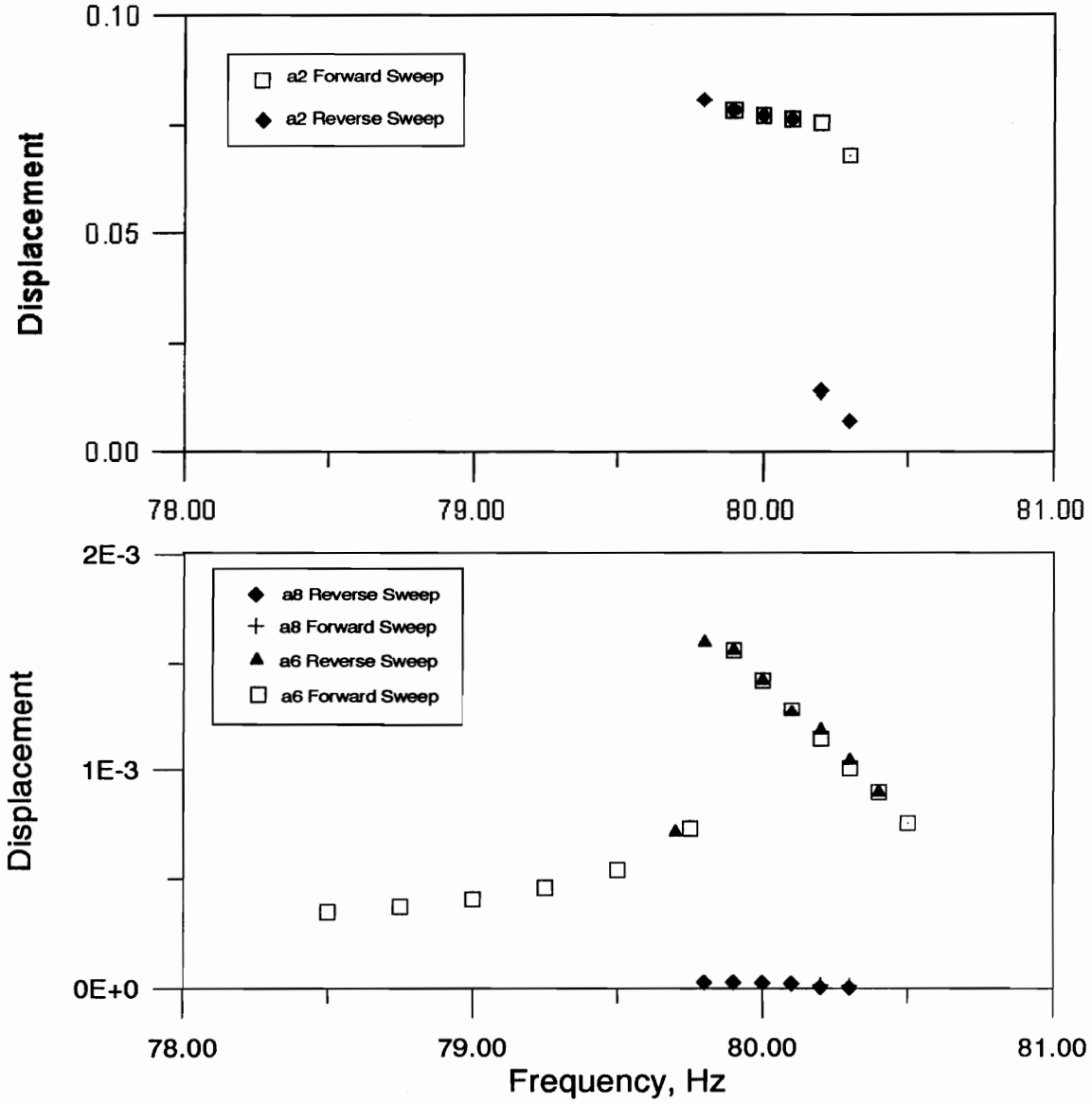

Figure 3.10 Frequency-response curves for an excitation amplitude of 0.9 *g*.

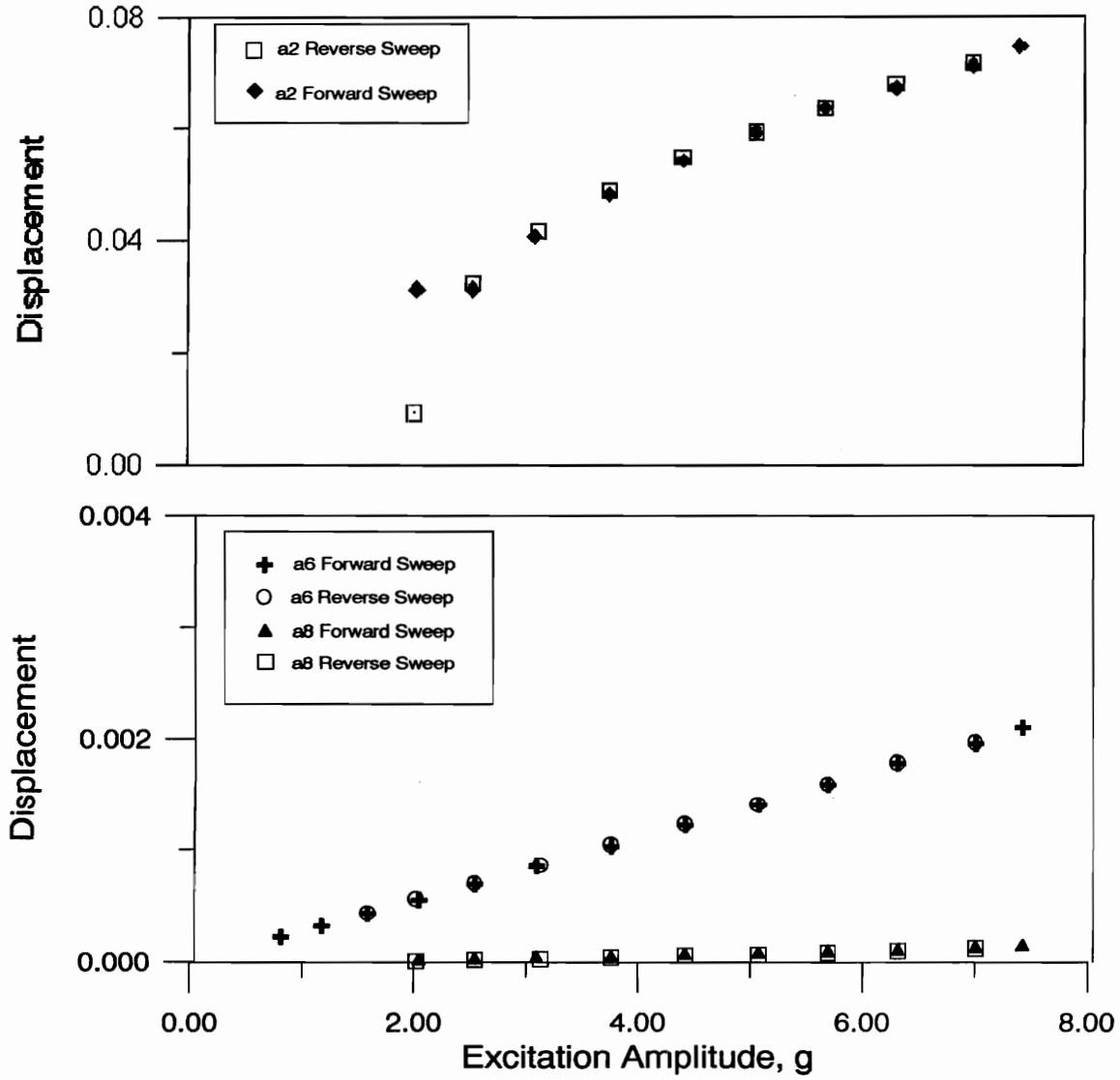

Figure 3.11 Amplitude-response curves for an excitation frequency of 78.5 Hz.

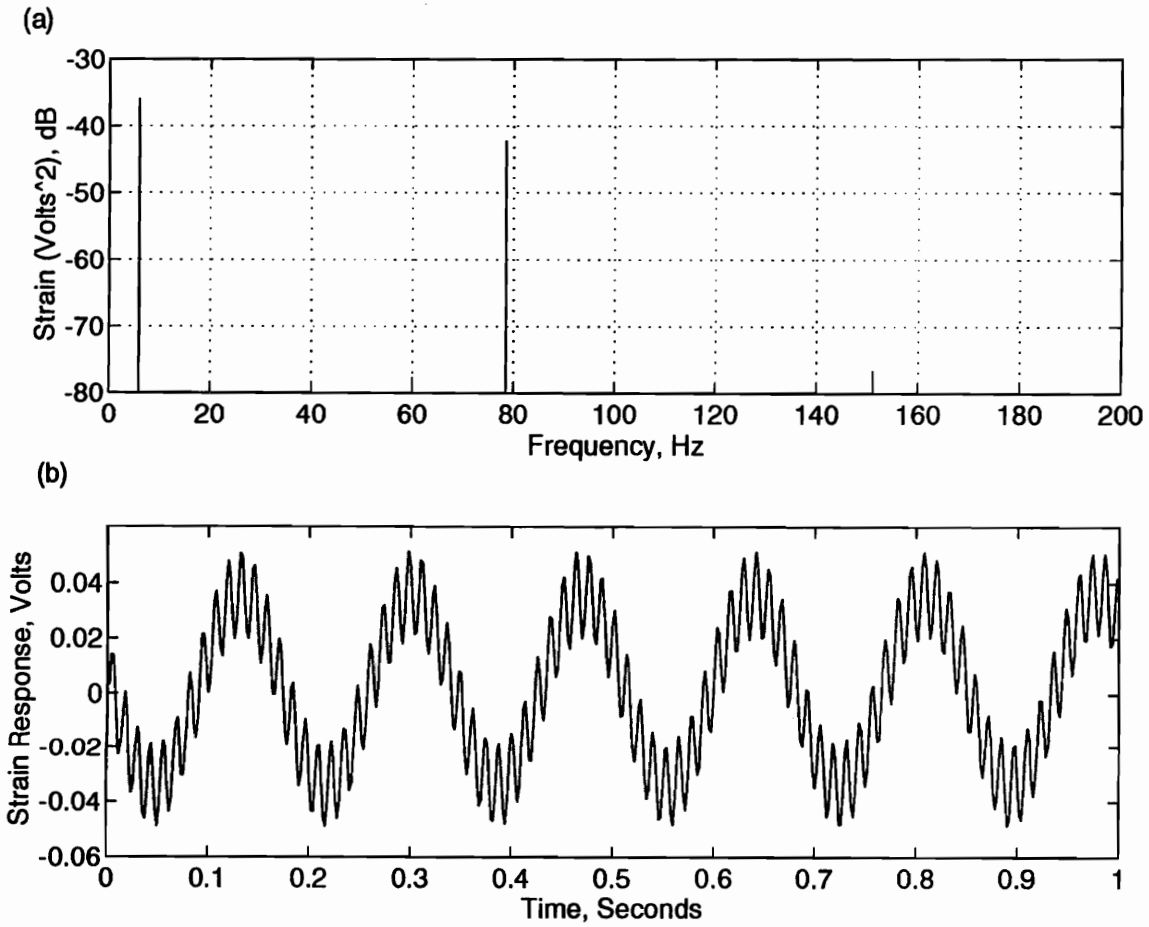

Figure 3.12 Motion at 78.5 Hz for an excitation amplitude of 0.9 g : (a) power spectrum (b) time series.

CHAPTER FOUR

Influence of Nonlinear Boundary Conditions on the Single-Mode Response of a Cantilever Beam

'Myself when young did eagerly frequent
Doctor and Saint, and heard great argument
About it and about: but evermore
Came out by the same door as in I came"
Rubaiyat of Omar Khayyam 1859 (translated by E. Fitzgerald)

In this final chapter on the nonlinear vibration of cantilever beams, we compare experimentally and theoretically obtained single-mode responses of cantilever beams. The analytical portion involves solving an integro-differential equation via the method of multiple scales. For the single-mode response, a large discrepancy is found between theory and experiment for an assumed ideal clamp model. Through some experimental detective work, it was found, and later shown through analysis, that the inclusion of a torsional spring at the supported end brought the theoretical and experimental results into excellent agreement. The torsional spring has both linear and nonlinear (cubic) stiffness components.

4.1 INTRODUCTION

In the study of structures, the modeling of boundary conditions, such as clamps, joints, and other connectors is difficult. In most analyses, the typical boundary conditions are free, sliding, clamped, and pinned. Of course, at times, these idealizations are bound to fall short and it then becomes necessary to raise the level of realism of the model. The most popular refinement of the classical boundary conditions is the substitution of rotational and translational springs to

account for boundary flexibility (Gorman, 1975). Furthermore, damping elements and mass elements are added features that can improve the ability of a model to approximate the physics of a structure.

4.2 EQUATION OF MOTION

To study the nonlinear response of a cantilever beam, we apply the equations developed by Crespo da Silva and Glynn (1978a). These equations are simplified to the case of planar motion of a metallic uniform cantilever beam to an external harmonic excitation. In addition, we add at this early point a term quadratic in velocity and account for torsional flexibility of the clamped end in anticipation of their future need. The integro-differential equation, under assumptions outlined in Crespo da Silva and Glynn (1978a), then becomes

$$m\frac{\partial^2\hat{v}}{\partial\hat{t}^2}+\hat{\mu}\frac{\partial\hat{v}}{\partial\hat{t}}+EI\frac{\partial^4\hat{v}}{\partial\hat{s}^4}=-EI\frac{\partial}{\partial\hat{s}}\left\{\frac{\partial\hat{v}}{\partial\hat{s}}\frac{\partial}{\partial\hat{s}}\left[\frac{\partial\hat{v}}{\partial\hat{s}}\frac{\partial^2\hat{v}}{\partial\hat{s}^2}\right]\right\}-\frac{\partial}{\partial\hat{s}}\left\{\frac{1}{2}\int_L^{\hat{s}}m\frac{\partial^2}{\partial\hat{t}^2}\left[\int_0^{\hat{s}}\left(\frac{\partial\hat{v}}{\partial\hat{s}}\right)^2 d\hat{s}\right]d\hat{s}\right\} + m\hat{a}_b\cos\left(\hat{\Omega}\hat{t}\right)-\hat{c}\left|\frac{\partial\hat{v}}{\partial\hat{t}}\right|\frac{\partial\hat{v}}{\partial\hat{t}}. \tag{4.1}$$

The variables are defined as follows: m is the mass per unit length, L is the beam length, E is Young's modulus, I is the area moment of inertia, $\hat{v}$ is the transverse displacement, $\hat{s}$ is the arclength, $\hat{t}$ is time, $\hat{a}_b$ is the acceleration of the supported end of the beam, $\hat{c}$ is the coefficient of quadratic damping, $\hat{\Omega}$ is the frequency of the support motion, and $\hat{\mu}$ is the linear viscous damping coefficient. Note that the displacement is a function of the arclength and time while all other variables are assumed to be constant.

The first two terms on the right-hand side of Eq. (4.1) are the *nonlinear* terms accounting for *curvature* and *inertia* effects. The third term is the harmonic external base excitation while the last term is the quadratic damping.

The boundary conditions for a beam with nonlinear support flexibility at one end are

$$\frac{\partial \hat{v}}{\partial \hat{s}}(0,\hat{t}) = 0,\ EI\frac{\partial^2 \hat{v}}{\partial \hat{s}^2}(0,\hat{t}) = \kappa_1 \frac{\partial \hat{v}}{\partial \hat{s}}(0,\hat{t}) + \kappa_3\left(\frac{\partial \hat{v}}{\partial \hat{s}}\right)^3,$$
$$\frac{\partial^2 \hat{v}}{\partial \hat{s}^2}(L,\hat{t}) = 0,\ \frac{\partial^3 \hat{v}}{\partial \hat{s}^3}(L,\hat{t}) = 0 \tag{4.2}$$

where κ_1 and κ_3 represent the linear and cubic rotational stiffness coefficients, respectively. The limiting cases for an elastically restrained support at one end are the clamped-free (infinite stiffness) and pinned-free (zero stiffness) boundary conditions.

The next step is to nondimensionalize the equation of motion and boundary conditions. Nondimensionalization allows for greater generality and simplicity in the analysis at the same time. We choose to nondimensionalize the variables according to the following scheme:

$$s = \frac{\hat{s}}{L},\ v = \frac{\hat{v}}{L},\ t = \hat{t}\sqrt{\frac{EI}{mL^4}},\ \tilde{\mu} = \hat{\mu}\frac{L^2}{\sqrt{mEI}},\ \tilde{c} = \hat{c}\frac{L}{m},\ \tilde{\Omega} = \hat{\Omega}\sqrt{\frac{mL^4}{EI}},\ \tilde{a}_b = \hat{a}_b\frac{mL^3}{EI}. \tag{4.3}$$

Using these variables, we rewrite Eq. (4.1) as

$$\ddot{v} + \tilde{\mu}\dot{v} + v'''' = -\left(v'\left(v'v''\right)'\right)' - \frac{1}{2}\left(v'\int_1^s\left(\int_0^s (v')^2\,ds\right)''ds\right)' + \tilde{a}_b\cos\left(\tilde{\Omega}t\right) - \tilde{c}|\dot{v}|\dot{v}. \tag{4.4}$$

We perform another scaling of the equation of motion and the boundary conditions. The purpose of this scaling is to reduce the numerical values of the nonlinear coefficients and help in the ordering of the terms for application of the perturbation method. The scaling factor z_n will be related to a linear natural frequency of the system. The relationship is set to be $\omega_n = z_n^2$ so that the natural frequency of interest will become unity. The two independent variables are scaled according to $s^* = z_n s$ and $t^* = z_n^2 t$. Using these scalings, we find that the equation of motion becomes

$$\ddot{v} + \frac{\tilde{\mu}}{z_n^2}\dot{v} + v'''' = \frac{\tilde{a}_b}{z_n^4}\cos\left(\frac{\tilde{\Omega}}{z_n^2}t\right) - \tilde{c}|\dot{v}|\dot{v} - z_n^2\left(v'\left(v'v''\right)'\right)' - \frac{z_n^2}{2}\left(v'\int_{z_n}^s\left(\int_0^s v'^2\,ds\right)''ds\right)' \tag{4.5}$$

where the prime and overdot denote spatial and time derivatives, respectively, and the asterisk superscript has been dropped. The boundary conditions become

$$v''(1,t)=0,\ \ v'''(1,t)=0,\ \ v(0,t)=0,\ \ v''(0,t)=\tilde{\alpha}_1 v'(0,t)+\tilde{\alpha}_3 v'(0,t)^3 \tag{4.6}$$

where

$$\tilde{\alpha}_1=\frac{\kappa_1 L}{EI} \quad \text{and} \quad \tilde{\alpha}_3=\frac{\kappa_3 L}{EI}.$$

4.3 PERTURBATION SOLUTION

As in most nonlinear continuous systems, Eq. (4.5) subject to (4.6) is not amenable to a closed-form solution. The ability to model the diverse dynamics embedded in such equations by analytical functions might not be feasible. At this point, a solution can be obtained via numerical methods for a very specific set of parameter values. With each change in the numerical value of a parameter, the equations subject to the boundary conditions must be integrated anew. To develop any sort of parameter sensitivity or bifurcation analysis would be computationally unwieldy. However, perturbation methods offer an alternate approach that can provide qualitative insight in addition to reliable quantitative results in a relatively simple fashion.

4.3.1 METHOD OF MULTIPLE SCALES

As the name implies, the method of multiple scales takes advantage of the scaling that appears to be inherent in nature. This scaling can take many forms, but for problems of our interest time is the focus. This method takes advantage of the time scaling involved in the occurrence of nonlinear phenomena in systems. In a very simplified explanation, the example of our solar system makes this concept clearer. For us, the stability of our earthly orbit and that of the other planets in our solar system is of primary concern. Dynamicists have developed nonlinear equations that attempt to model the motions of these cosmic bodies. In applying a perturbation method, such as the multiple scales method, one can determine the motion and

stability of the planetary orbits for various time scales. That is, the perturbation solution may indicate for the next 100 million years the planets in the solar system will not collide with any other planet. However, the analysis may be carried out further in time by including and determining the dependence of the solution on more time scales. Such an analysis may show that, for a million million trillion years from now, the orbits of several planets, including our earth, will overlap and the chance of a collision is enhanced or that the earth may even leave the solar system and stray in an entirely new orbit. This means that the viability of a solution at each order depends upon the relevant time scale of the phenomenon being examined.

To apply the method of multiple scales requires that the equation of motion be in a suitable form. The nondimensionalizations carried out in the earlier part of this chapter were part of this process. One final scaling is necessary. This involves defining the remaining parameters in terms of a parameter ε. This parameter will provide a convenient expansion parameter and determine the ordering of the various terms in the equation.

Defining

$$\frac{\tilde{\mu}}{z_n^2} = \varepsilon^2\mu, \quad \frac{\tilde{a}_b}{z_n^4} = \varepsilon^3 a_b, \quad \frac{\tilde{\Omega}}{z_n^2} = \Omega, \quad \tilde{c} = \varepsilon c$$

leads to

$$\ddot{v} + \varepsilon^2\mu\dot{v} + v^{iv} = \varepsilon^3 a_b \cos(\Omega t) - \varepsilon c\dot{v}|\dot{v}| - z_n^2\left[v'\left(v'v''\right)'\right]' - \frac{1}{2}z_n^2\left[v'\int_{z_n}^{s}\left(\int_0^s v'^2 ds\right)^{\cdot\cdot} ds\right]' \tag{4.7a}$$

subject to

$$v(0,t) = 0, \quad v''(z_n,t) = 0, \quad v'''(z_n,t) = 0, \quad v''(0,t) = \alpha_1 v'(0,t) + \alpha_3 v'(0,t)^3 \tag{4.7b}$$

where

$$\alpha_1 = \frac{\kappa_1 L}{EIz_n} \quad \text{and} \quad \alpha_3 = \frac{\kappa_3 L z_n}{EI} \; . \tag{4.8}$$

Now the foundation of the method of multiple scales is that time t can be broken down into a succession of independent time scales given by the relationship $T_n = \varepsilon^n t$ (Nayfeh. 1981). The parameter ε can also serve as an expansion parameter for the dependent variable. The form of the expansion is

$$v(s,T_0,T_1,\ldots;\varepsilon) = \varepsilon v_1(s,T_0,T_1,\ldots;\varepsilon) + \varepsilon^2 v_2(s,T_0,T_1,\ldots;\varepsilon) + \varepsilon^3 v_3(s,T_0,T_1,\ldots;\varepsilon) + \ \ldots \tag{4.9}$$

and the time derivatives become

$$\frac{\partial}{\partial t} = \frac{\partial}{\partial T_0} + \varepsilon\frac{\partial}{\partial T_1} + \varepsilon^2\frac{\partial}{\partial^2 T_2} + \ \ldots \ = D_0 + \varepsilon D_1 + \varepsilon^2 D_2 + \ \ldots \tag{4.10a}$$

and

$$\frac{\partial^2}{\partial t^2} = D_0^2 + 2\varepsilon D_0 D_1 + \varepsilon^2 D_1^2 + 2\varepsilon^2 D_0 D_2 + \ \ldots \ . \tag{4.10b}$$

The procedure is to substitute Eqs. (4.9) and (4.10) into Eqs. (4.7). Then the coefficient of each power of ε is set equal to zero. The result is a hierarchy of linear equations and associated boundary conditions. Restricting our analyses to the first three orders, we have the following:

Order ε:

$$D_0^2 v_1 + v_1^{iv} = 0$$

$$v_1(0,t) = 0,\ v_1''(z_n,t) = 0,\ v_1''(0,t) = \alpha_1 v_1'(0,t) \tag{4.11}$$

Order ε^2:

$$D_0^2 v_2 + v_2^{iv} = -2D_0 D_1 v_1$$

$$v_2(0,t) = 0,\ v_2''(z_n,t) = 0,\ v_2'''(z_n,t) = 0,\ v_2''(0,t) = \alpha_1 v_2'(0,t) \tag{4.12}$$

Order ε^3:

$$D_0^2 v_3 + v_3^{iv} = -2D_0 D_1 v_2 - 2D_0 D_1 v_1 - \mu D_0 v_1 - D_1^2 v_1 - z_n^2 \left(v' \left(v' v'' \right)' \right)' - \frac{z_n^2}{2} \left[v' \int_{z_n}^{s} \int_{0}^{s} \left(v'^2 ds \right)^{\cdot\cdot} ds \right]' + a_b \cos(\Omega t)$$

$$v_3(0,t) = 0, \quad v_3''(z_n,t) = 0, \quad v_3'''(z_n,t) = 0, \quad v_3''(0,t) = \alpha_1 v_3'(0,t) + \alpha_3 v_3'(0,t)^3 . \tag{4.13}$$

Beginning with the first-order equation and boundary conditions, Eqs. (4.11), we seek a solution. This solution then allows consideration of the next order equation, and so on. The first-order equation is the linear problem and this what we turn to next.

4.3.2 FIRST-ORDER EQUATION

The first-order equation and boundary conditions, Eqs. (4.11), is a linear problem whose solution is assumed in the following separable form:

$$v_1(s, T_0, \ldots : \varepsilon) = \sum_{m=1}^{\infty} \left[\varphi_m(s) A_m(T_1, \ldots) e^{i\omega_m T_0} + cc \right] \tag{4.14a}$$

where cc is the complex conjugate of the preceding term, $\omega_m = \frac{z_m^2}{z_n^2}$, and $\varphi_m(s)$ is the linear mode shape. The linear mode shape for a free-elastically restrained beam (Chun, 1972) can be expressed as

$$\varphi_m(s) = -\alpha_1 \gamma \left(\cos(s) - \cosh(s) \right) + \gamma \left(\sin(s) + \sinh(s) \right) + \left(\sin(s) - \sinh(s) \right) \tag{4.14b}$$

where

$$\alpha_1 = \frac{\sin(z_n)\cosh(z_n) - \cos(z_n)\sinh(z_n)}{1 + \cosh(z_n)\cos(z_n)} , \tag{4.14c}$$

$$\gamma = \frac{1+p}{1-p}, \text{ and}$$

$$p = \frac{\cosh(z_n)\cos(z_n) - \sinh(z_n)\sin(z_n) + 1}{\cos(z_n)\cosh(z_n) + \sinh(z_n)\sin(z_n) + 1} .$$

The orthogonality condition for the linear mode shapes is

$$\int_0^{z_n} \varphi_m(s)\,\varphi_n(s)\,ds = \delta_{mn}\,z_n$$

where δ_{mn} is the Dirac delta function.

Since we are considering a single-mode response, only a one-term expansion of Eq. (4.14a) will be considered, specifically, that consisting of the directly excited fourth mode ($m = 4$); that is,

$$v_1 = A_4\varphi_4(s)e^{iT_o} + cc \qquad (4.14d)$$

This is an assumption that the other modes of the beam do not significantly affect the motion of the beam and that only the directly excited mode determines the type of motion being observed (Nayfeh and Mook, 1979).

4.3.3 SOLVABILITY CONDITIONS

Moving onto the second-order problem, we substitute Eq (4.14a) into Eq. (4.12) and obtain

$$D_0^2 v_2 + v_2^{iv} = -2D_1A_4i\varphi_4e^{iT_0}$$

where $\omega_4 = 1$. The solution at each order must insure uniformity of the expansion Eq. (4.9). This is known as the *solvability condition* and will be presented in more detail for the third-order problem. For now we state that the solvability condition together with the orthogonality condition leads to $D_1A_4 = 0$ which implies that the coefficient A_4 is not a function of T_1. It can be determined by imposing the solvability condition for the third-order problem. So v_2 is trivial.

At this point, it is prudent to introduce a detuning parameter σ that is a measure of the nearness of the forcing frequency to the frequency of the fourth mode. It is defined according to the relation : $\Omega = \omega_4 + \varepsilon^2\sigma$.

For the solution of the third-order problem, Eq. (4.13), we assume that

$$v_3 = V_3(s,T_2,\ldots)\,e^{iT_0} + cc\ . \qquad (4.15)$$

We substitute Eqs. (4.15) and (4.14d) into Eq. (4.13), recall that $v_2 = 0$, and arrive at

$$
\begin{aligned}
&-V_3 + V_3^{iv} = \mathrm{H} \\
&V_3(0,T_2) = 0,\ \ V_3''(z_4,T_2) = 0,\ \ V_3'''(z_4,T_2) = 0,\ \ V_3''(0,T_2) = \alpha_1 V_3'(0,T_2) + 3\alpha_3 \varphi_4'^3 A_4^2 \bar{A}_4
\end{aligned}
\tag{4.16}
$$

where

$$
\mathrm{H} = -\mu i \varphi_4 A_4 - 2i\varphi_4 D_2 A_4 - 3z_4^2 \left[\varphi_4' \left(\varphi_4' \varphi_4'' \right)' \right]' A_4^2 \bar{A}_4 + 2z_n^2 \left(\varphi_4' \int_{z_n}^{s} \int_{0}^{s} \varphi_4'^2 ds ds \right)' A_4^2 \bar{A}_4
$$

$$
+ a_b \cos(\Omega t) e^{-iT_0} .
$$

The solvability condition insures uniformity of the expansion of the dependent variable; it is found by using the concept of adjoint. To begin, the first of Eqs. (4.16) is multiplied by the adjoint Ψ and integrated as follows:

$$
\int_0^{z_n} \Psi(-V_3 + V_3^{iv}) ds = \int_0^{z_n} \Psi \mathrm{H} ds . \tag{4.17}
$$

To determine the adjoint problem, we follow the procedure outlined in Nayfeh (1981) and find that the third-order problem is self-adjoint; that is, $\Psi = \varphi_4$. Consequently, the solvability condition becomes

$$
\int_0^{z_4} \varphi_4 \mathrm{H} ds - 3\alpha_3 \varphi_4'^4(0) A_4^2 \bar{A}_4 = 0 . \tag{4.18}
$$

Integrating Eq. (4.18) and applying the polar transformation $A_4 = \frac{1}{2} a_4 e^{i\beta 4}$, we obtain the following *modulation equations* governing the amplitude and phase of the fourth mode:

$$
\begin{aligned}
&a_4' = -\frac{1}{2}\mu a_4 + \frac{a_b}{z_4} \sin\vartheta - \breve{c} a_4^2 \\
&a_4 \vartheta' = a_4 \sigma + \frac{1}{8}\delta_1 a_4^3 + \frac{a_b}{z_4} \cos\vartheta
\end{aligned}
\tag{4.19}
$$

where $\vartheta = \sigma T_2 - \beta_4$ and δ_1 denotes the effective nonlinear coefficient (excluding damping) in the solvability condition, Eq. (4.18). It is given by

$$\delta_1 = \int_0^{z_4} \left[-3z_4^2 \left(\varphi_4' \left(\varphi_4' \varphi_4'' \right)' \right)' + 2z_4^2 \left(\varphi_4' \int_{z_4}^{s} \int_0^{s} \varphi_4'^2 ds ds \right)' \right] \varphi_4 ds - 3\alpha_3 \varphi_4'^4(0), \tag{4.20}$$

To study the solutions of Eqs. (4.19), we begin with the constant solutions (fixed points), which correspond to periodic motions of the beam. To this end, we set the time variation of the amplitude and phase in Eqs. (4.19) equal to zero. The stability of the fixed points can be found by investigating the eigenvalues of the Jacobian of Eqs. (4.19). It follows from Eq. (4.20) that if we neglect the contribution of the nonlinear torsional spring and consider only a clamped-free beam, the sign of the nonlinear coefficient is determined by the relative contributions of the nonlinear curvature and inertia terms. For the first mode, the nonlinear curvature term dominates and the frequency-response curve will display a hardening-type behavior. For higher modes, the nonlinear inertia term is larger than the nonlinear curvature term and, therefore, the frequency-response curve displays a softening-type behavior. Inclusion of the nonlinear (cubic) elastic element at the boundary allows for the further hardening (or softening) of the frequency-response curve, depending on whether the nonlinear stiffness coefficient is negative (or positive).

Solving for the fixed points, we set the right-hand side of Eqs. (4.19) equal to zero. Using some algebraic manipulations, we reduce the two equations to one single equation known as the *frequency-response equation* written as

$$\left[\left(\frac{1}{2}\mu + \hat{c}a_4 \right)^2 + \left(\sigma + \frac{1}{8}\delta_1 a_4^2 \right)^2 \right] a_4^2 = \frac{a_b^2}{z_4^2} \ . \tag{4.21}$$

For most of our experiments, the detuning parameter and the forcing amplitude comprise the control parameters. Fixing one control parameter while varying the other provides a set of plots that detail the pattern of behavior of the fixed points (i.e., periodic motions of the beam). In the following sections, we compare theoretical and experimental results for such plots for a response consisting of the fourth mode of the beam.

4.4 CLAMPED-FREE BOUNDARY CONDITIONS

In this section, we attempt to match the experimental results with the above theoretical analysis. The experimental results are of the fourth-mode responses of the horizontal beam presented in Chapter 3. The properties of this beam are noted in Chapter 2. The theoretical results involve the assumption of a perfectly clamped end. The comparison may reveal deficiencies in the model and/or experiment.

For the experimental results, we consider the fourth-mode response ($z_4 \approx 10.996$) of the horizontal cantilever beam, specifically, the frequency-response curves for an excitation amplitude of 0.7 g and the amplitude-response curves for an excitation frequency of 32.00 Hz. Assuming clamped-free conditions in the analysis, we find that $\delta_1 \approx 7557 (\approx 7952 - 395)$, which combines the contributions from the inertia nonlinearity (-395) and the curvature nonlinearity (7952). From the half-power point, we find that the damping ratio $\hat{\xi} = 0.001$. Figure 4.1 shows a comparison between the theoretically, Eq. (4.21), and experimentally obtained frequency-responses curves. Two discrepancies were found. The first, not shown, is that the frequency-response curve with only a linear viscous damping term exhibited a jump down frequency very far from the experimental jump down frequency. The inclusion of quadratic damping allowed for a curve fitting process whereby the jump down frequency for the theoretical results was forced to match that of the experimental results by choosing an appropriate quadratic damping coefficient. The addition of the quadratic damping for a blunt body is physically reasonable as the large deflections observed during the experiment most probably gave rise to significant air damping, which is proportional to the square of the velocity. The second obvious discrepancy is the difference in the slopes of the theoretically and experimentally obtained frequency-response curves. The experimentally obtained frequency-response curve is softer than the theoretically

obtained frequency-response curve. This implies that the nonlinear coefficient δ_1 requires modification. Possible sources of this revision are discussed in the next section.

4.5 ERROR ANALYSIS

The difference in the slopes of the experimentally and theoretically obtained frequency-response curves may have several sources. Each source may affect either the experimental or theoretical results. We note that, in a comparison between experimental and theoretical results, sometimes it is taken for granted that the experimental results are the correct ones and that one should strive to match theory to experiment. However, it may happen that the experimental results will need to be adjusted. Errors in measurement, transducer placement, and faulty calibration curves are just a few of the possible sources of error in experimental measurements (Wilson, 1996; Dally, Riley, and McConnell, 1993). We hypothesize three possible sources that may be responsible for the discrepancy, namely,

(1) Nonlinear strain gage calibration curve,

(2) Midplane stretching, and

(3) Nonlinear stiffness at the clamped boundary.

The nonlinear strain gage calibration curve may be due to unusually large strains induced by vibrations of the beam. This would most likely harden the experimental data points, thereby bringing them closer to the theoretical results. From the literature and manufacturer information, this source was found to be an unlikely culprit. Attempts to obtain a dynamic calibration curve for the fourth mode by placing an accelerometer on the beam to provide displacement related measurements in conjunction with strain measurements proved inconclusive. Also such measurement may include the effect of the second possible error source. midplane stretching. The theoretical development is based on the assumption of inextensionality of the midplane of the beam. This is found to be very adequate for beams with one end unrestrained. However, it

is an assumption and possibly, under very large deflections and curvatures, the midplane stretching effect may become important. This effect was much harder to measure and, once again, a search through the literature on this topic made the likelihood of midplane stretching very small. The inclusion of midplane stretching would have hardened the theoretical results.

Finally, consideration of a nonideal clamping boundary lead us to perform an exploratory experiment whereby two small accelerometers were placed on the clamping fixture. One was centered while the other was placed close to the edge of the clamp, on the side where the beam was extending out. As forcing frequency and amplitude sweeps were performed, we observed a significant relative change in acceleration levels between the two transducers. At low levels, the accelerations matched quite well, while during large-amplitude motions the accelerometer closer to the edge displayed larger values than those displayed by the center accelerometer. Note that all motions were restricted to unimodal responses consisting of the fourth mode. A comparison of the readings of the center and edge accelerometers revealed a hardening-type behavior. Therefore, the inclusion of a hardening-type spring at the clamped end would appear to be the most viable explanation of the difference between the experimentally and theoretically obtained frequency-response curves. As a qualifying insight, the difference in acceleration levels may be due to flexure of the metallic clamping fixture and/or rotation of the shaker armature to which the clamping fixture is attached. From our experience in the laboratory, the latter is the more likely source. However, from a modeling point of view, the mathematical formulation is the same for both. So in the next section, we refine our analysis to include boundary flexibility and reexamine the results vis a vis the experimental data.

4.6 NONIDEAL CLAMPS

Next we consider the case of a torsional spring with linear and cubic stiffness terms in the theoretical analysis. By incorporating the boundary flexibility, we have introduced two additional

unknowns into our analysis, the linear and cubic stiffness coefficients. The linear stiffness coefficient can be found by taking the first experimentally obtained linear natural frequency and substituting it into Eq. (4.14c). Then we deduce the value of the cubic stiffness term by curve fitting the theoretically obtained frequency-response curve for one excitation amplitude. Again, we use the experimental jump down frequency to ascertain the value of the quadratic damping coefficient. Once these parameters are determined, we check whether the remaining theoretically obtained frequency- and amplitude-response curves match the experimentally obtained curves. Reasonable agreement will thereby lend credibility to the assertion that the previously observed discrepancy is attributable to a nonideal clamping boundary.

First, we need to estimate the linear stiffness coefficient. The value for α_1 is found by improving the agreement between the theoretically and experimentally obtained linear natural frequencies. We find that a change in the value of the linear stiffness term only affects the second decimal of z_4 (Blevins, 1979). As such, we chose $z_4 \approx 10.977$ as a value that best fit the first four natural frequencies of our beam. This choice gives $\alpha_1 z_n \approx 581$. Next we consider the frequency-response curve for an excitation amplitude of 0.7 g. Performing the curve fitting, we find that we can match the theoretically and experimentally obtained frequency-response curves as shown in Figure 4.2. We find the value for the quadratic damping coefficient, $\hat{c} \approx 0.33$, from curve fitting the jump down frequency of the theoretical model to the experimentally obtained jump down frequency and $\delta_1 \approx 4560$ from curve fitting the backbone curve of the experimentally obtained frequency-response curve and using this value for the theoretical model. Using these values and Eqs. (4.20) and (4.8), we can then estimate that $\alpha_3 \approx 10^7$. From the half-power point method, we find $\mu \approx 0.0003$. Using these values, we obtain an equally excellent match between the experimentally and theoretically obtained frequency-response curves for an excitation amplitude of 0.9 g as shown in Figure 4.3. As an additional boost of confidence, we compare the theoretically and experimentally obtained amplitude-response curves

in Figure 4.4 for an excitation frequency of 32 Hz. Again a fairly good match is realized. A final fine tuning was performed where the forcing amplitude was adjusted. It was found that a 10% reduction in the forcing amplitudes improved the agreement. The physical explanation for this apparent energy loss is that the measured input signal is from the accelerometer placed on the clamping fixture. This signal is then transformed into the frequency domain by the dynamic signal analyzer. The magnitude of the peak in the spectrum at the forcing frequency is then assumed to be the total forcing amplitude. However, some structural feedback to the shaker occurs at the same frequency which would result in an observed increase in the magnitude of the forcing. The contributions from these different sources can not be separated in the frequency domain. Therefore, the actual force imparted to the beam by the shaker is lower.

Since the choice of the expansion parameter affects the coefficients of the terms in the expansion, a final step is required. The forcing frequency, forcing amplitude, and linear viscous damping were the experimentally obtained parameters that were fed into the theoretical model by scaling the values according to the transformations outlined in Sections 4.2 and 4.3.1. However, the scalings and perturbation solution require a numerical value for one last parameter, the perturbation parameter ε. For this case, we chose $\varepsilon \approx 0.01$. To complete the perturbation analysis, we need to evaluate the smallness of our perturbation terms based on our particular choice of the perturbation parameter. We use the chosen value of the perturbation parameter to check that the ratio $\frac{\kappa_3}{\kappa_1}\varepsilon^2 << 1$ is satisfied to insure the validity of our perturbation expansion. Using the estimated values for the boundary stiffness coefficients, we find that $\frac{\kappa_3}{\kappa_1}\varepsilon^2 \approx \frac{\alpha_3}{\alpha_1 z_n^2} \approx 0.01$. An alternate procedure would involve comparing the multiple scales solution with a solution obtained by integrating the original differential equation.

4.7 CHAPTER REMARKS

The unimodal dynamics of a cantilever beam subject to a harmonic external excitation was examined both experimentally and theoretically for the fourth mode. The experimentally obtained frequency-response curves exhibit a hardening-type nonlinearity. However, in a comparison with a theoretical analysis for an ideal clamp, we found a large discrepancy. This discrepancy was found to be due to two sources: air damping and boundary flexibility. The former was modeled by adding a quadratic damping term while the latter was modeled by replacing the clamped end by a torsional spring. This rotational elastic element possesses linear and cubic stiffness components. The addition of these two elements to our model was found to improve dramatically the agreement between the experimentally and theoretically obtained frequency- and amplitude-response curves.

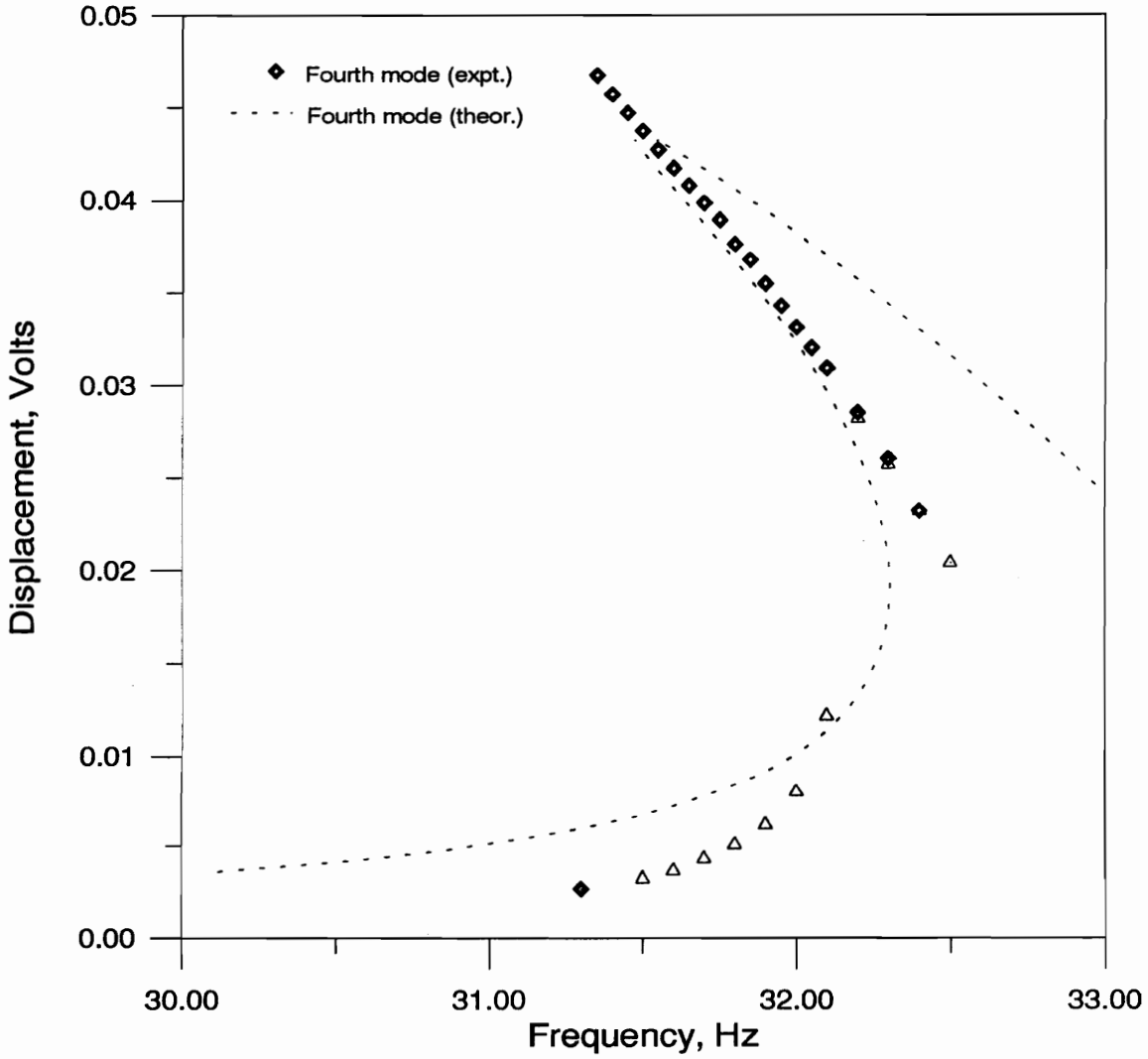

Figure 4.1 Experimentally and theoretically (clamped-free ends) obtained frequency-response curves for an excitation amplitude of 0.7 g.

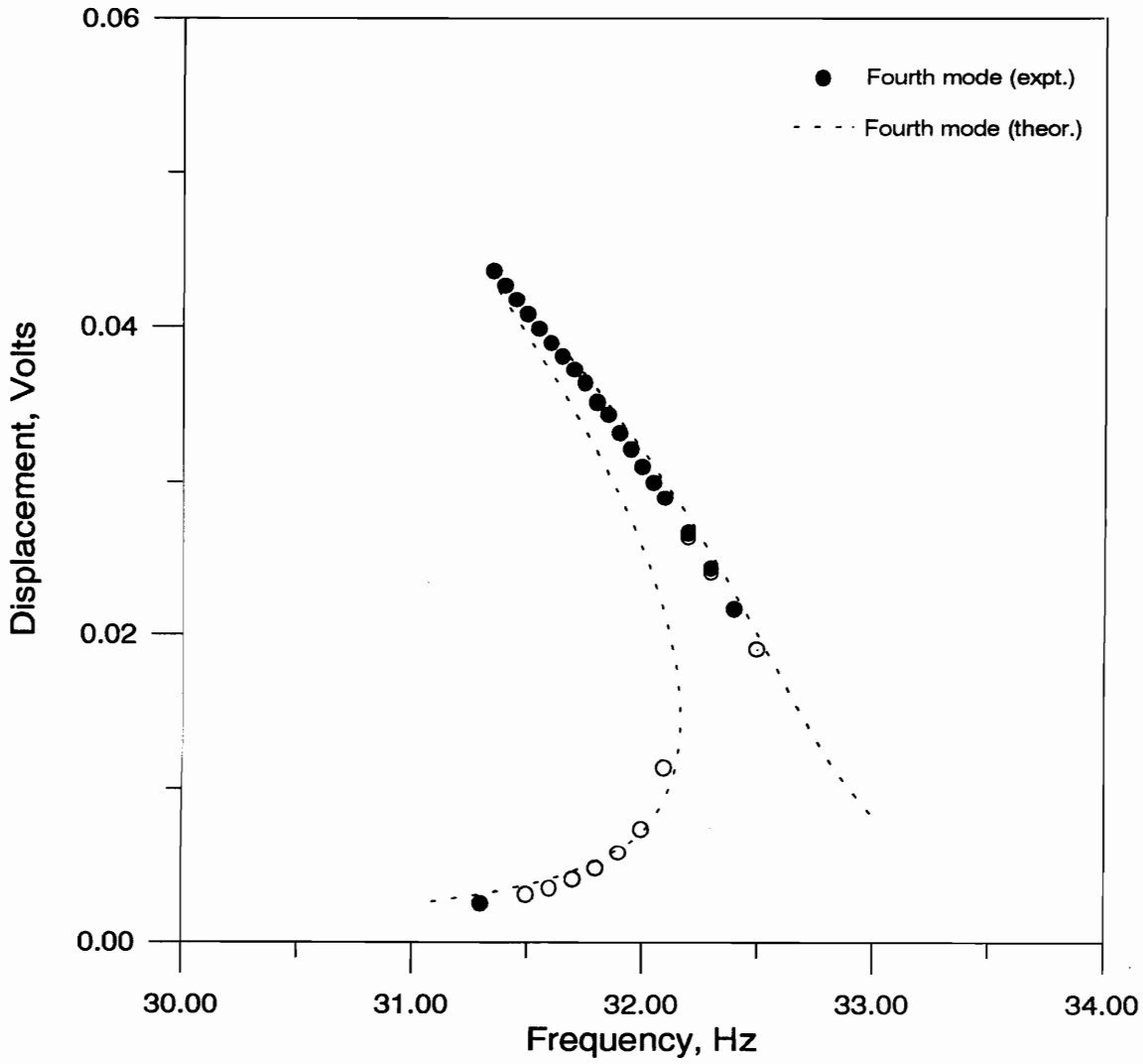

Figure 4.2 Experimentally and theoretically (spring-hinged-free end) obtained frequency-response curves for an excitation amplitude of 0.7 *g*.

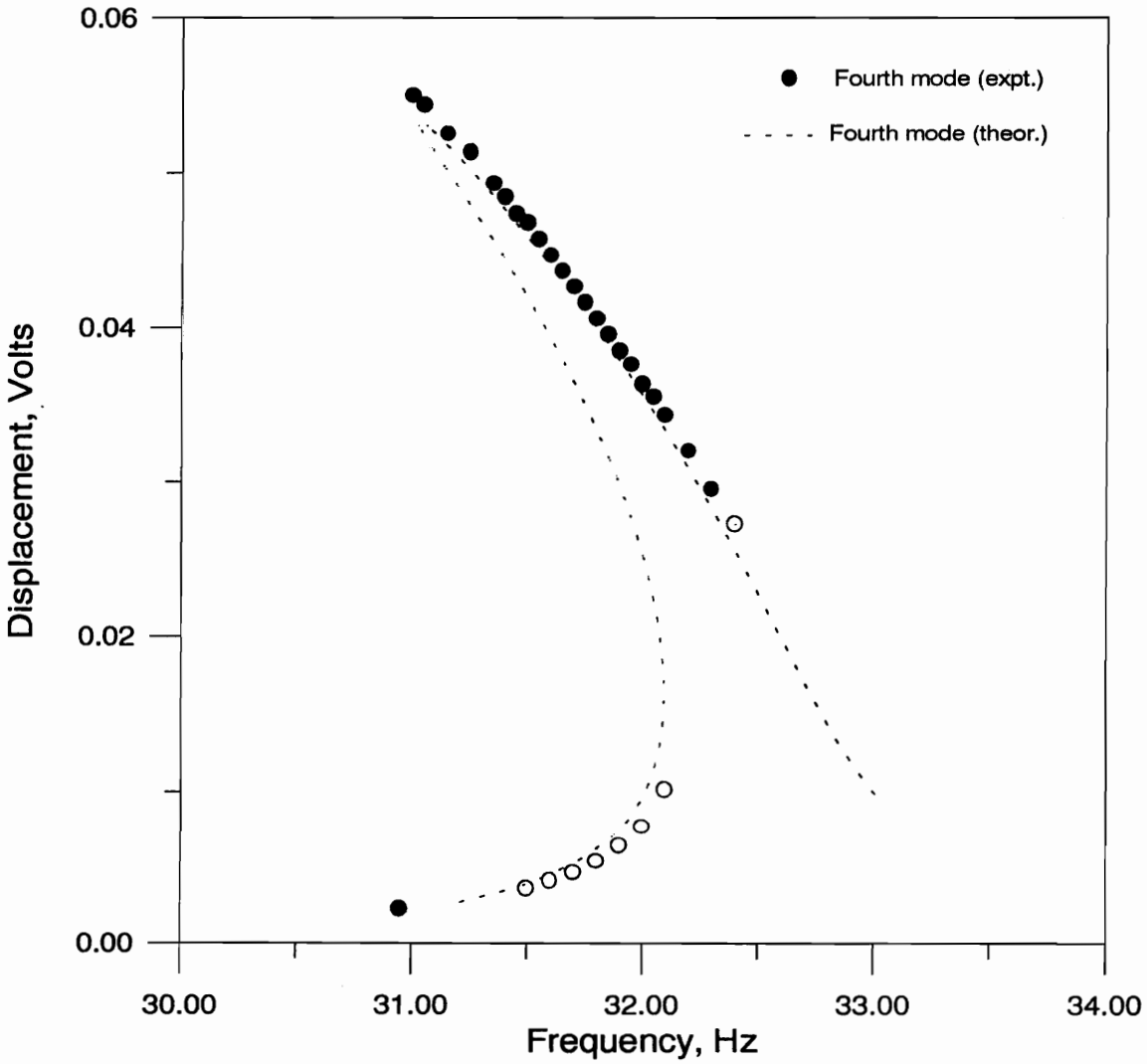

Figure 4.3 Experimentally and theoretically (spring-hinged-free ends) obtained frequency-response curves for an excitation amplitude of 0.9 *g*.

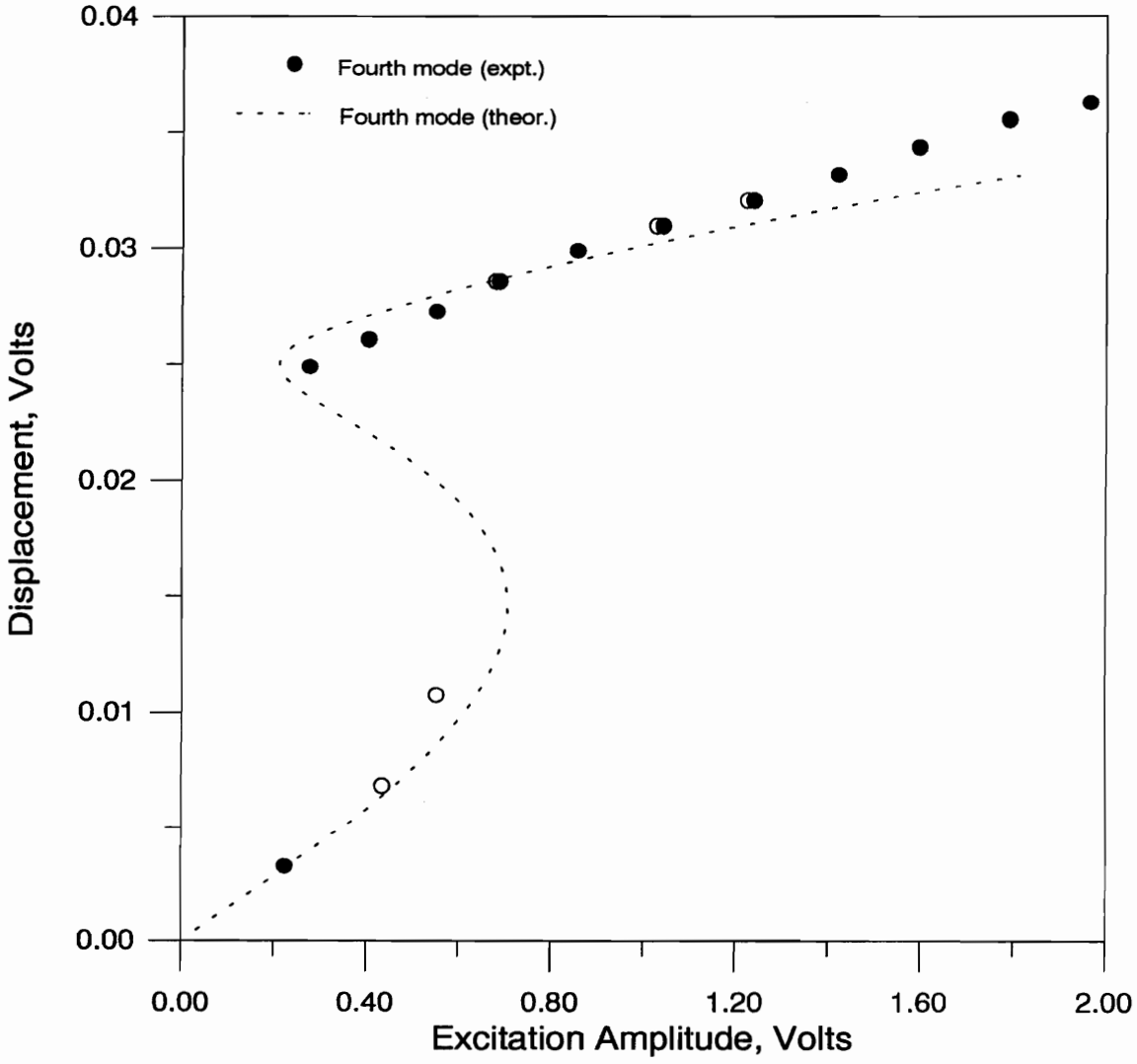

Figure 4.4 Experimentally and theoretically (spring-hinged-free ends) obtained amplitude-response curves for an excitation frequency of 32.00 Hz.

CHAPTER FIVE

Theoretical Modeling of a Portal Frame

'Ignorance of the cause of variation does not make such variation random' A. Freudenthal

The present chapter presents a theoretical model of a portal frame. The dominant nonlinearity for the portal frame is quadratic. A linear model of the portal frame is also shown. An accurate linear model is essential for the determination of the linear natural frequencies and mode shapes. However, instead, a finite element analysis is performed to obtain the linear natural frequencies and mode shapes. A methodology for estimating the experimentally obtained natural frequencies is discussed. A comparison between the experimentally and theoretically obtained linear natural frequencies exhibits a discrepancy that points to the need to include the effect of gravity, as discussed in Chapter 2.

5.1 INTRODUCTION

The study of the portal frame provides a contrast to that of the cantilever beam presented in the previous chapters. The dominant nonlinearity of the frame is quadratic whereas that of the cantilever beam is cubic. The importance of this mathematical distinction is that the order of the nonlinearity determines the type of modal interactions that can be observed in a system.

5.2 THEORETICAL MODELING

A schematic of the frame is shown in Figure 5.1. It consists of two vertical beams, one horizontal crossbar, two corner masses, and a single middle mass.

5.2.1 NONLINEAR MODELING

In this section, we outline the components of the energy terms necessary for modeling the nonlinear vibrations of the portal frame.

The derivation is based on the division of the portal frame into four separate sections. Each section is then modeled as an Euler-Bernoulli beam. The analysis includes the rotary inertia of the rigid masses while those of the beams are neglected. However, the finiteness of the rigid masses is not taken into account. A Lagrangian description based on the undeformed arclength x_j, as a convenient measure of distance along each beam section j of the portal frame, is used. The axial and transverse displacements of each beam section are denoted by $u_j(s_j,t)$ and $v_j(s_j,t)$. The rigid body rotation is represented by $\psi_j(s_j,t)$ where

$\sin\psi_j = \partial v_j/\partial s_j$.

Finally, we assume that the midsurface of each beam section is inextensional: that is,

$$\left[1+\partial u_i/\partial s_i\right]^2+\left[\partial v_j/\partial s\right]^2=1.$$

Next, we derive the kinetic energy T and potential energy V of the portal structure. The energy terms are the basis for the development of the equations of motion by using the concept of a *time-averaged Lagrangian* (Nayfeh, 1973). The kinetic energy is given by

$$\begin{aligned}T=&\tfrac{1}{2}\int_0^{L_1}\rho_1\left[\dot v_1^2+\left(\dot u_1+\dot X\right)^2\right]dx_1+\tfrac{1}{2}m_1\left[\left(\dot X+\dot u_1(L_1)\right)^2+\dot v_1^2(L_1)\right]+\tfrac{1}{2}\int_0^{L_2}\rho_2\left[\dot v_2^2+\left(\dot u_2+\dot X\right)^2\right]dx_2\\&+\tfrac{1}{2}m_2\left[\left(\dot X+\dot u_2(L_2)\right)^2+\dot v_2^2(L_2)\right]+\tfrac{1}{2}J_2\dot\psi_2^2+\tfrac{1}{2}\int_0^{L_3}\rho_3\left[\left(\dot X+\dot u_1(L_1)-\dot v_3\right)^2+\left(\dot v_1(L_1)\right)^2\right]dx_3+\tfrac{1}{2}J_3\dot\psi_3^2\\&+\tfrac{1}{2}\int_0^{L_4}\rho_4\left[\left(\dot X+\dot u_2(L_2)-\dot v_4\right)^2+\left(\dot v_2(L_2)\right)^2\right]dx_4+\tfrac{1}{2}m_3\left[\left(\dot X+\dot u_1(L_1)-\dot v_3(L_3)\right)^2+\left(\dot v_1(L_1)+\dot u_3(L_3)\right)^2\right]\\&+\tfrac{1}{2}J_1\dot\psi_1^2\end{aligned}$$

where E is Young's modulus, I is the area moment of inertia, L is beam length, m is mass of rigid masses, X is the displacement of the base, ρ is the mass per unit length of the beam, J is the

polar moment of inertia of the rigid masses, g is the local gravitational acceleration, and the subscripts refer the specific beam sections.

The potential energy is given by

$$V = \tfrac{1}{2}\int_0^{L_1}(EI)_1(\partial\psi_1/\partial x_1)^2\,dx_1 + \tfrac{1}{2}\int_0^{L_2}(EI)_2(\partial\psi_2/\partial x_2)^2\,dx_2 + \tfrac{1}{2}\int_0^{L_3}(EI)_3(\partial\psi_3/\partial x_3)^2\,dx_3$$
$$+ \tfrac{1}{2}\int_0^{L_4}(EI)_4(\partial\psi_4/\partial x_4)^2\,dx_4 + \int_0^{L_3}\rho_3 g(X - v_3 + u_1(L_1))dx_3 + \int_0^{L_4}\rho_4 g(X - v_4 + u_2(L_2))dx_4$$
$$+ m_1\left[u_1(L_1) + X\right]g + m_2\left[u_2(L_2) + X\right]g + m_3\left[u_1(L_1) + X - v_3(L_3)\right]g + \rho_1 L_1 gX + \rho_2 L_2 gX$$
$$+ \int_0^{L_1}\rho_1 g u_1 dx_1 + \int_0^{L_2}\rho_2 g u_2 dx_2$$

To complete the methodology, we need to incorporate the inextensionality constraints by introducing Lagrange multipliers and thereby obtain the *augmented Lagrangian*. The augmented Lagrangian is averaged over the period of the primary oscillation. Requiring the averaged Lagrangian to be stationary with respect to the dependent variables v leads to the Euler-Lagrange equations. To study any specific resonance, we assume the form of the solution by restricting the expansion in terms of the directly and indirectly excited modes. All other modes are presumed to decay with time. Similar to other multibeam systems with concentrated masses, the dominant nonlinearity can be shown to be quadratic whose source derives from the kinetic energy term. We refer the reader to Balachandran (1990) for details of the above methodology.

5.2.2 LINEAR MODELING

A linear model for the portal frame is necessary for calculation of the linear natural frequencies and modes shapes. The linear model can be attained by either linearizing the nonlinear Euler-Lagrange equations derived from the time-averaged Lagrangian or by applying Newton's laws of motion. The second approach is described here.

The *linear equations of motion* for the portal frame based on the division into four separate sections is as follows:

For beam section 1,

$$(EI)_1 \frac{\partial^4 v_1}{\partial x_1^4} + \rho_1 \frac{\partial^2 v_1}{\partial t^2} + \left[m_1 + \tfrac{1}{2}m_3 + \tfrac{1}{2}(\rho_3 L_3 + \rho_4 L_4)\right] g \frac{\partial^2 v_1}{\partial x_1^2} + \underline{\rho_1 (L_1 - x_1) g \frac{\partial^2 v_1}{\partial x_1^2} - \rho_1 g \frac{\partial v_1}{\partial x_1}} = 0$$

For beam section 2,

$$(EI)_2 \frac{\partial^4 v_2}{\partial x_2^4} + \rho_2 \frac{\partial^2 v_2}{\partial t^2} + \left[m_2 + \tfrac{1}{2}m_3 + \tfrac{1}{2}(\rho_3 L_3 + \rho_4 L_4)\right] g \frac{\partial^2 v_2}{\partial x_2^2} + \underline{\rho_2 (L_2 - x_2) g \frac{\partial^2 v_2}{\partial x_2^2} - \rho_2 g \frac{\partial v_2}{\partial x_2}} = 0$$

For beam section 3,

$$(EI)_3 \frac{\partial^4 v_3}{\partial x_3^4} + \rho_3 \frac{\partial^2 v_3}{\partial t^2} + \rho_3 g = 0$$

For beam section 4,

$$(EI)_4 \frac{\partial^4 v_4}{\partial x_4^4} + \rho_4 \frac{\partial^2 v_4}{\partial t^2} + \rho_4 g = 0.$$

The *boundary conditions* of the frame are found to be

Clamped ends at the base

$$v_1(0,t) = 0,\ \partial v_1/\partial x_1(0,t) = 0,\ v_2(0,t) = 0,\ \partial v_2/\partial x_2(0,t) = 0$$

Continuity of slope at the rigid masses

$$\partial v_1/\partial x_1(L_1,t) = \partial v_3/\partial x_3(0,t),\ \partial v_2/\partial x_2(L_2,t) = \partial v_4/\partial x_4(0,t),\ \partial v_3/\partial x_3(L_3,t) = \partial v_4/\partial x_4(L_4,t)$$

Displacement of the crossbar beam sections

$$v_3(0,t) = 0,\ v_4(0,t) = 0,\ v_3(L_3,t) = -v_4(L_4,t)$$

Force equilibrium equation on the crossbar

$$(EI)_1 \frac{\partial^3 v_1}{\partial x_1^3}(L_1,t) + (EI)_2 \frac{\partial^3 v_2}{\partial v_2^3}(L_2,t) = \left[m_1 + m_2 + m_3 + \rho_3 L_3 + \rho_4 L_4\right] \frac{\partial^2 v_1}{\partial t^2}(L_1,t)$$

Moment equilibrium equations of the corner masses

$$(EI)_1 \frac{\partial^2 v_1}{\partial x_1^2}(L_1,t) + J_1 \frac{\partial^3 v_1}{\partial x_1 \partial t^2}(L_1,t) = (EI)_3 \frac{\partial^2 v_3}{\partial x_3^2}(0,t)$$

$$(EI)_2 \frac{\partial^2 v_2}{\partial x_2^2}(L_2,t) + J_2 \frac{\partial^3 v_2}{\partial x_2 \partial t^2}(L_2,t) = (EI)_4 \frac{\partial^2 v_4}{\partial x_4^2}(0,t)$$

Tip displacements of the vertical beams

$$v_1(L_1,t) = v_2(L_2,t)$$

Equilibrium equations of the middle rigid mass

$$(EI)_3 \frac{\partial^3 v_3}{\partial x_3^3}(L_3,t) + m_3 g \frac{\partial v_3}{\partial x_3}(L_3,t) = (EI)_4 \frac{\partial^3 v_4}{\partial x_4^3}(L_4,t) + m_3 \frac{\partial^2 v_3}{\partial t^2}(L_3,t)$$

$$(EI)_3 \frac{\partial^2 v_3}{\partial x_3^2}(L_3,t) + J_3 \frac{\partial^2 v_3}{\partial t^2 \partial x_3}(L_3,t) = (EI)_4 \frac{\partial^2 v_4}{\partial x_4^2}(L_4,t)$$

The underlined terms in the equations of motion capture the effect of gravity (Chapter 2). The solution of these equations results in an eigenvalue problem. The resulting characteristic equation is then solved numerically to obtain the linear natural frequencies. As an alternative, we resorted to the commercial finite element code ABAQUS to solve for the linear natural frequencies and mode shapes of the portal frame. The obtained linear eigenfrequencies (natural frequencies) are shown in Table 5.1. The dimensions of the frame are mentioned in the next section. The linear eigenfunctions (mode shapes) for the first eleven modes are shown in Figure 5.3.

5.3 LINEAR NATURAL FREQUENCIES

5.3.1 EXPERIMENTAL RESULTS

The linear natural frequencies were estimated experimentally for a frame where the dimensions of its vertical beams were 0.451 *m* x 1.27 *cm* x 0.08 *cm* and the dimensions of its horizontal crossbar were 0.248 *m* x 0.08 *cm* x 1.91 *cm*. The center mass was fixed at the midpoint of the crossbar and weighed approximately 40 *gm* and the two corner masses each weighed about 131 *gm*. The interfaces between the masses and the beams were clamped. The beam material

consisted of spring steel. The density was approximately 7800 kg/m^3 and Young's modulus was 207 *Gpa*. The base to which the frame was clamped was aluminum.

Figure 5.2 shows the experimental setup. The frame was placed on top of a 900-lb shaker. A signal generator provided a harmonic input to the shaker. Once the frame was mounted to the shaker, the only two control parameters were the forcing frequency and excitation. An accelerometer was placed on the aluminum base while a laser vibrometer was aligned with one of the vertical beams of the frame. Signals from both transducers were passed through a dynamic signal analyzer for calculating the real-time power spectra and an oscilloscope for displaying the time traces. Finally, the data were digitized and stored in a computer for further processing.

To estimate the linear natural frequencies, we used a band-limited random support motion. The readings of an accelerometer, measuring the support motion, and a laser vibrometer focusing on a point on one of the vertical beams, measuring the frame response, were fed into a dynamic signal analyzer that could produce frequency-response functions. It was assumed that a measurement at any point on the frame was representative of the response of the entire frame. Of course, the choice of the laser measurement point depends on the modes involved in the response. The measuring point should be away from nodal points of any of the active modes.

Next, each well-defined peak in the magnitude portion of the frequency-response function was assumed to represent an estimate of one of the linear natural frequencies of the system. To refine these estimates, we conducted slow sine sweeps around them. A stroboscopic device was used to observe visually the mode shape associated with the natural frequency being identified. Due to the high flexibility of the structure, some mode shapes could not be identified since the required forcing levels would activate modal interactions, which corrupt the single-mode response. However, the experimentally obtained mode shapes that were observed did match the corresponding mode shapes obtained with ABAQUS.

The modal testing was performed for different laser measurement locations along one of the vertical beams. In this way, the possibility of missing a linear natural frequency due to the measuring point being near a nodal point was reduced. The modal tests were conducted for different forcing levels to insure that the estimated frequencies do not depend on the vibration amplitude.

The identified 13 lowest frequencies and their associated modal damping values are listed in Table 5.1. The modal damping was found through the half-power point method. Inspecting these frequencies, we conclude that many of them are commensurate and hence the frame may possess numerous internal resonances. Because the dominant nonlinearity is quadratic, the most likely resonances are either two-to-one or combination internal resonances. A combination of any of these is also possible as will be shown in the next chapter.

Table 5.1: Linear natural frequencies of portal frame

Mode No.	FEM	Experimental	Damping
1	1.562	1.069	0.0025
2	11.970	10.974	0.0023
3	18.839	18.140	0.0015
4	25.539	22.618	0.0015
5	42.708	43.020	0.0011
6	52.900	51.590	0.0010
7	68.278	64.693	0.0017
8	74.013	74.081	0.0012
9	119.65	112.312	0.0008
10	121.06	116.701	0.0006
11	184.64	181.220	0.0007
12	-	187.995	0.0005
13	-	189.581	0.0008

5.3.2 FINITE ELEMENT RESULTS

A finite element modal analysis of the frame was carried out to compare the analytical results with those obtained experimentally. The ABAQUS code was used for this purpose (ABAQUS, 1989). Various modeling approaches can be adapted for such an analysis. One approach is to utilize beam elements and concentrated masses to discretize the frame. The beam elements are one-dimensional elements in the sense that there is only one independent variable in the formulation. The dependent variables can be as many as six, three translations and three rotations at each node. Another approach is to use two-dimensional plane stress or plane strain elements, where the geometry of the frame and the joints can be modeled in more detail. This approach was chosen. The analysis limits the response prediction only to the plane of the frame. Finally, one can use three-dimensional elements so that the geometry can be very accurately modeled and all the modes, inplane and out-of-plane modes, can all be captured.

For two-dimensional modeling, linear elements are not appropriate since these elements perform poorly for bending modes and result in significant overestimates of the stiffness. This is particularly more severe in thin beams. This situation can be partly remedied by the use of a reduced integration technique. The most appropriate technique is, however, to use higher-order elements for bending. The eight-node plane-stress elements were thus used for modal analysis. The frame was modeled with 618 nodes and 123 eight-node elements. An initial study was carried out to make sure that the level of refinement was sufficient, so that further refinement would not significantly alter the results. The analysis with the eight-node elements and reduced integration technique was also carried out. No appreciable changes in the calculated linear natural frequencies were seen. The natural frequencies are obtained from the solution of the linear eigenvalue problem.

5.3.3 COMPARISON

A comparison between the theoretically and experimentally obtained natural frequencies reveals a discrepancy for several of the low-frequency modes. The physical source of this discrepancy is most likely due to the exclusion of the gravity effect from the analysis. The finite-element analysis ignores the gravity effect of the vertical beams. Gravity, as outlined in Chapter 2 for the cantilever beam, reduces the theoretically obtained linear natural frequencies. The terms that would capture this effect in an analysis are underlined in the equations of motions for beam sections 1 and 2. Though it is not pursued here, the linear natural frequencies including the effect of gravity could be found by applying a perturbation method to the equations of motion developed in this chapter, as shown by Balachandran (1990).

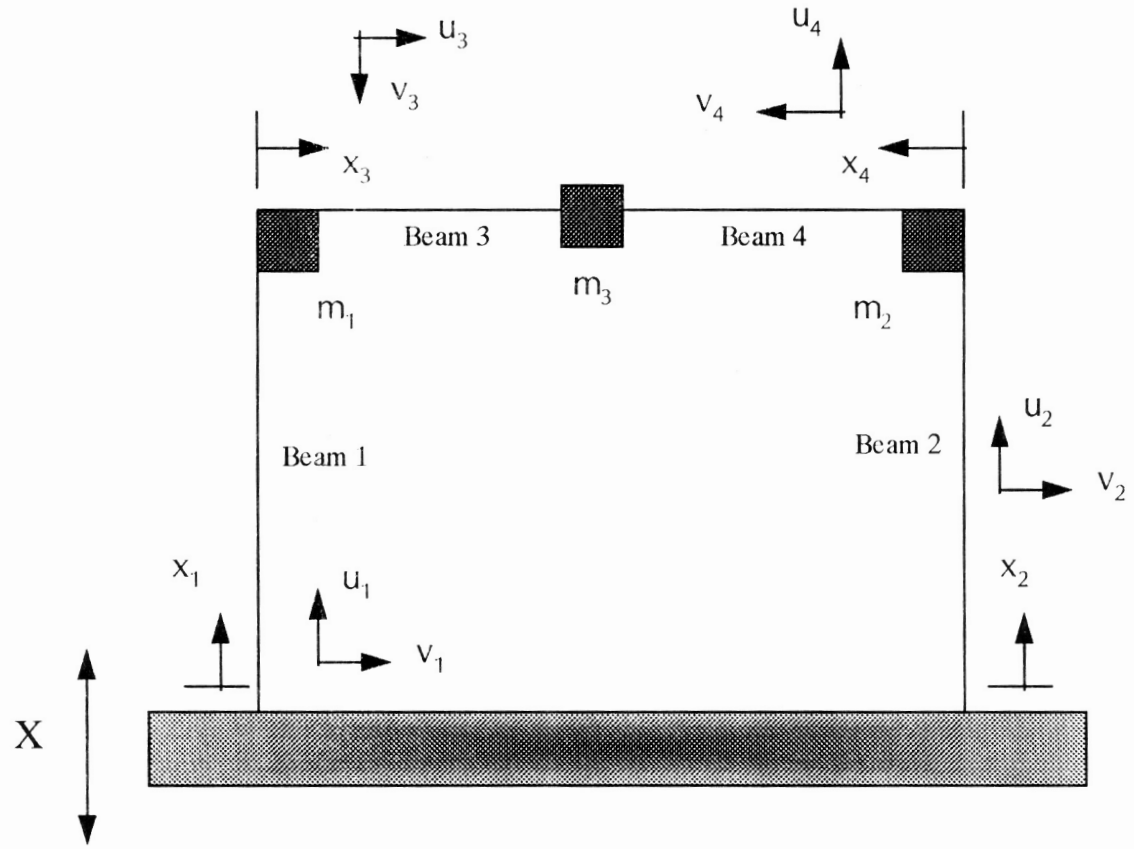

Figure 5.1 Portal frame with coordinate systems.

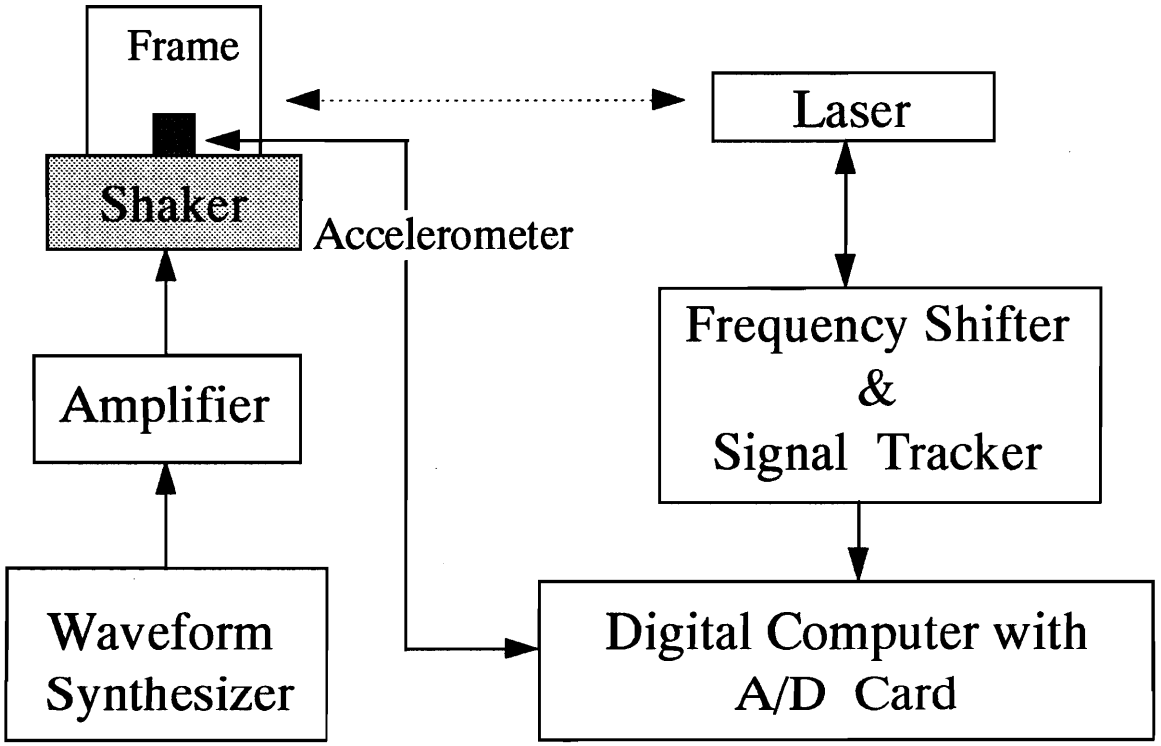

Figure 5.2 A schematic of the experimental setup.

5.4 CHAPTER REMARKS

The linear natural frequencies of a portal frame were calculated both theoretically and experimentally. In a frequency region below 200 Hz, 13 planar linear natural frequencies were observed. The type of transducer used in measuring the structural response is a key element in obtaining accurate measurements of modal contributions. The laser, being a point measuring device, had to be moved to several different locations on the frame to insure proper identification of modes within the frequency region of interest. This point becomes crucial especially for quantitative measurements in multimode dynamics. The frame proves to have a rich modal density, which enhances the possibility of nonlinear modal interactions.

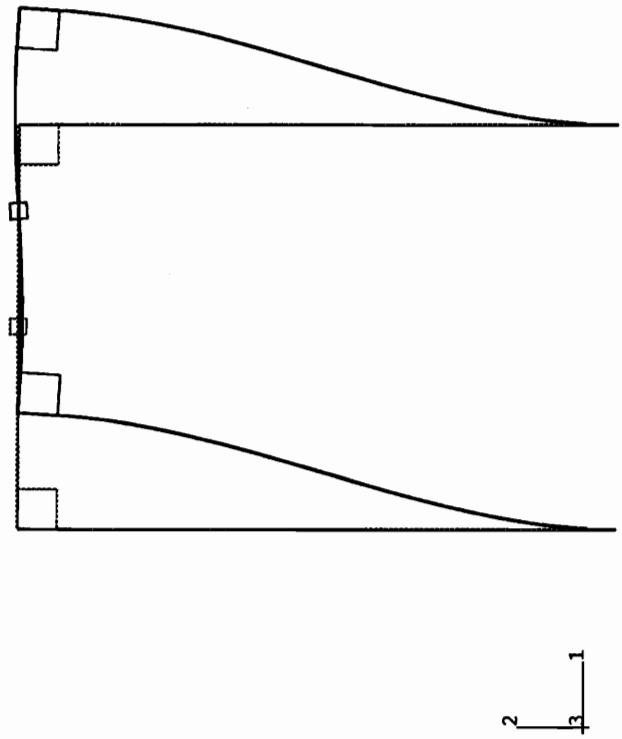

Figure 5.3(a) Shape of the first mode of the portal frame (ABAQUS).

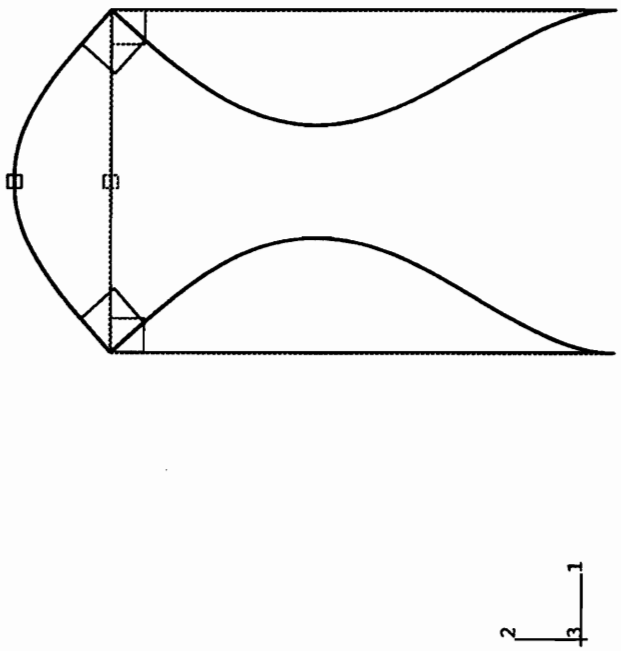

Figure 5.3(b) Shape of the second mode of the portal frame (ABAQUS).

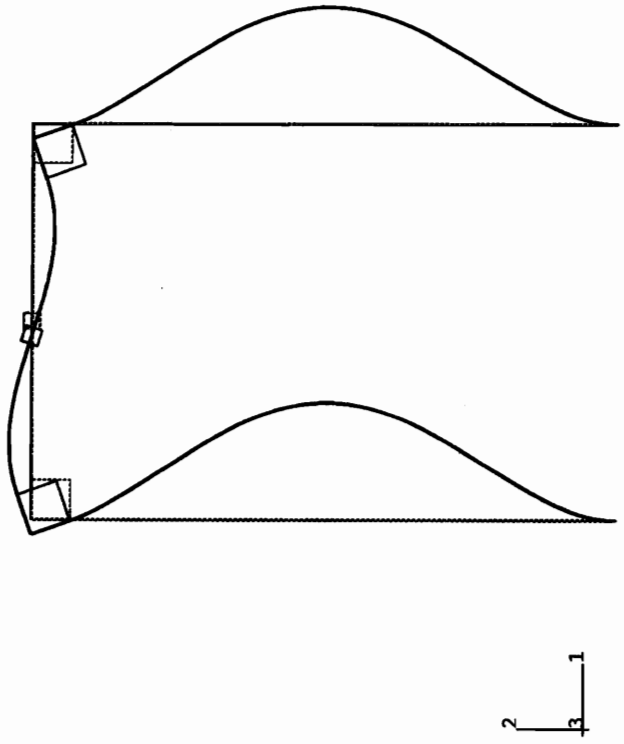

Figure 5.3(c) Shape of the third mode of the portal frame (ABAQUS).

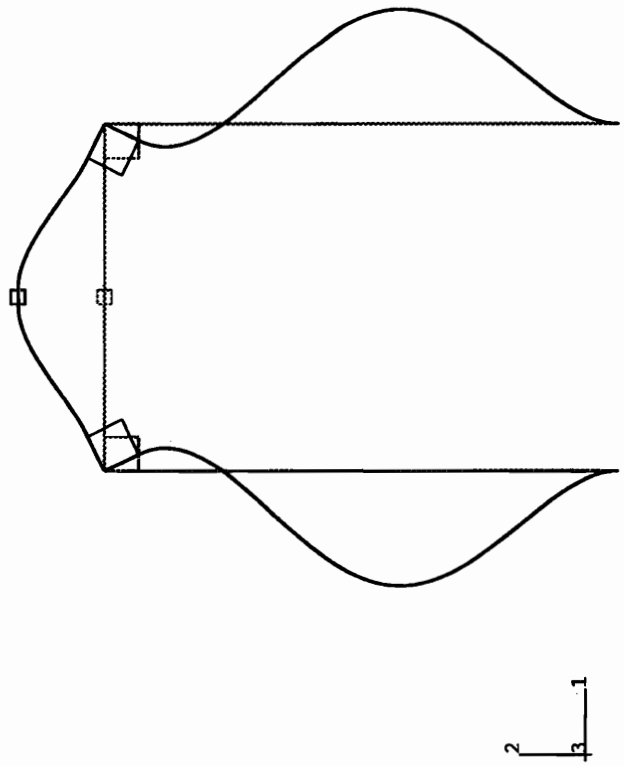

Figure 5.3(d) Shape of the fourth mode of the portal frame (ABAQUS).

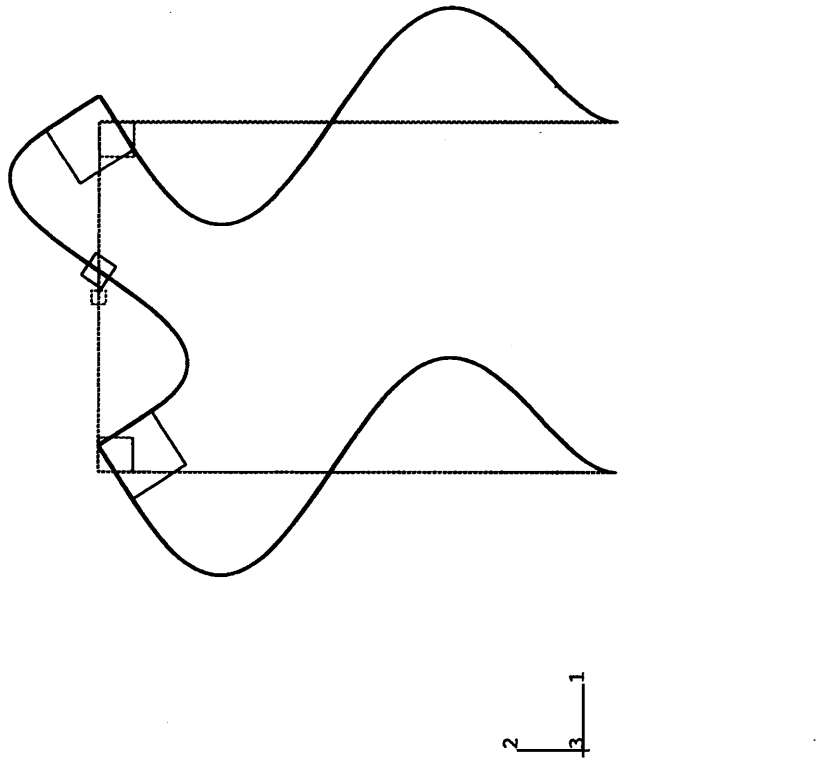

Figure 5.3(e) Shape of the fifth mode of the portal frame (ABAQUS).

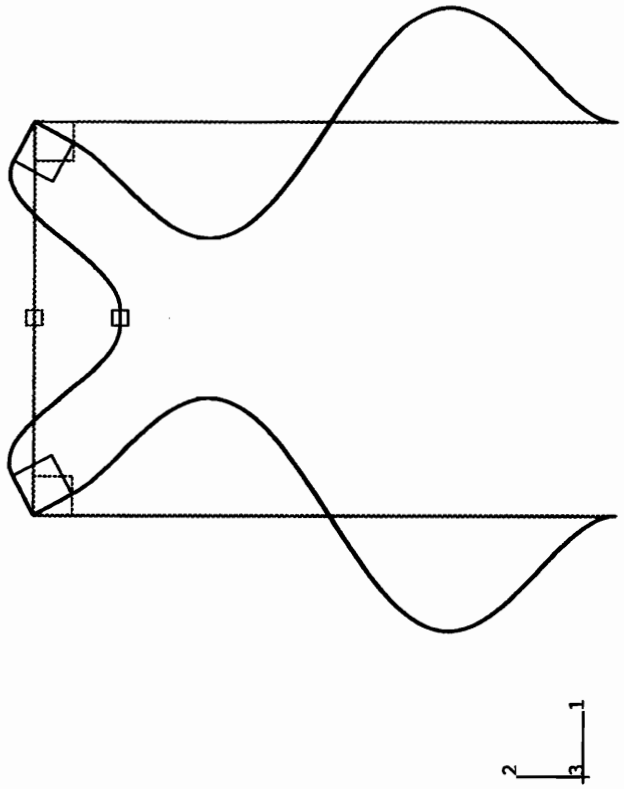

Figure 5.3(f) Shape of the sixth mode of the portal frame (ABAQUS).

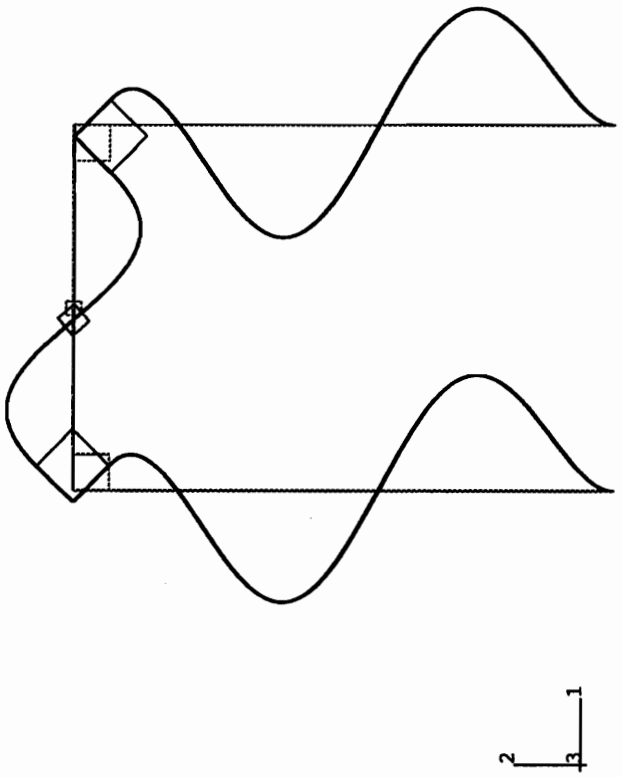

Figure 5.3(g) Shape of the seventh mode of the portal frame (ABAQUS).

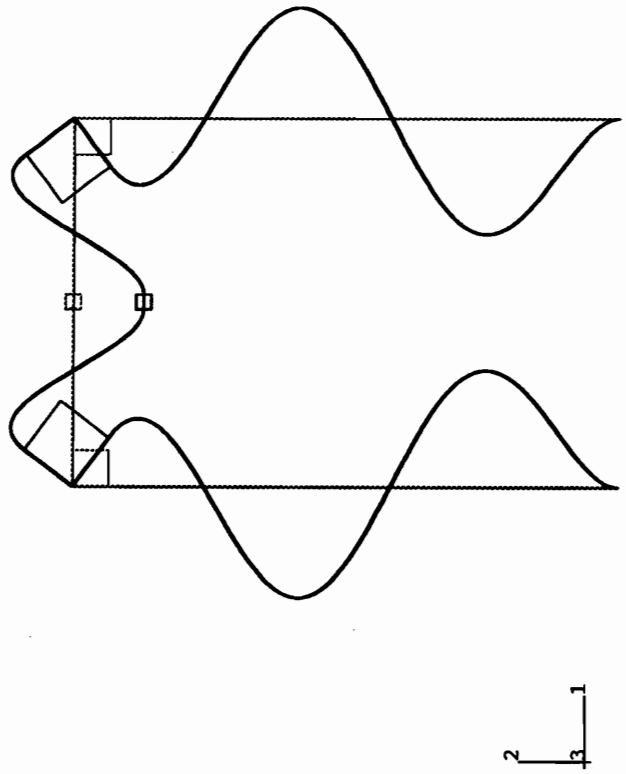

Figure 5.3(h) Shape of the eighth mode of the portal frame (ABAQUS).

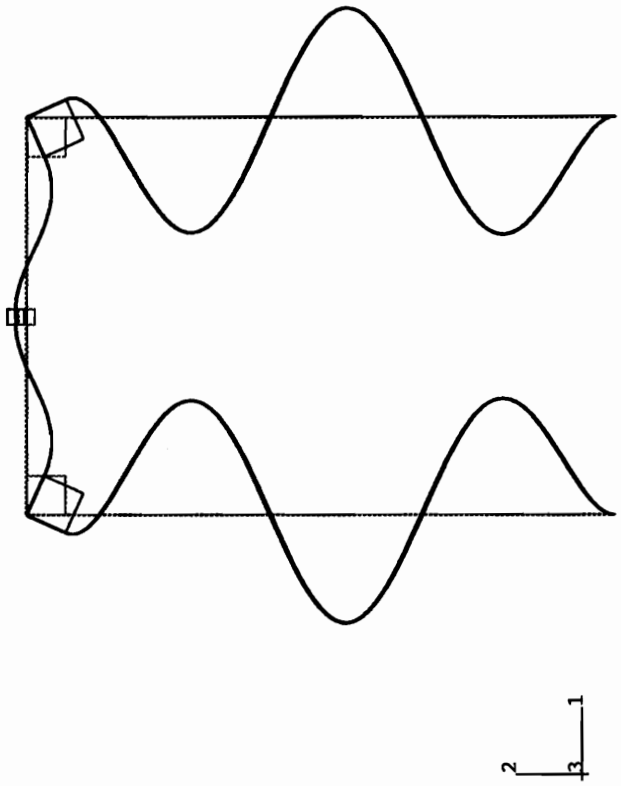

Figure 5.3(i) Shape of the tenth mode of the portal frame (ABAQUS).

CHAPTER SIX

Modal Interactions in a Flexible Portal Frame Under Support Motions

'It is much easier to criticize than to be correct' Anonymous

This chapter discusses an experimental investigation into the planar, multimode response of a metallic portal frame to a harmonic support excitation. Forcing frequency and amplitude sweeps near the frequencies of the eighth and tenth modes of the structure revealed multimode responses. In the frequency interval surrounding that of the eighth mode, two additional lower-frequency modes, the fourth and the sixth, were excited. The mechanism responsible for the multimode behavior of the frame is a combination internal resonance of the additive type. Forcing amplitude sweeps for forcing frequencies below the eighth linear natural frequency produced a saturation type phenomenon and a chaotically modulated motion. For the frequency interval surrounding that of the tenth mode, the response contained contributions from seven modes; they were excited through the simultaneous satisfaction of several internal resonance conditions.

6.1 INTRODUCTION

The nonlinear vibration of multibeam systems has been the topic of very recent research. The subject of our study is the portal frame detailed in Chapter 5. It has 13 planar linear natural frequencies in a frequency region below 200 Hz. Looking at Table 5.1 one can identify numerous commensurate relationships amongst its linear natural frequencies. The experiments that follow were designed to take advantage of the rich modal density and the structural flexibility of the portal frame to activate modal interactions in its forced response.

6.2 EXPERIMENTAL SETUP

The experimental setup is the same as that outlined in Chapter 5. The key point to be aware of is the issue of transducer type. With the improvements in technology, instrumentation has advanced significantly (Noltingk, 1995; Stanbridge and Ewins, 1996). For structural vibrations, usually a transducer whose output is proportional to the displacement and has the least effect in terms of mass and stiffness loading on the structure is desirable. Laser vibrometers and fiber optic displacement transducers satisfy these criteria very well. In the experiments that follow, a laser vibrometer, which measures velocity at a point was used to sense the structural response. However, as mentioned in the previous chapter, the transducer may not be measuring exactly what we seek. In choosing a point on the frame for response sensing, we had to know what type of behavior we were seeking to study; that is, we had to have knowledge of the active modes in the response so that the placement of the laser vibrometer measuring point can be chosen to insure a fair accounting of the contributions of the active modes. It is important to have a measuring point that is not near a nodal point of any particular mode. Obviously, it will be difficult to have a single point measurement be near the antinodes of all the active modes for the general case of multimode response of a structure. However, this complication is only one side of the coin. The other side is that the relative contribution of each mode may not be properly recorded. For example, if we are measuring a response consisting of three modes, the measuring point may coincide with the antinode of one of the modes but will most likely not coincide with the antinodes of the two other modes. So the measurement may give the false impression that the mode whose antinode is coincident with the measuring point contributes more than the other two modes to the structural response. The sensing point only measures a partial contribution of the two other modes. Of course, this can be corrected with some difficulty as an accurate knowledge of the mode shape is required.

The magnitudes of the velocity (in volts) associated with each peak were scaled by the frequency of each peak to obtain a numerical measure that is proportional to displacement. The calibration constant for the laser vibrometer would be necessary to convert to the actual displacement. The assumption is that the qualitative aspects of the analysis are not affected by the transducer calibration.

Other problems can arise depending on the nature of the test. For instance, the effect of fatigue and temperature (Mitchell and Neumann, 1995) on the response of a structure can be considerable.

6.3 DYNAMICAL RESPONSE

Once the linear natural frequencies have been determined, they are organized based on the satisfaction of frequency relationships known as resonances or conditions of commensurability. These resonances could be internal, combination, or both (Nayfeh and Mook, 1979). The specific relationship of commensurability depends on the order of the dominant system nonlinearity. The two most widely studied are quadratic and cubic nonlinearities (Nayfeh and Balachandran, 1989). As shown in Chapter 5, for the portal frame with large concentrated masses, the dominant nonlinearity is quadratic and inertial in nature (Balthazar and Brasil, 1995). The possibility of modal interactions is enhanced by the modal density and commensurability of some of the modes.

Testing for the purpose of identifying nonlinear mechanisms in the dynamic response of structures requires a methodical approach combined with powerful experimental tools. These tools include forcing frequency and amplitude sweeps, power spectra, time series, pseudo Poincare' sections, pseudo state plots, and dimension calculations. Some or all are necessary for the proper characterization of the complicated nonlinear responses of a structure (Nayfeh and Balachandran, 1995). Here, we use as many of these tools as possible.

The results discussed next are from experiments conducted in two different frequency regions: (i) near the natural frequency of the eighth mode where a single internal resonance was activated and (ii) near the natural frequency of the tenth mode where several different internal resonances were simultaneously activated.

6.3.1 A SINGLE COMBINATION INTERNAL RESONANCE

Figure 6.1 shows the frequency-response curves for an excitation level of 1.75 g. The forcing frequency was varied in an interval around the natural frequency of the eighth mode. The frequency-response curve for the eighth mode exhibits two local maxima and a local minimum, as shown in Figure 6.1(a). The minimum is near the eighth linear natural frequency. Starting at a frequency below the linear natural frequency and slowly increasing the forcing frequency, we found that the amplitude of the eighth mode increased, jumped to a peak, and then began to decrease as it approached the linear natural frequency. Once the linear natural frequency was passed, the amplitude of the eighth mode increased, experienced a jump to a peak amplitude, and then began to decrease with increasing forcing frequency.

For a decreasing forcing frequency starting at a point above the linear natural frequency, we found that the amplitude of the eighth mode increased, reaching a maximum lower than that in the forward sweep. After the peak, the amplitude decreased significantly and reached a minimum near the linear natural frequency at nearly the same point as in the forward sweep. Once past the linear natural frequency, the amplitude of the eighth mode increased until it peaked for a second time, this time jumping down to a lower amplitude and gradually decreasing with decreasing forcing frequency.

The multimode response for the forward sweep was observed for the point at 73.90 Hz rather after the first peak. The multimode response consisted of contributions from the fourth and sixth modes, as evident from Figure 6.1(b). These two modes were activated by a combination internal resonance of the additive type where $\omega_8 \approx \omega_6 + \omega_4$. This type of

resonance occurs for systems with a dominant quadratic nonlinearity. We note that the amplitudes of the indirectly excited modes are larger than that of the directly excited eighth mode. The amplitudes of the fourth and sixth modes also appear to display minima near the linear natural frequency. The combination resonance for the forward sweep ends after the second peak is passed at 74.35 Hz where the amplitudes of the fourth and sixth modes also display a jump to a smaller amplitude motion.

For the reverse sweep, the combination resonance was activated at the same point, 74.35 Hz, as it ended for the forward sweep. In this case, the amplitudes of the fourth and sixth modes jumped to larger values and once again displayed minima near the eighth linear natural frequency. The interval during which the combination resonance was activated in the reverse direction was longer than that in the forward direction, eventually disappearing at 73.60 Hz after the second peak.

Now using some of the tools of nonlinear dynamical analysis, we examine in detail the response at three points on the frequency-response curves labeled as A, B and C.

Figure 6.2 shows the power spectrum and pseudo-state plane for the motion at point A. The power spectrum for the response shows a single frequency motion with very low level harmonics. The response at this point is essentially linear. The pseudo-state plane strengthens this assessment as it shows a closed curve. The pseudo-state plane is obtained by plotting a single state variable versus a time delayed value of the same state variable. For a single frequency motion, the pseudo-state plane is a closed curve as the motion is periodic (The sampling frequency for the time plots and power spectra was 1000 Hz; the pseudo-state planes were obtained using a time delay of 2; though not shown here due to the poor signal-to-noise ratio, the sampling frequency for the Poincare sections was equal to the forcing frequency).

Figure 6.3 shows the power spectrum and time trace of the motion at point B. The power spectrum now reveals two additional frequency components, both below the excitation

frequency. They correspond to the fourth and sixth natural frequencies. Harmonics of the active modes are also present as the nonlinearity gains strength. Figure 6.3(b) shows the time trace of the motion. For multimode responses, time traces prove to be less effective in discerning the type of motion being observed. The pseudo-state plane (Figure 6.4) shows a nonclosed curve. Both of these are indicative of quasiperiodic behavior.

Finally, Figure 6.5 shows the power spectrum of the response at point C. We note both an increase in the strength of the active modes (fourth, sixth and eighth) and in the amplitudes of the sums, differences, and multiples of the frequencies of these active modes (secondary modes) in the response of the structure. As the strength of the nonlinearity increases, the contributions from the secondary modes increases.

Next we show the results from a series of forcing amplitude sweeps conducted near, above, and below the eighth linear natural frequency.

Figure 6.6 shows the amplitude-response curves obtained for a forcing frequency of 74.06 Hz. Starting with a low excitation level and gradually increasing it, we found that the amplitude of the fourth mode gradually increased as the response of the frame consisted of this single mode. At slightly above 0.4 g (accelerometer sensitivity 0.1 V/g) the amplitude of the fourth mode reached a maximum. After the peak there was a slight drop in the amplitude of the fourth mode while the nature of the response bifurcated from a single-mode response to a multimode response, including the fourth and sixth modes. Once again, the amplitudes of the indirectly excited modes were larger than that of the directly excited eighth mode. With further increases in the forcing amplitude, the amplitude of the eighth mode appeared to level off, possibly indicating a saturation type phenomenon, while the amplitudes of the fourth and sixth modes continued to increase.

Decreasing slowly the excitation amplitude, we observed that the amplitude of the eighth mode remained constant until near 0.4 g, where it began to gradually decrease, no longer

exhibiting any peak as in the forward sweep. The amplitudes of the fourth and sixth modes gradually decreased beyond the point of initiation in the forward sweep. However, once past 0.4 g the rate of decrease in the amplitudes of the fourth and sixth modes increased. The amplitude sweep for this frequency revealed, jumps, hystereses, and multimode behavior, all characteristics of a structure behaving in a nonlinear manner.

Figure 6.7 shows the amplitude-response curves obtained for a forcing frequency of 74.5 Hz. In this case, the amplitude of the eighth mode gradually increased with increasing forcing amplitude and only at an excitation level slightly above 0.7 g did the single-mode response lose stability and give way to a multimode response consisting of the eighth, sixth, and fourth modes. However, for this combination internal resonance, the amplitudes of the indirectly excited modes were smaller than that of the directly excited eighth mode. Further increases in the excitation amplitude lead to the instability of the multimode response and the activation of a nonresonant modal interaction at an excitation level of approximately 0.9 g (point A in Figure 6.7). This nonresonant modal interaction involved the directly excited eighth mode transferring energy to the first mode of the frame. As can be seen from amplitude-response curves, the amplitude of the first mode is significantly larger than that of the eighth mode.

Examining the response at point A more closely, we infer from the response power spectrum of the transient motion in Fig. 6.8(a) that the combination internal resonance gave way to an interaction between widely spaced modes. Figure 6.8(a) shows sidebands at 74.5 Hz, 51.75 Hz, 22.75 Hz, and 1.12 Hz, representing the contributions from the eighth, sixth, fourth, and first modes, respectively. The simultaneous decay of the contributions of the fourth and sixth modes and the growth of the first mode occurred over a relatively long-time span in comparison to the previous bifurcation of the single-mode response to the combination response and vice versa. We also note asymmetric sidebands around the frequencies of the eighth, sixth, and fourth modes with a spacing equal to the frequency of the first mode. This indicates a phase and

amplitude modulation of the responses of the primary modes even though contributions of the sixth and fourth modes were decaying. The time trace for this transient phase of the response is shown in Figure 6.8(b). Figure 6.9 shows the power spectrum for the long-term response, where now only the eighth and first modes remain. The peak corresponding to the eighth mode continued to be surrounded by asymmetric sidebands whose spacing approximately equals the frequency of the first mode. Figure 6.10(a) shows the time trace of motion for this nonresonant modal interaction. Figure 6.10(b) shows the pseudo-state plane for the motion at point A.

Finally, we consider a frequency level below the eighth linear natural frequency. Figure 6.11 shows the amplitude-response curves at a forcing frequency of 73.62 Hz. Starting at a very low excitation amplitude and gradually increasing it, we found that the amplitude of the eighth mode increased until an excitation amplitude of 0.25 g where it peaked. After that, the amplitude of the eighth mode dropped and remained essentially constant. Moreover, the single-mode response lost stability and a combination internal resonance activated the fourth and sixth modes. Once again, the amplitudes of the indirectly excited modes were larger than that of the directly excited eighth mode. However, for this forcing frequency, modulated motions were observed for a restricted excitation amplitude range. This region is delineated by dotted lines in Figure 6.11. Though we only show a forward sweep, we begin to examine the nature of the response in the modulated region by starting at point A, the point farthest away.

Figure 6.12 shows a power spectrum of the response at point A. The peaks associated with the three primary modes are surrounded by sidebands with a spacing of nearly 0.6 Hz, indicating modulated motions. Figure 6.13 shows the power spectra of the motions for points A, B, C, and D, where only changes in the sideband structure occurring around the natural frequency of the eighth mode are considered; similar changes occur for the sidebands of the other two primary modes. First comparing the power spectra of the motions at points A and B, we note the addition of sidebands at point B at one-half the spacing of the sidebands at point A. This

suggests the occurrence of a period-doubling bifurcation of the modulation frequency. The power spectrum of the response at point C shows further sidebands, possibly revealing another period-doubling bifurcation of the modulation frequency. Already a slight broadening of the sideband base is observed. Finally, at point D, the base broadening has grown, suggesting a chaotically modulated behavior. Further tools such as dimension calculations and Lyapunov exponents, would be prudent to add confidence to this assessment (Nayfeh and Balachandran, 1995 and Moon, 1987). So we suspect that, once the motion entered the modulated region through a Hopf bifurcation, it quickly experiences a series of period-doubling bifurcations that lead to a chaotically modulated multimode response near point D. With further increases in the excitation amplitude, the motion passed through a series of reverse period-doubling bifurcations, eventually returning to a steady-state multimode behavior through a reverse Hopf bifurcation. The time series of the motions at points A and D are shown in Figure 6.14. Some amount of breakdown in the periodicity of the time series of point A is evident in the time series of point B. The pseudo-state planes are shown in Figure 6.15 though definite conclusions are difficult to draw from these plots in this instance.

6.3.2 MULTIPLE COMBINATION INTERNAL RESONANCES

In this section, the frame was excited in an interval containing the frequency of the tenth mode. Figure 6.16 shows the frequency-response curves for an excitation level of 0.2 g. Figure 6.16(a) shows variation of amplitude of the tenth mode as the forcing frequency was swept in both forward and reverse directions. It displays a qualitatively different pattern than that shown for the frequency interval surrounding that of the eighth mode. Starting below the tenth linear natural frequency and slowly increasing the forcing frequency, we observed that the amplitude of the eighth mode gradually increased until 116.65 Hz when it jumped to a large-amplitude single-mode solution. At 116.75 Hz, the amplitude of the tenth mode fell unexpectedly to a smaller value though the response was no longer a single-mode motion. We will discuss the multimode

motions later. After this fall. the amplitude of the tenth mode once again jumped to a larger value and continued to decrease with increasing forcing frequency.

On the reverse sweep, the amplitude of the tenth mode followed the same path as in the forward sweep, gradually increasing with decreasing forcing frequency until 116.75 Hz where it jumped down to a smaller value at approximately the same frequency as for the forward sweep. With decreasing forcing frequency, the amplitude of the tenth mode continued to increase, experiencing a smaller jump to a larger value until 116.50 Hz, afterwhich it jumped to a small value.

To locate the bifurcation points of the single-mode solution, we will first consider the reverse sweep. Starting at a forcing frequency above the tenth linear natural frequency and gradually decreasing it, we found that the single-mode motion gave way to a multimode response at 117.10 Hz. Figure 6.17(a) shows the power spectrum of the response at this point. Below 200 Hz, four peaks are apparent at 117.10 Hz, 51.75 Hz, 65.35 Hz, and 182.45 Hz, corresponding to contributions to the response from the tenth, sixth, seventh, and eleventh modes, respectively. When documenting the transient growth of this multimode motion, it was observed that the growth of the contributions of the sixth and seventh mode preceded that of the eleventh mode. The observed multimode motion is the result of a simultaneous activation of two combination internal resonances: $\omega_{10} \approx \omega_6 + \omega_7$ and $\omega_{11} \approx \omega_{10} + \omega_6$. The amplitudes of all of the indirectly excited modes are larger than that of the directly excited tenth mode. lowering the forcing frequency slightly to 117.05 Hz, we found that three additional modes appeared in the total response. Figure 6.17(b) shows the spectrum of the response at 117.05 Hz. The additional peaks below the frequency of the tenth mode are 22.6 Hz, 42.75 Hz, and 74.3 Hz, which indicate contributions from the fourth, fifth, and eighth modes, respectively. These frequencies satisfy the following relationships: $\omega_7 \approx \omega_4 + \omega_5$ and $\omega_8 \approx \omega_6 + \omega_4$. So the single-mode response lost stability and gave way to a multimode motion consisting of first four modes and then seven

modes. No discernible pattern of variation is apparent in the amplitudes of the indirectly excited modes though most appear to increase in amplitude with decreasing forcing frequency. Time traces of these motions are shown in Figure 6.18. The multimode motion consisting of seven modes remained stable until 116.50 Hz, when the response reverted back into a three-mode motion. At 116.45 Hz, the multimode motion disappeared and a single-mode motion consisting of the tenth mode regained stability. This disappearance corresponds to the final jump to a small-amplitude tenth mode.

For the forward sweep, the multimode response did not appear until 116.70 Hz. This response consisted of the aforementioned seven modes without any transition to the three-mode motion. For most of the primary modes of the response, their amplitudes in the reverse sweep matched those in the forward sweep. However, at 117.15 Hz the seven-mode response lost stability and was replaced by a three-mode motion that consisted of the tenth, fifth, and eighth modes since $\omega_{10} \approx \omega_5 + \omega_8$. At 117.20 Hz, the three-mode motion lost stability and was replaced by a single-mode motion.

Finally, Figure 6.19 shows the amplitude-response curves at a forcing frequency of 117.19 Hz. The curves for the tenth mode show a gradual increase in amplitude with an increase in the forcing amplitude. On the reverse sweep, the amplitude of the tenth was slightly lower. For the forward sweep, at an excitation amplitude of approximately 0.1 *g*, the single-mode response bifurcated to a multimode response. This multimode response consisted of the tenth mode in addition to the sixth, seventh, and eleventh modes. The amplitudes of the sixth and seventh modes were larger than that of the directly excited tenth mode. However, the amplitude of the higher-frequency eleventh mode is less than that of the tenth mode. Further along the forward sweep, three additional modes contributed to the response at an excitation level of approximately 0.16 *g*. The three additional modes are the fourth, fifth, and eighth modes. The following series of combination internal resonances are responsible for the observed response

during the forcing amplitude sweep: $\omega_{10} \approx \omega_6 + \omega_7$, $\omega_{10} + \omega_6 \approx \omega_{11}$, $\omega_{10} \approx \omega_5 + \omega_8$, and $\omega_8 - \omega_6 \approx \omega_4$.

6.4 CHAPTER REMARKS

In this chapter, an experimental investigation into the planar nonlinear response of a flexible portal frame to harmonic support motions was presented. The frame structure possessed 13 linear natural frequencies in the 0-200 Hz range. The rich modal density allowed for the possibility of complex behavior resulting from the activation of internal resonances.

For the frequency interval surrounding that of the eighth mode, forcing frequency and amplitude sweeps revealed nonlinear responses starting from an eighth-mode response and giving way to a multimode response consisting of contributions from the eighth, fourth, and sixth modes. The amplitudes of the lower-frequency modes were larger than that of the directly excited eighth mode. A combination internal resonance of the additive type is the mechanism responsible for the activation of the low-frequency modes. This type of resonance is observed in structures with a dominant quadratic nonlinearity. The combination internal resonance results in the creation of a minimum and two maxima in the frequency-response curve. For a fixed frequency below the eighth linear natural frequency and a slow variation in the excitation amplitude, a Hopf bifurcation produced modulated motions. For a brief interval, the modulated motions appeared to undergo a sequence of period-doubling bifurcations, eventually displaying characteristics of a chaotically modulated response. For a fixed forcing frequency above the eighth linear natural frequency and a gradual variation of the excitation amplitude, the response resulting from the internal combination resonance lost stability and gave way to a nonresonant modal interaction involving the eighth and first modes.

Finally, in a frequency region surrounding the tenth mode, forcing frequency and amplitude sweeps produced a multimode response with contribution from up to seven modes, most of

which having frequencies lower than that of the directly excited tenth mode but with larger amplitudes than that of the tenth mode.

For most structures, modal density results in the possibility of commensurate relationships amongst various modal frequencies. Depending on the forcing amplitude, forcing frequency, and initial conditions, a single-mode response may lose stability and give way to a multimode response. The multimode response will likely contain contributions from low-frequency modes with large amplitudes. These amplitudes are occasionally on the same order of and may sometimes exceed the amplitude of the directly excited mode by several orders of magnitude. Either way, if one relies in a design on a linear analysis, which can not account for the possibility of energy transfer from a high-frequency mode to a low-frequency mode through either resonant or nonresonant modal interactions, the actual dynamical behavior may cause premature structural failure because of additional dynamic stresses due to the low-frequency components. Also the results show that a series of resonances may lead to the activation of a low-frequency component whose appearance was not possible through any single resonance involving the directly excited mode.

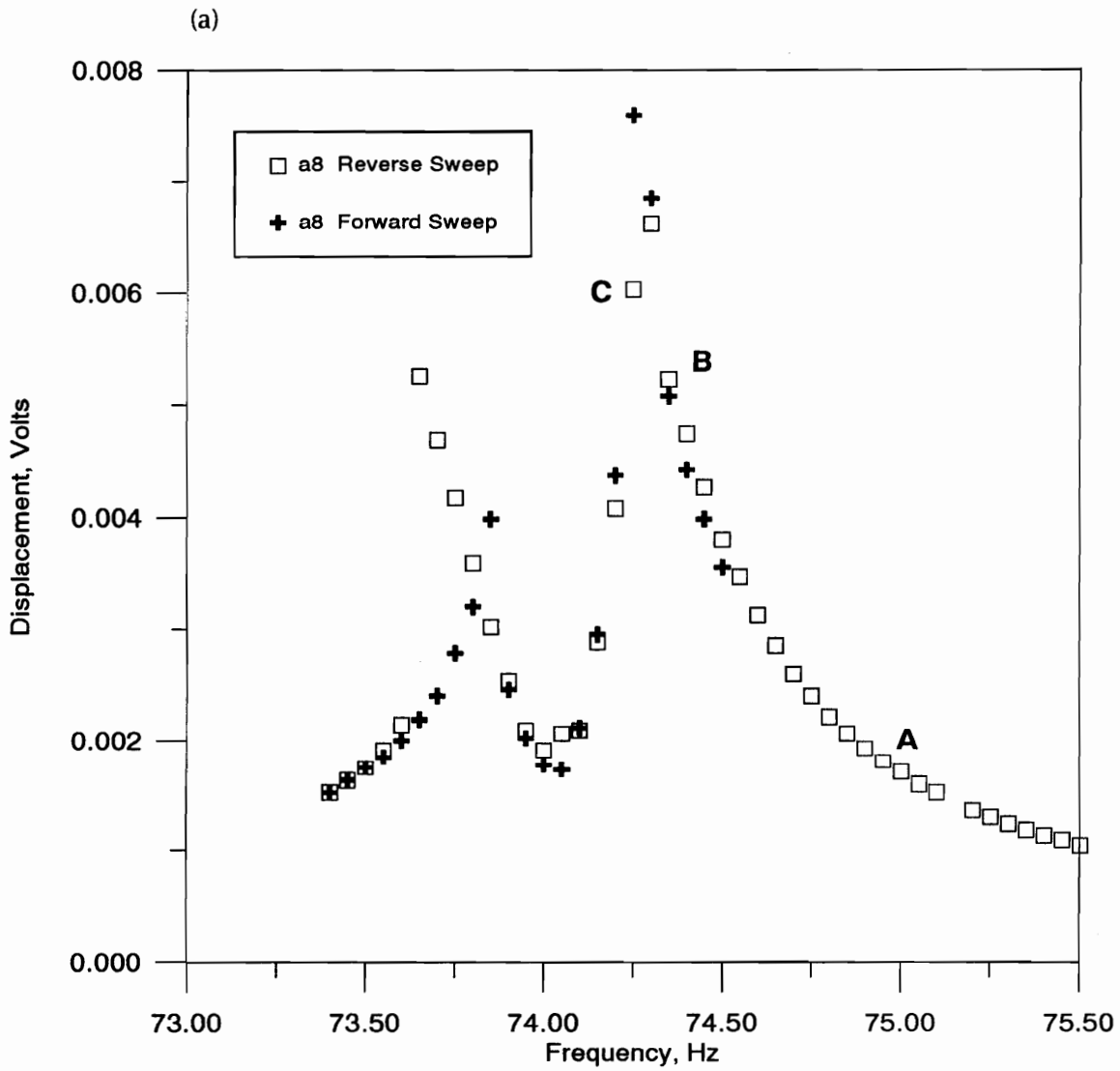

Figure 6.1 Frequency-response curves for an excitation amplitude of 1.75 g. (a) amplitude of the eighth mode and (b) amplitudes of the fourth and sixth modes.

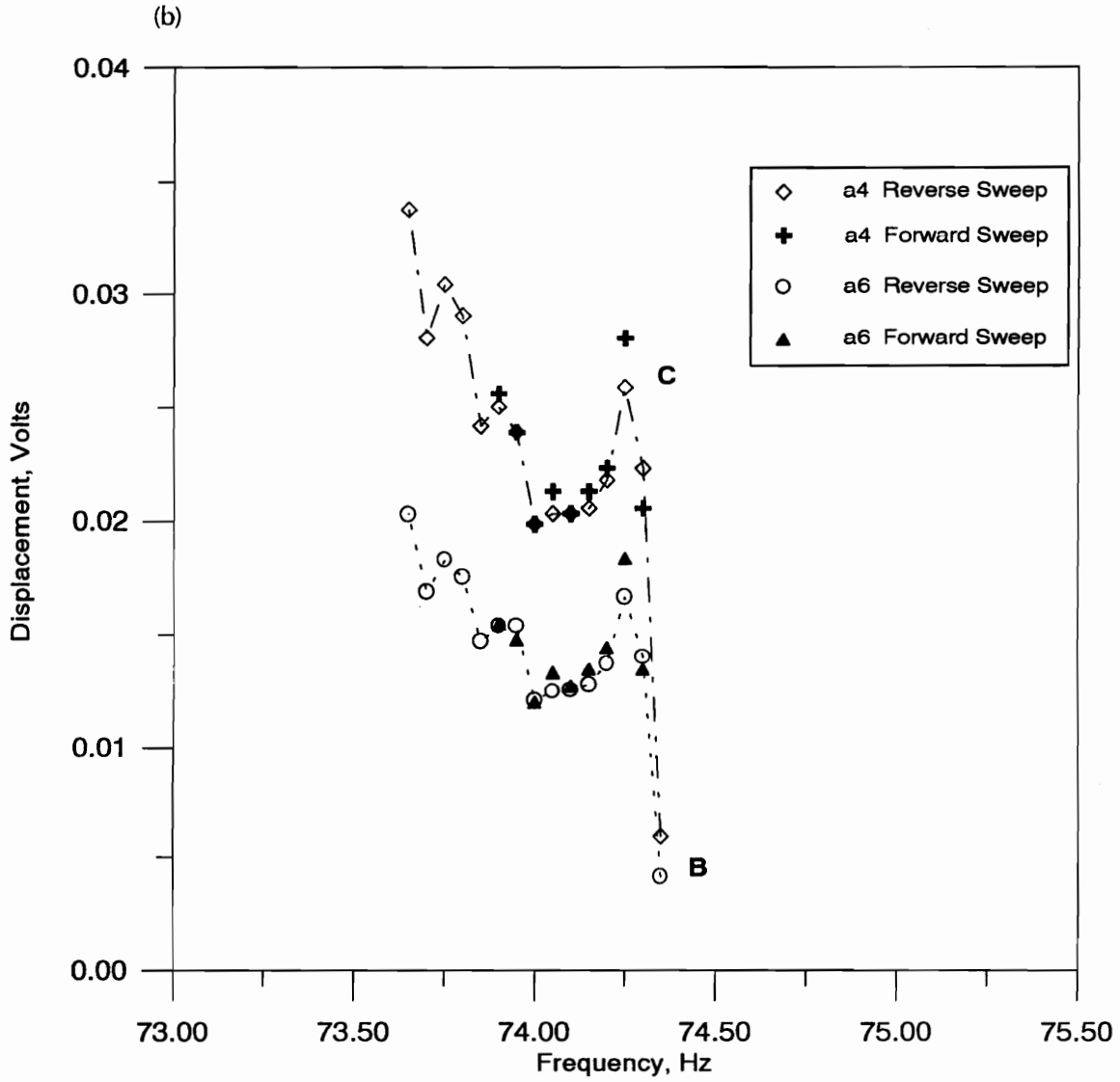

Figure 6.1 Continued

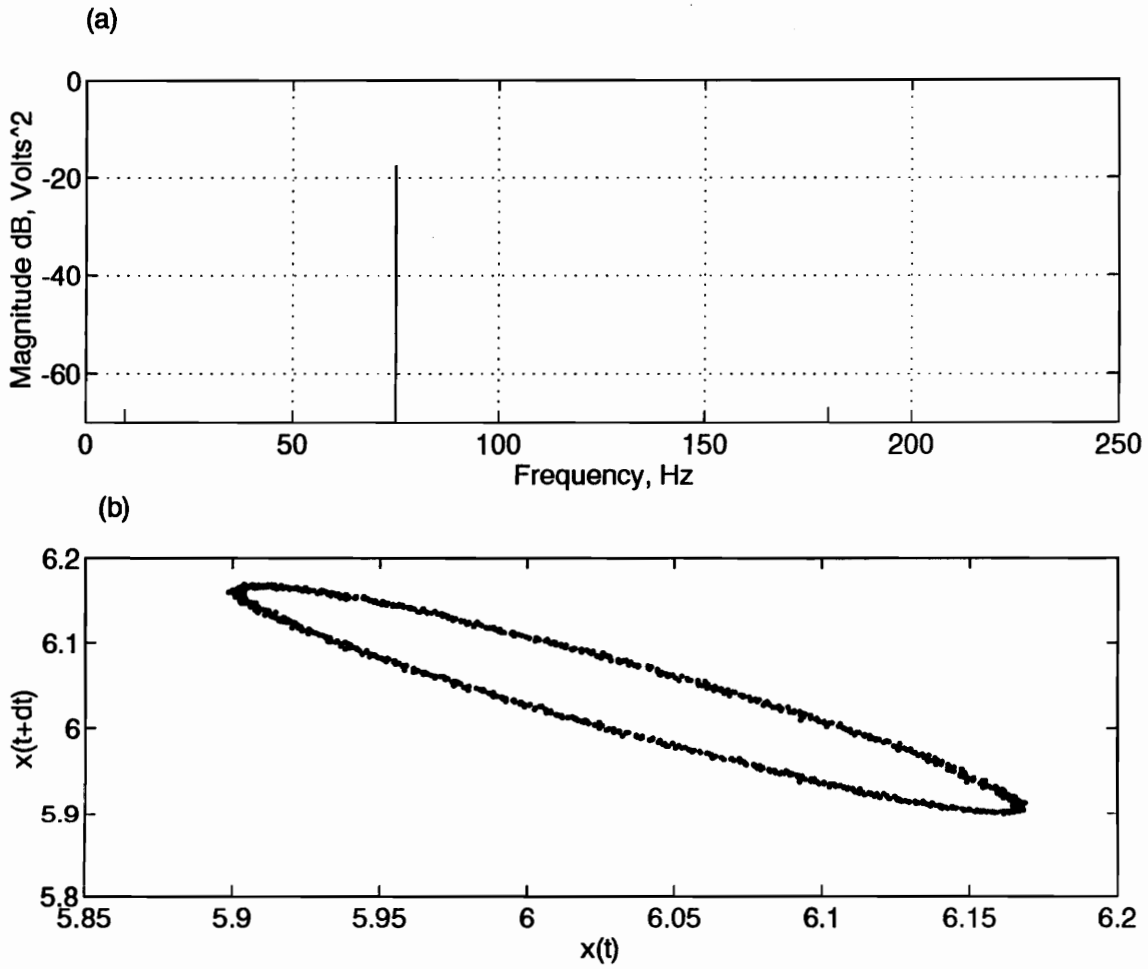

Figure 6.2 (a) Power spectrum and (b) pseudo-state portrait at point A.

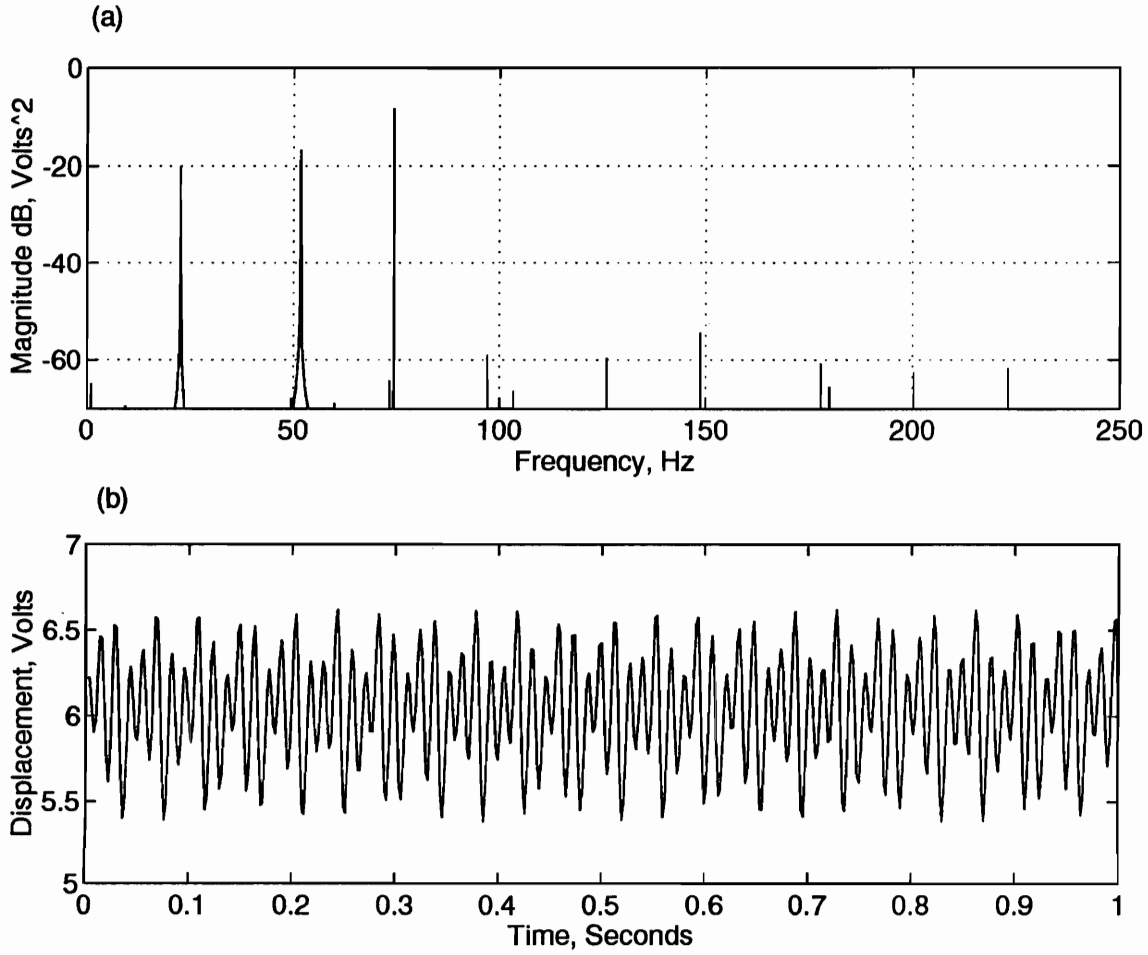

Figure 6.3 (a) Power spectrum and (b) time series at point B.

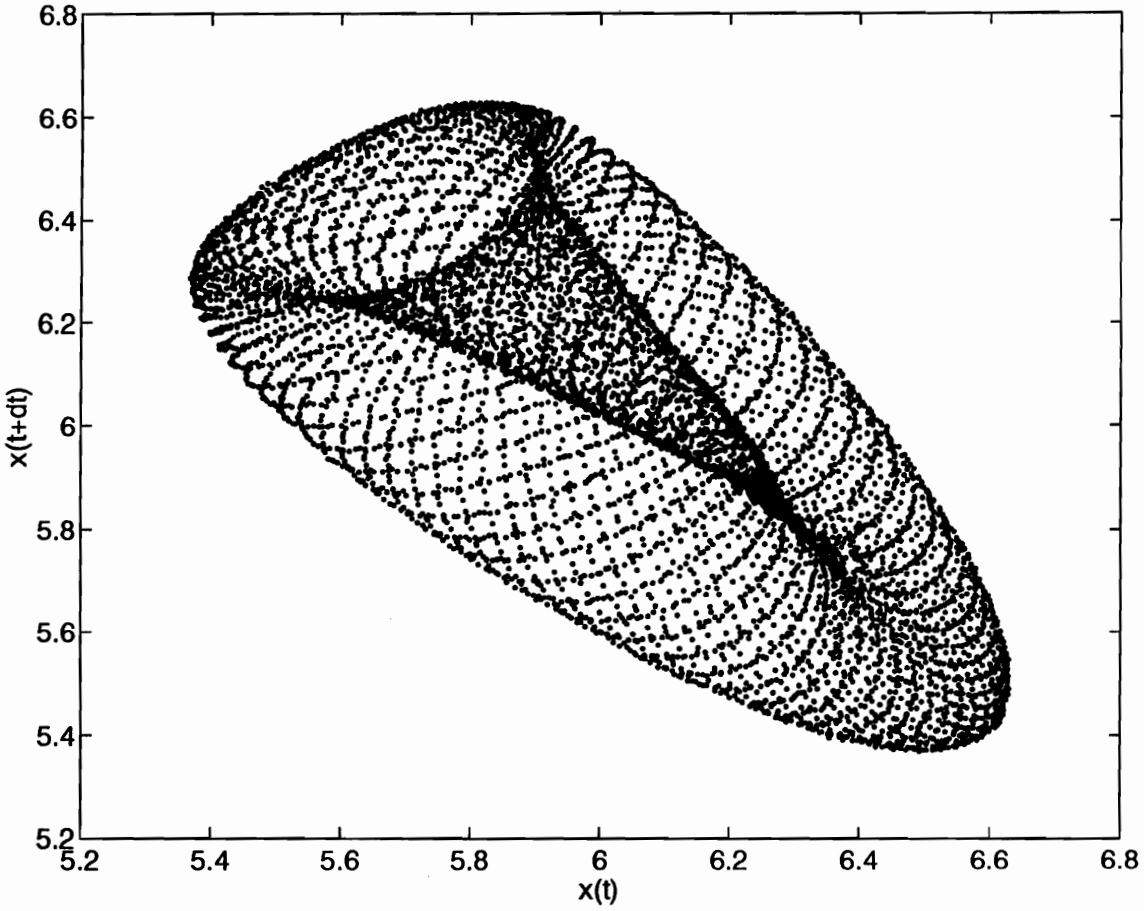

Figure 6.4 Pseudo-state plane at point B.

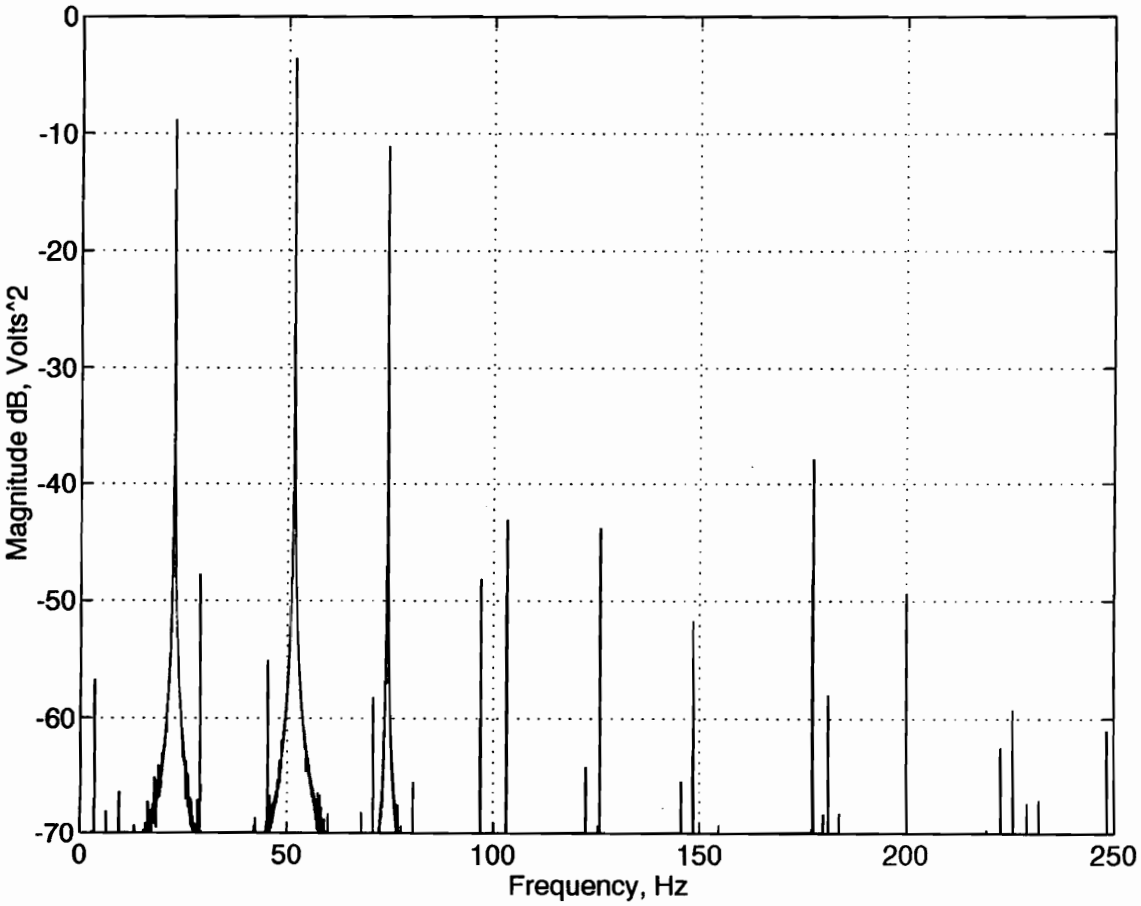

Figure 6.5 Power spectrum at point C.

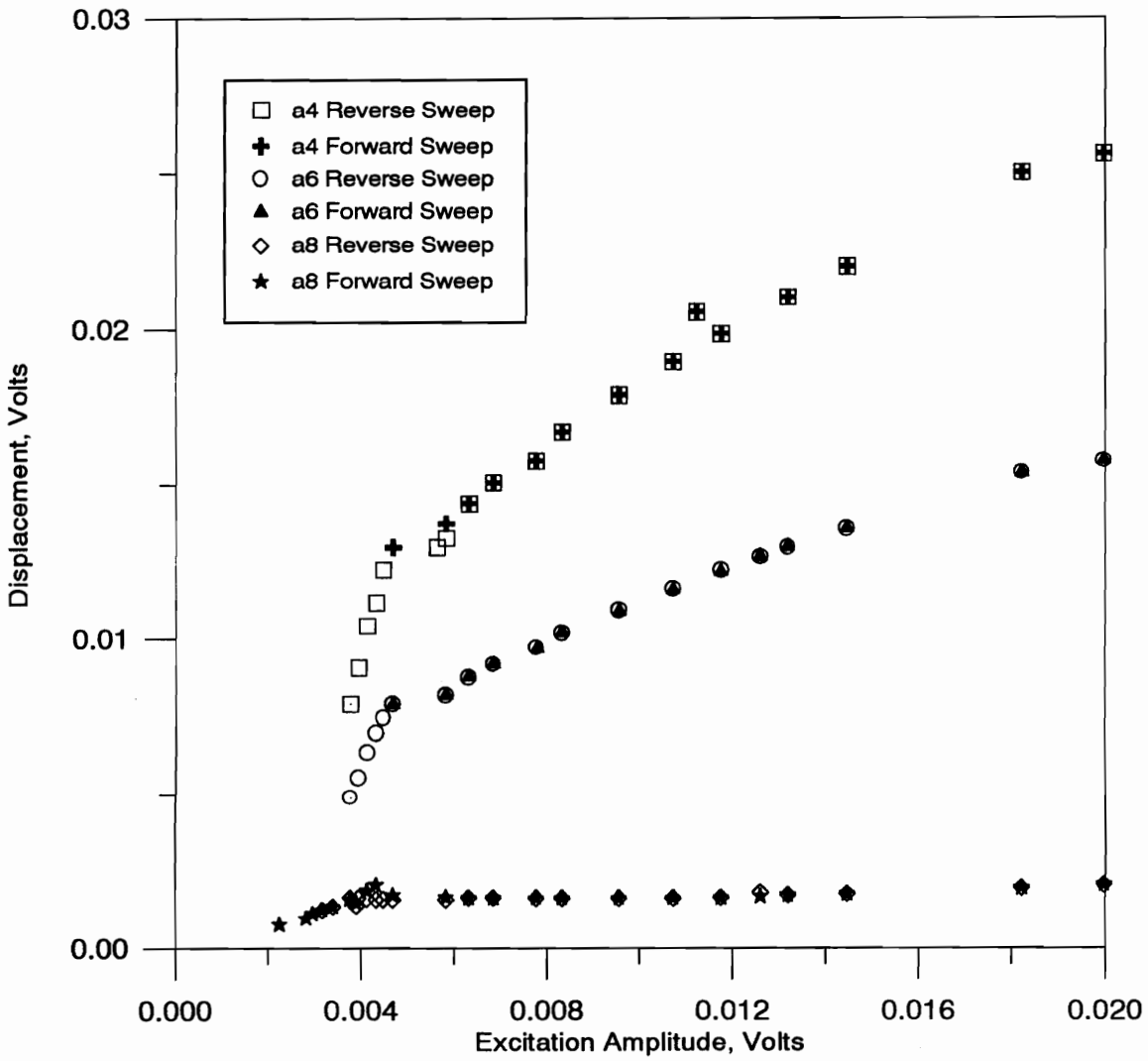

Figure 6.6 Amplitude-response curves for an excitation frequency of 74.06 Hz.

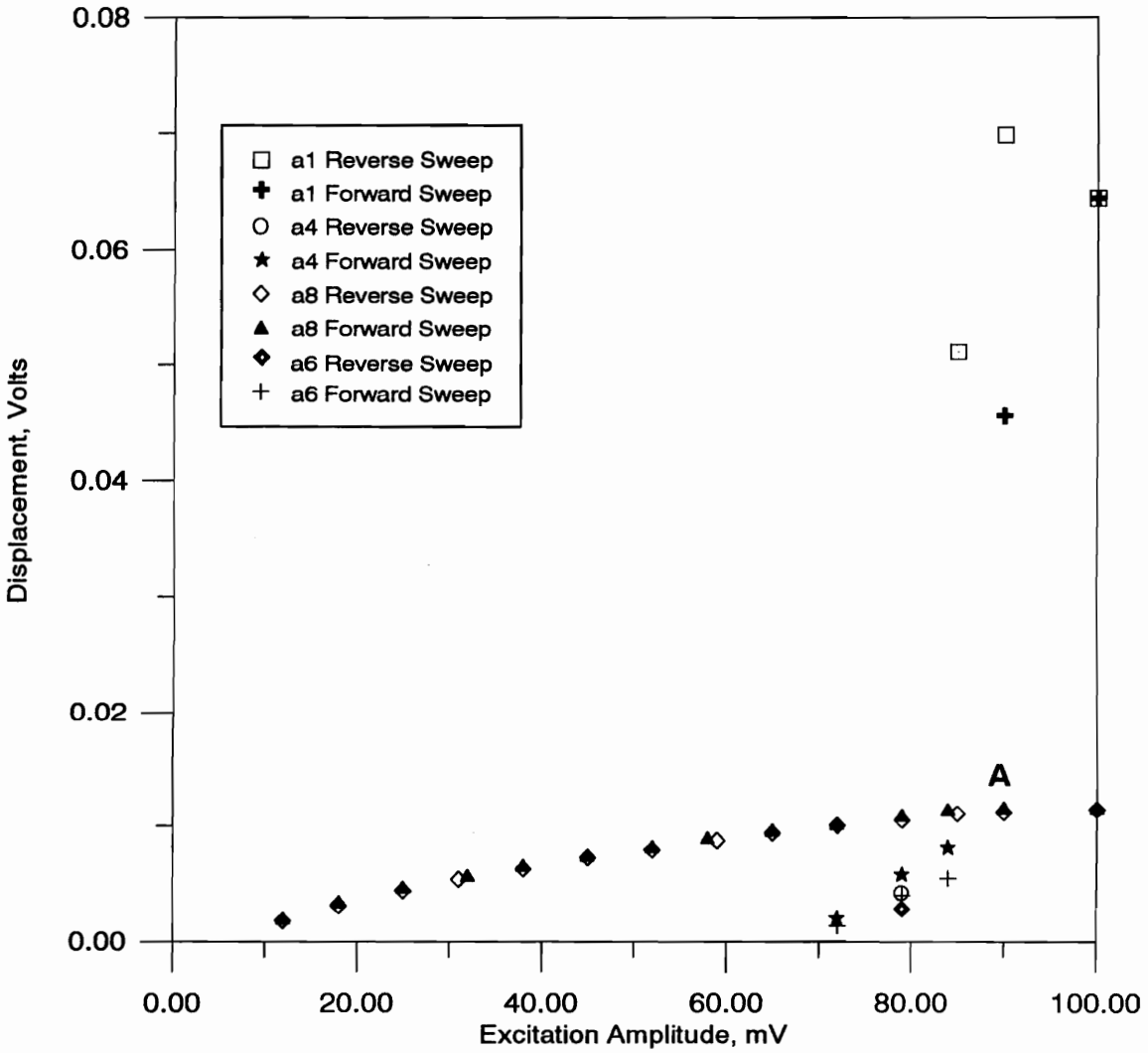

Figure 6.7 Amplitude-response curves for an excitation frequency of 74.50 Hz.

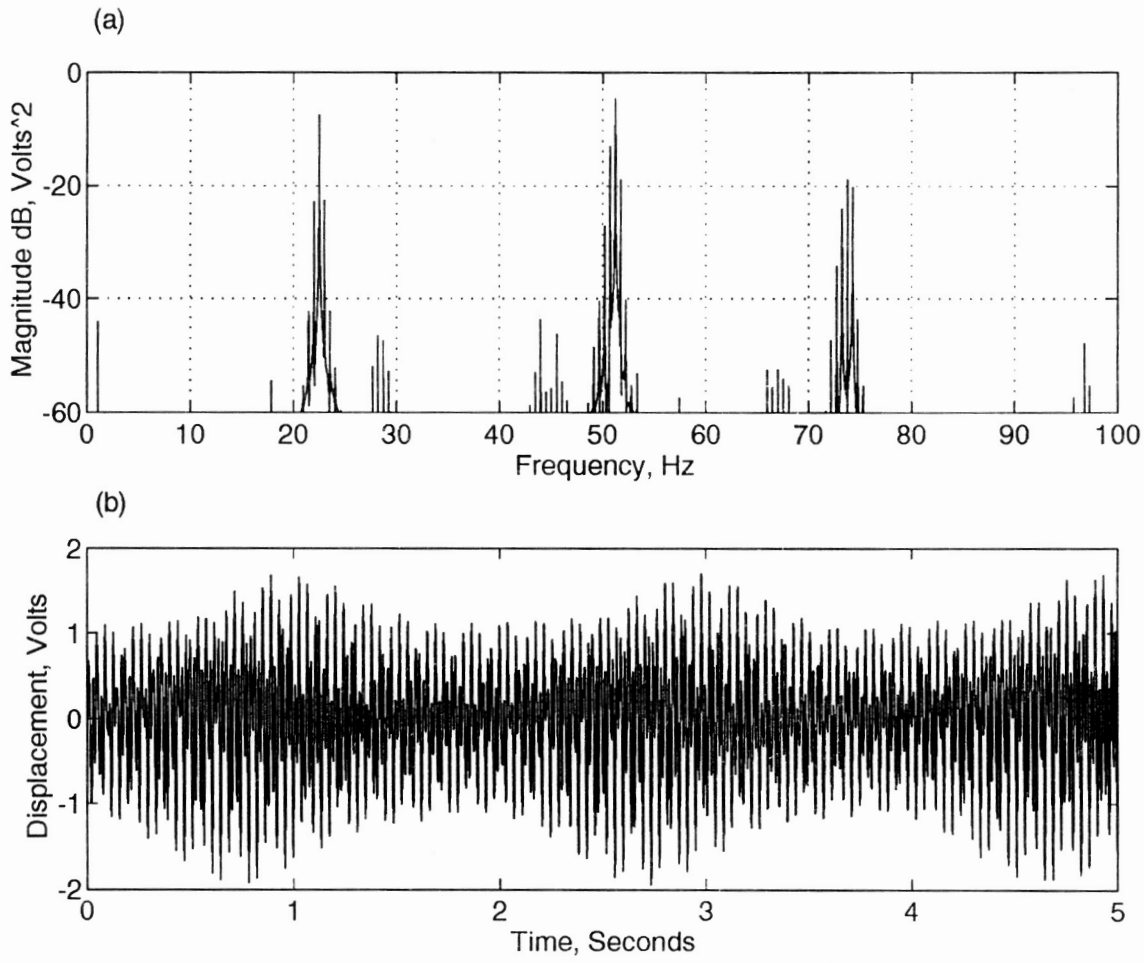

Figure 6.8 (a) Power spectrum and (b) time series of motion at point A.

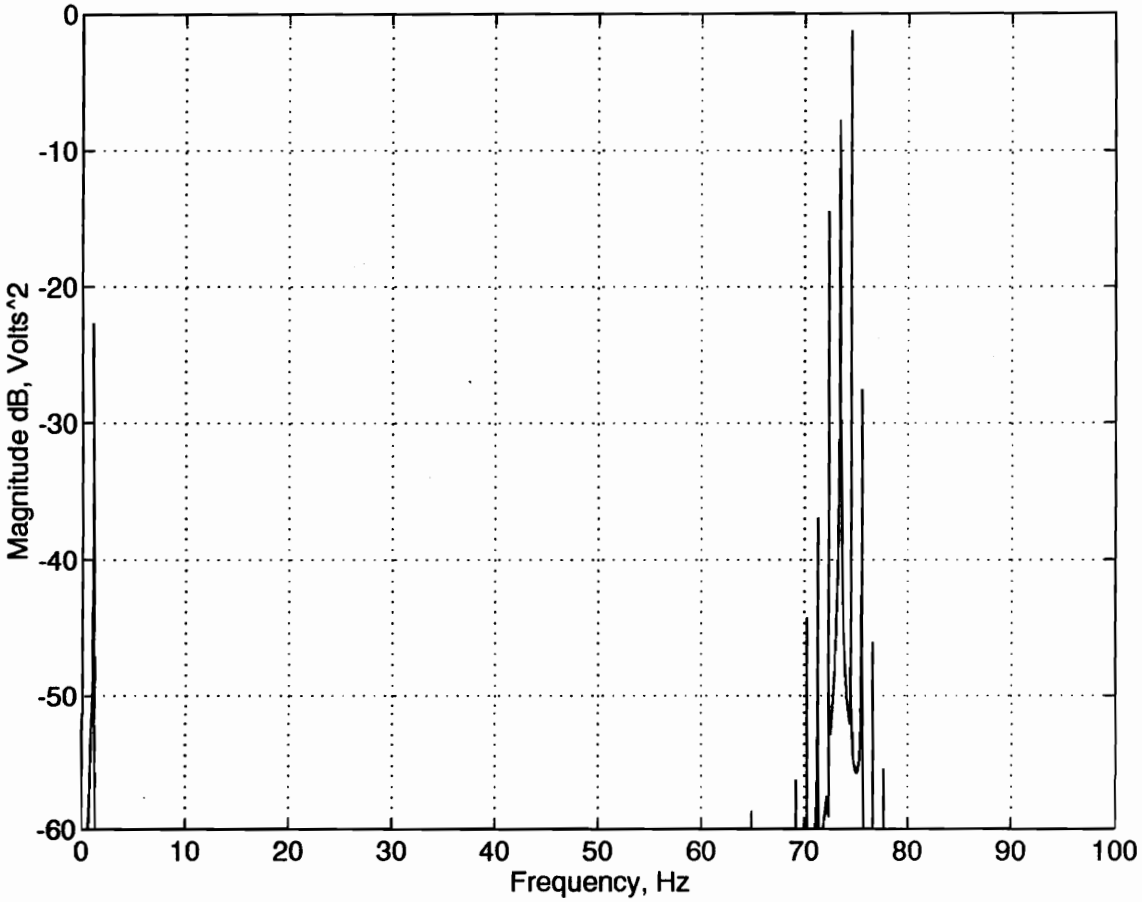

Figure 6.9 Power spectrum of the long-term behavior of the response at point A.

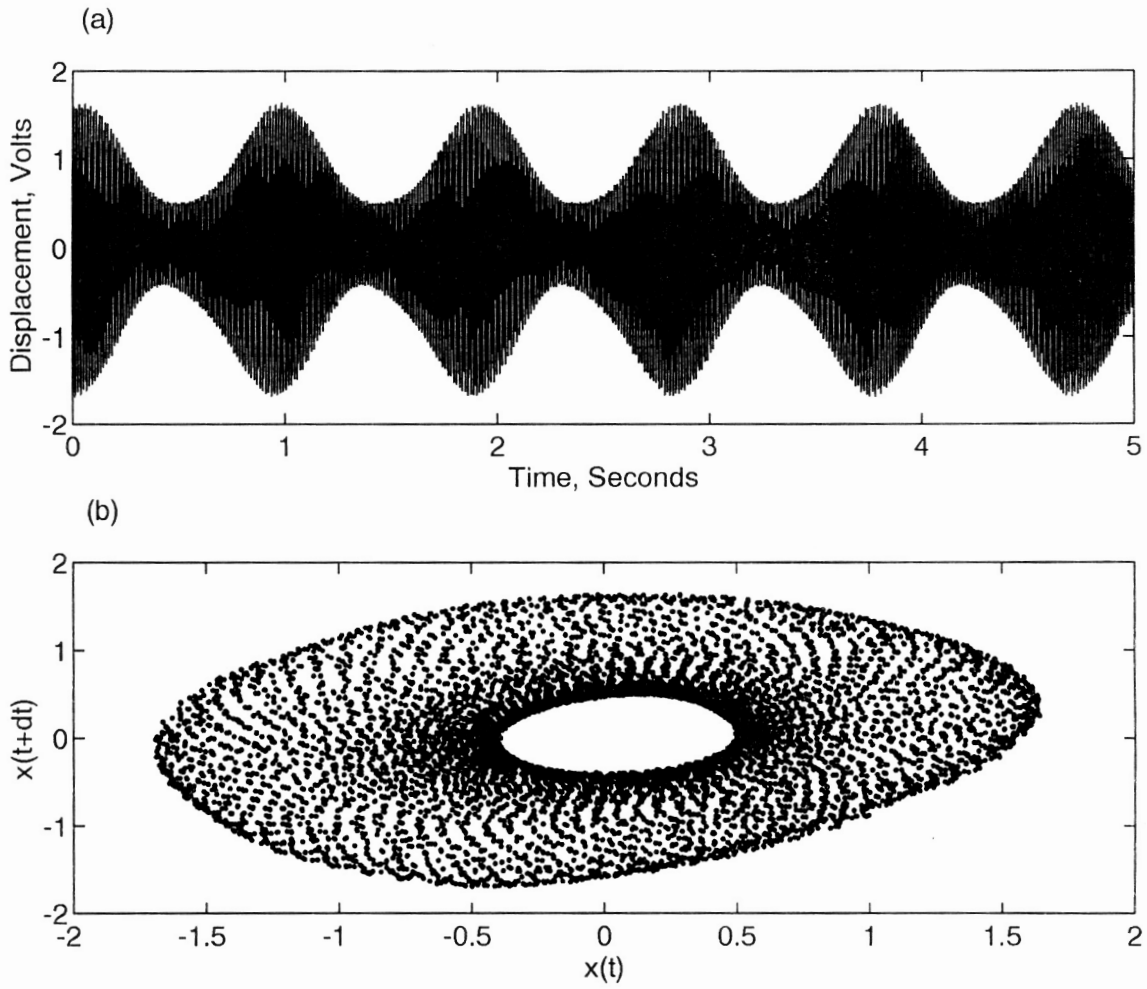

Figure 6.10 (a) Time trace and (b) pseudo-state plane for the motion at point A.

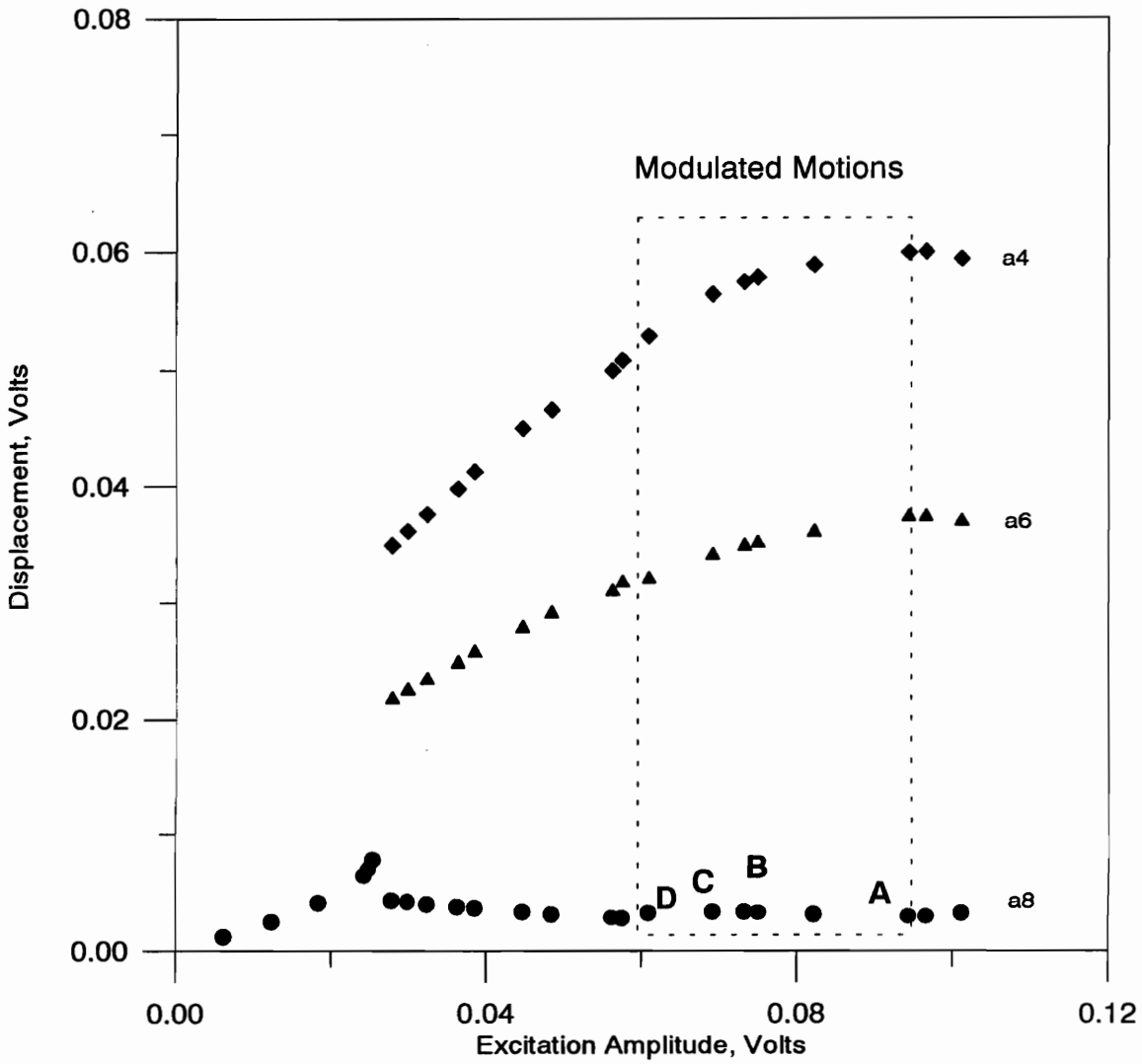

Figure 6.11 Amplitude-response curves at an excitation frequency of 73.62 Hz.

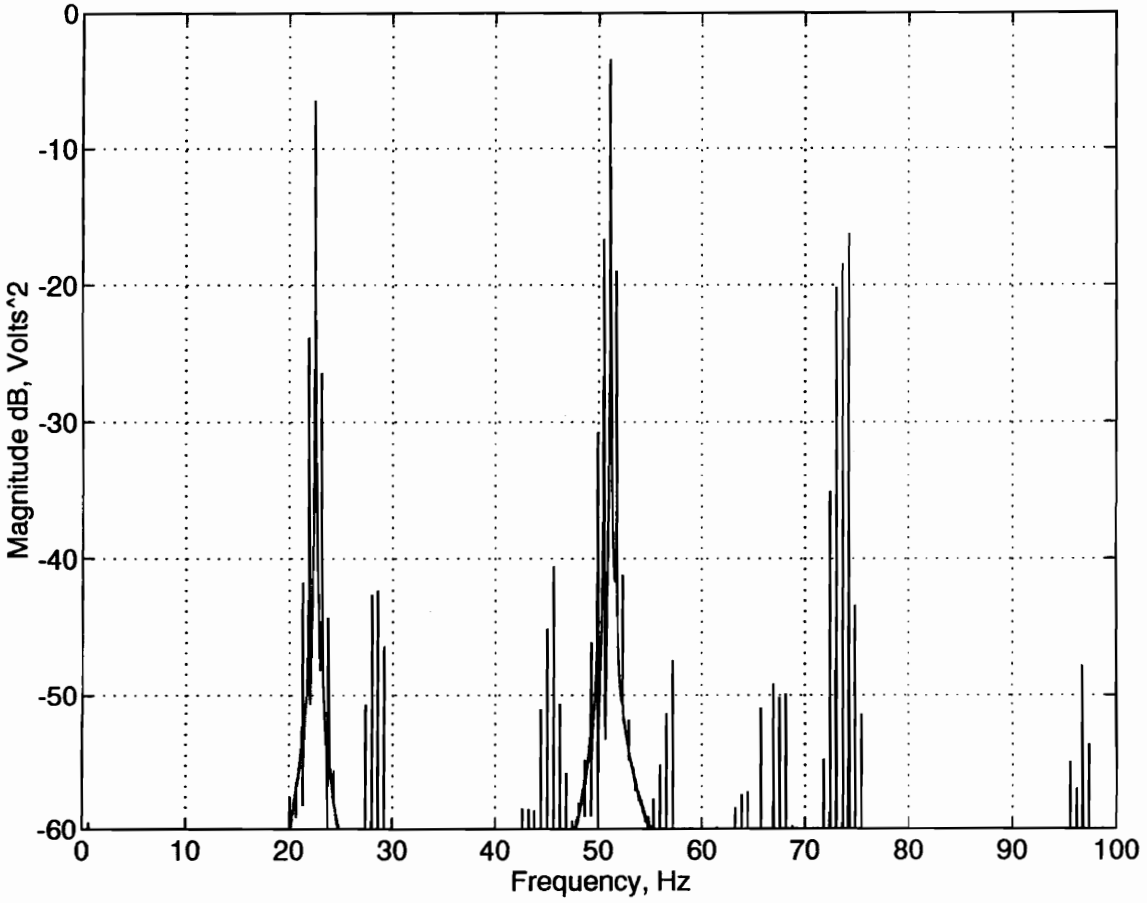

Figure 6.12 Power spectrum of the response at point A.

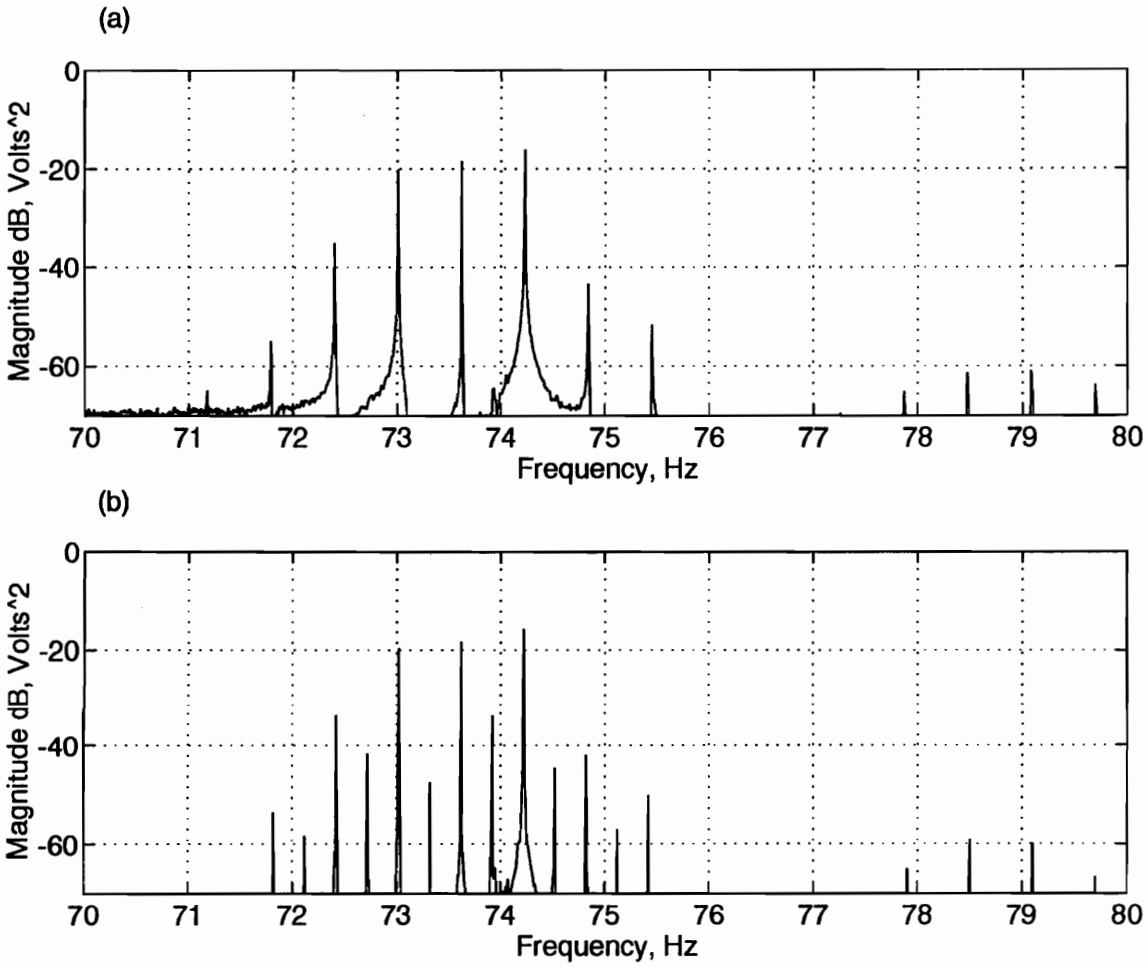

Figure 6.13 Power spectrum (zoom) of the motion at (a) point A, (b) point B, (c) point C, and (d) point D.

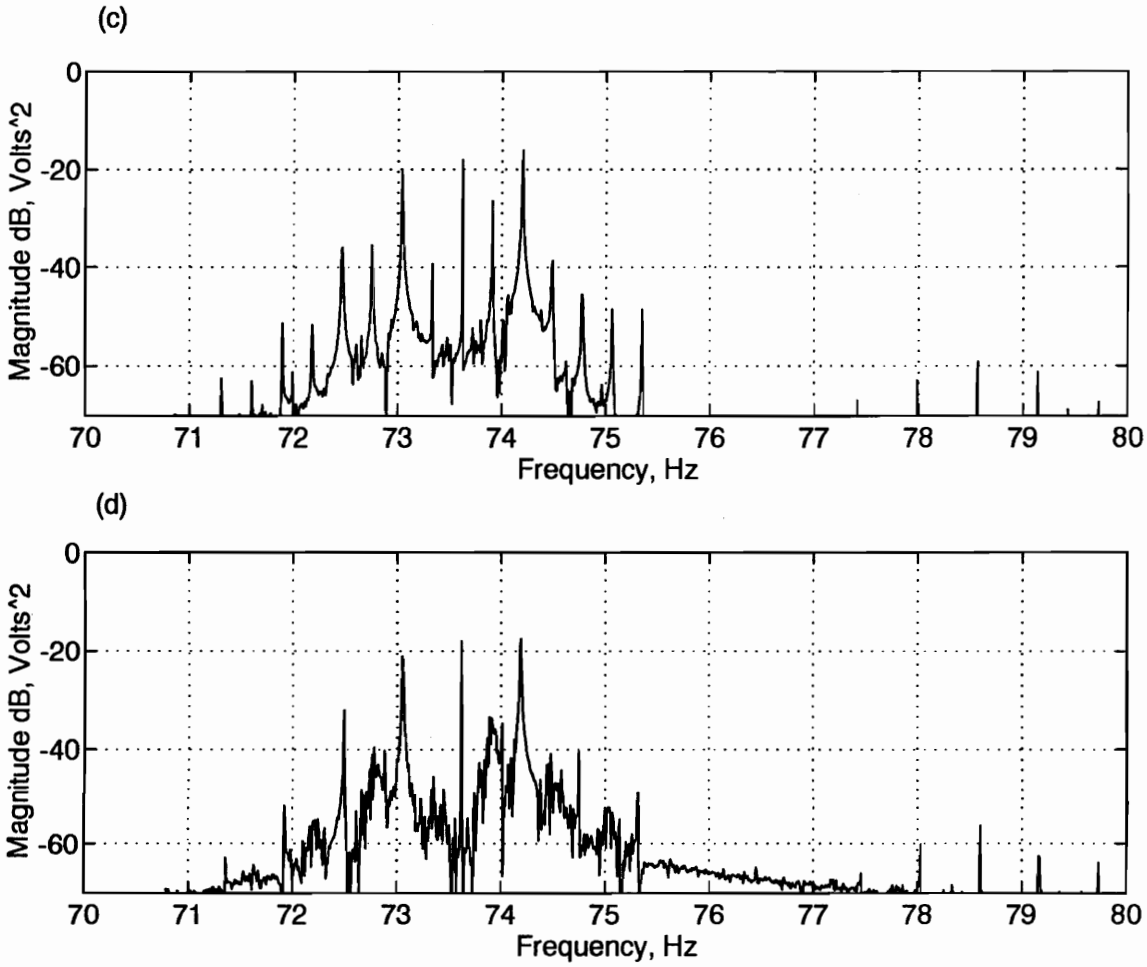

Figure 6.13 Continued

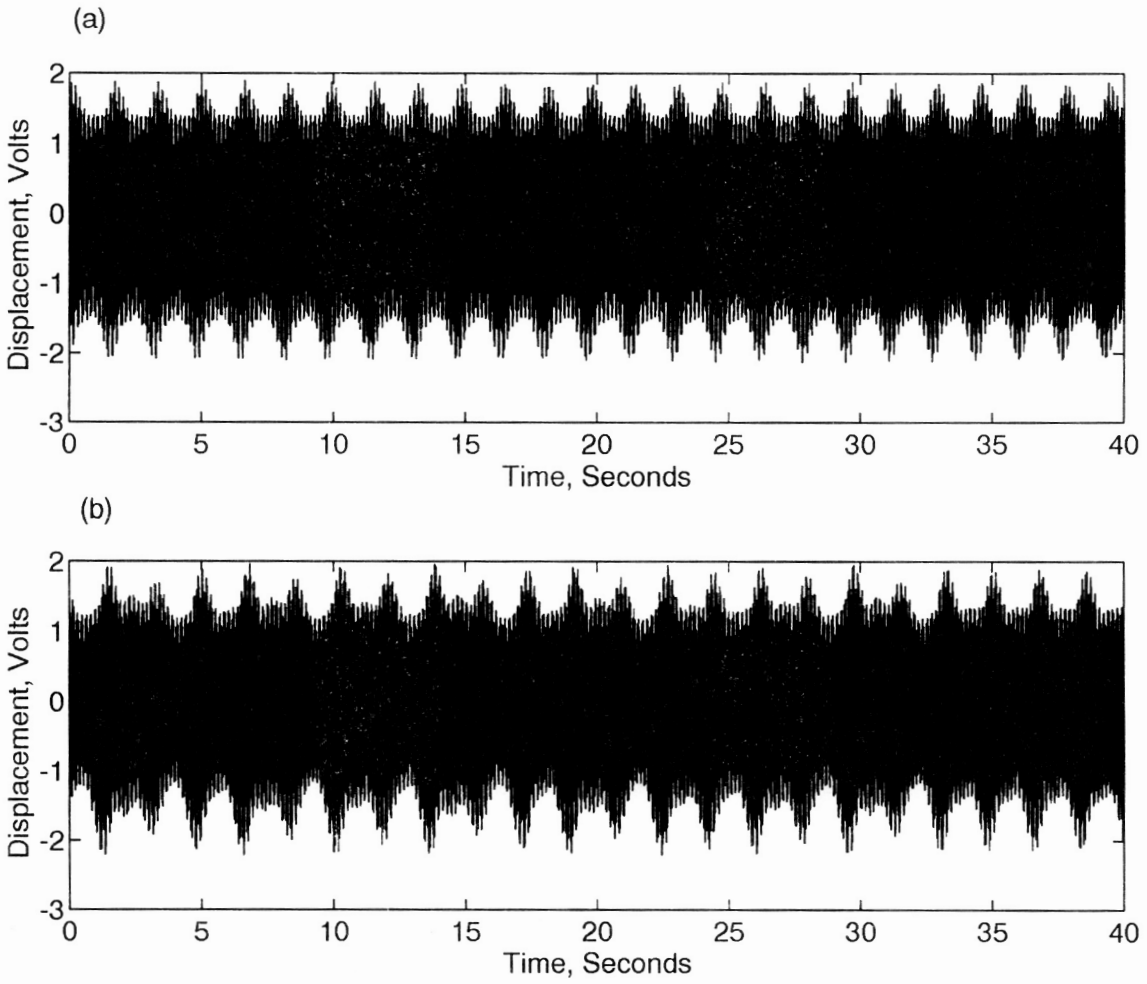

Figure 6.14 Time series for motions at (a) point A and (b) point D.

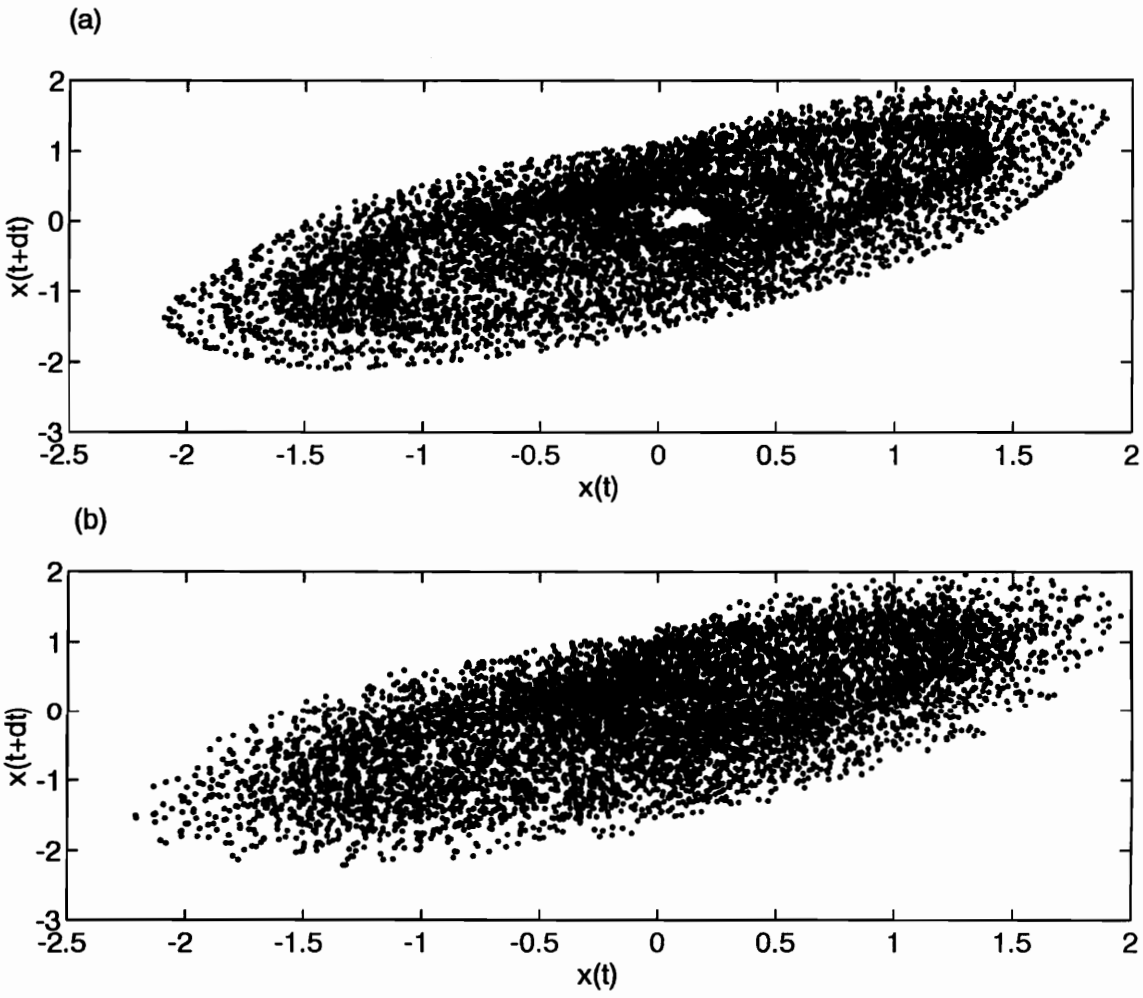

Figure 6.15 Pseudo-state planes for motions at (a) point A and (b) point D.

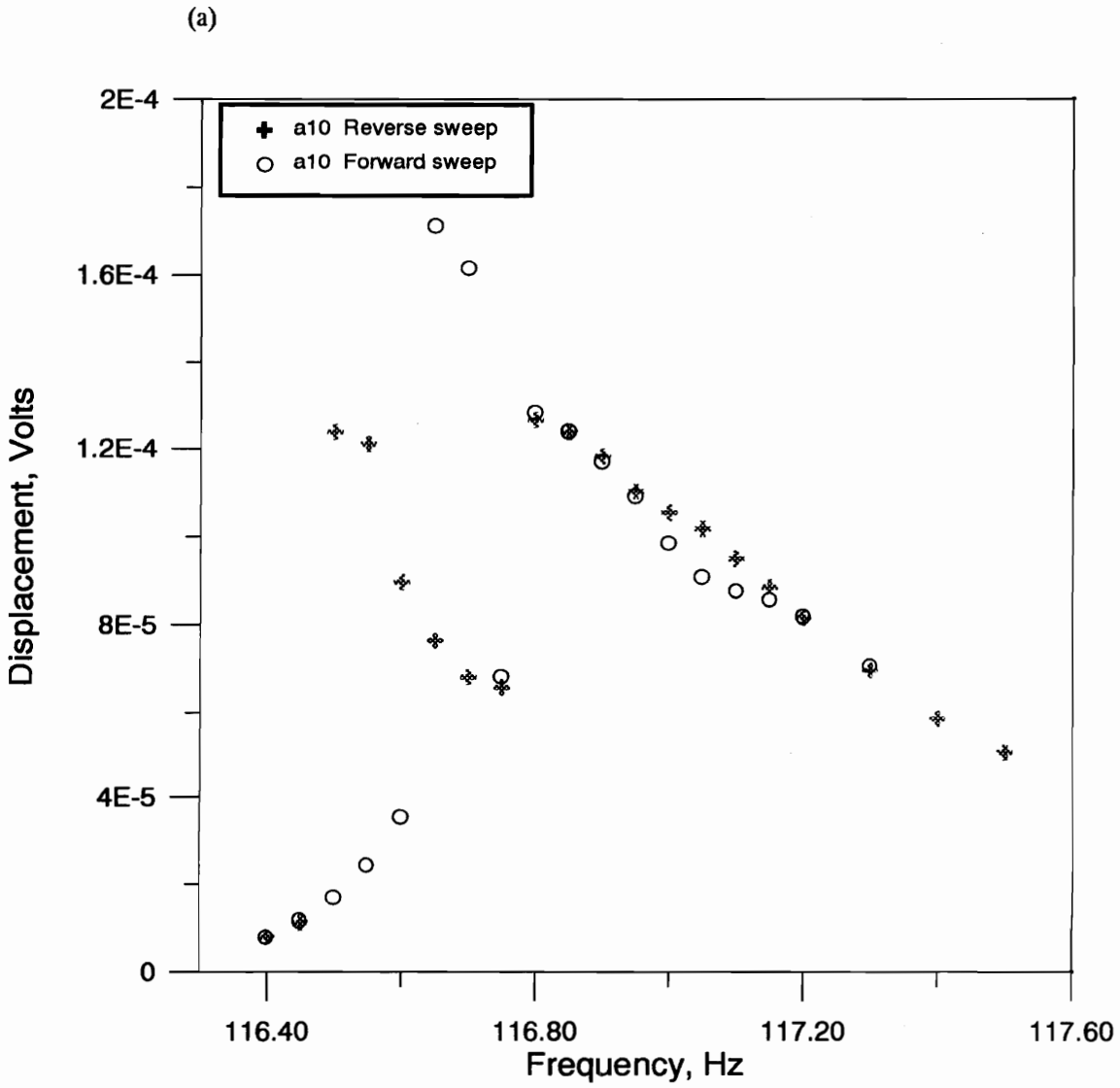

Figure 6.16 Frequency-response curves for an excitation amplitude of 0.2 *g*. (a) amplitude of the tenth mode. (b) amplitudes of the seventh and eleventh modes, (c) amplitude of the eighth mode, (d) amplitudes of the fifth and fourth modes, and (e) amplitude of the sixth mode.

(b)

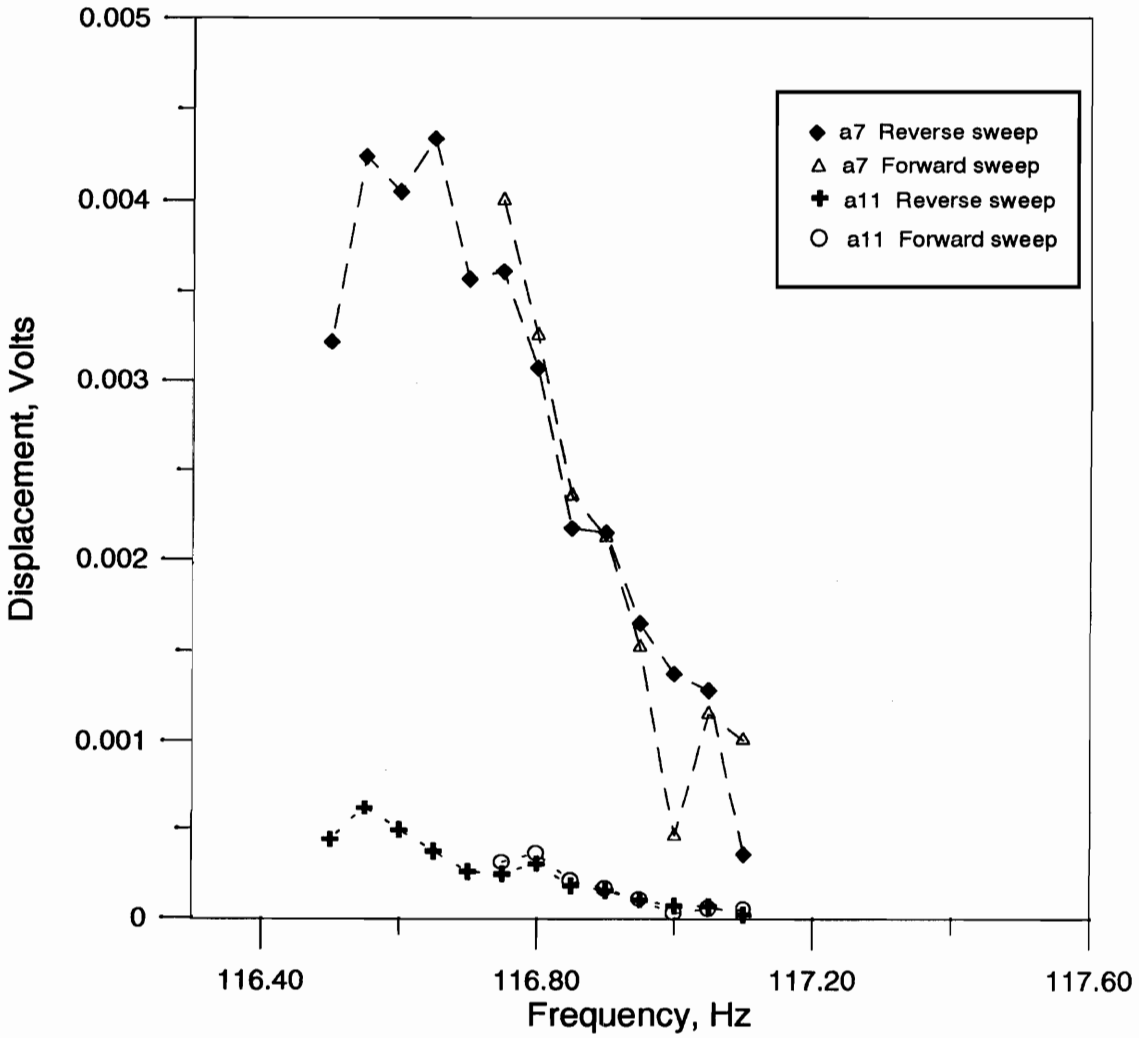

Figure 6.16 Continued

(c)

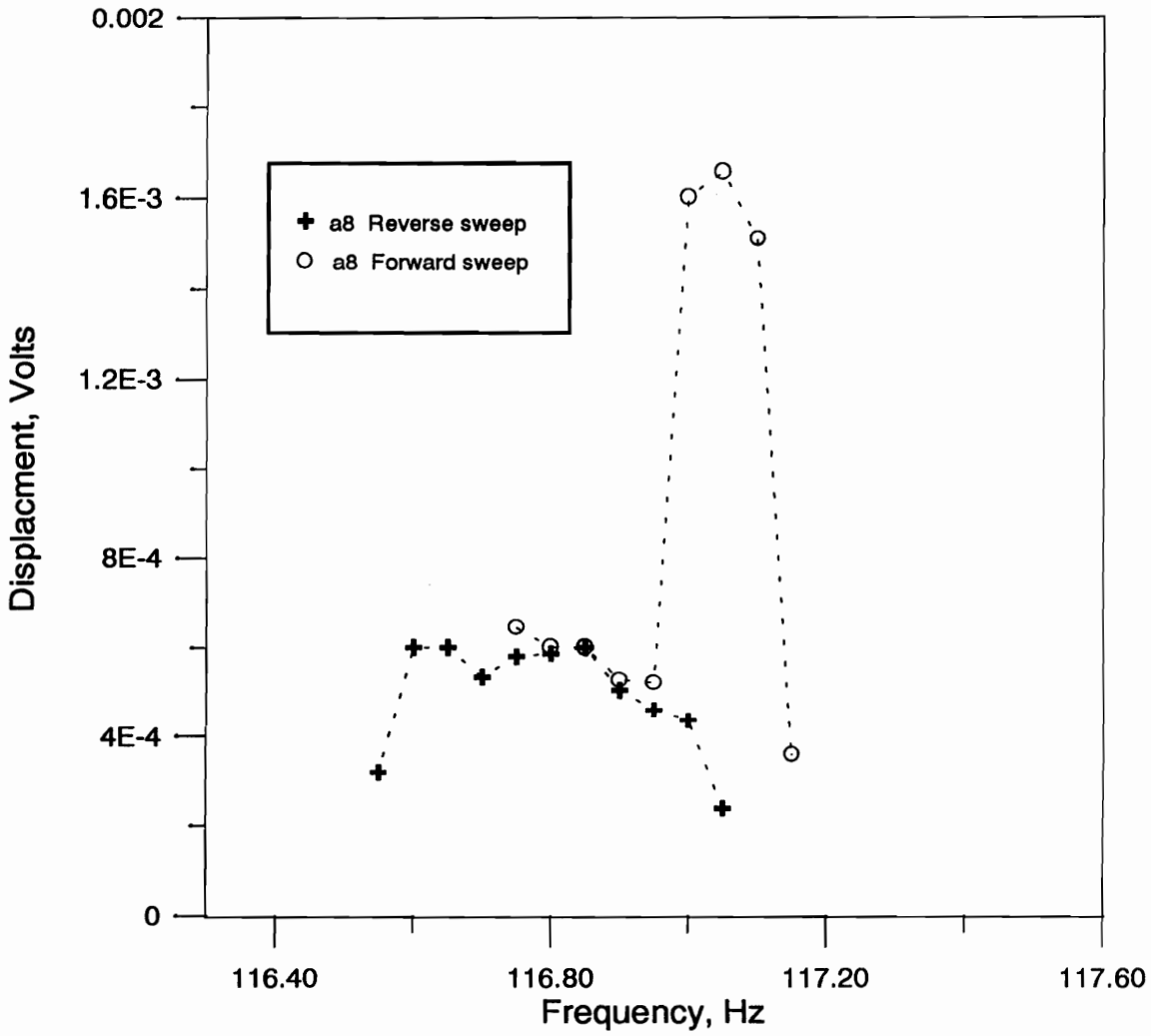

Figure 6.16 Continued

(d)

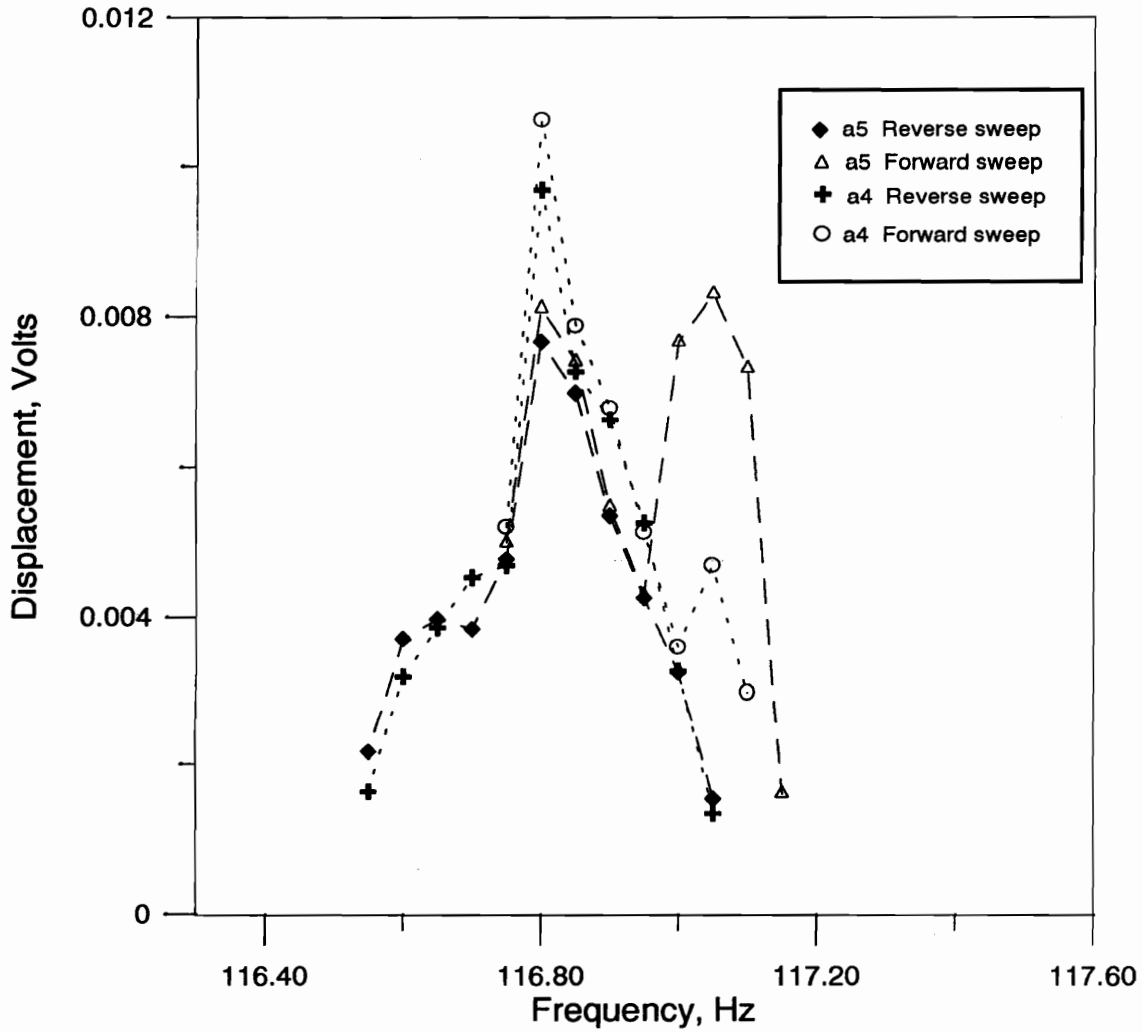

Figure 6.16 Continued

(e)

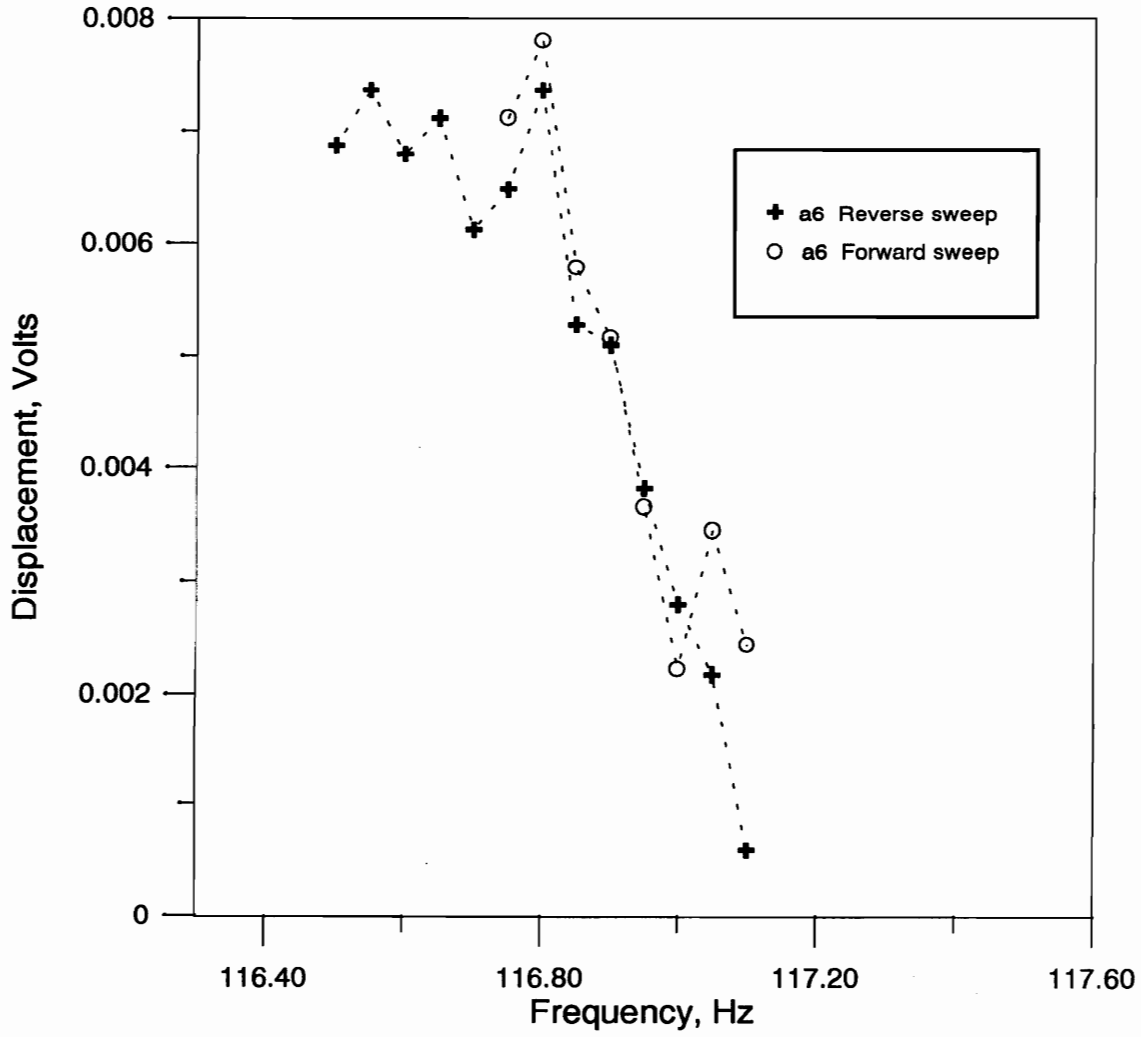

Figure 6.16 Continued

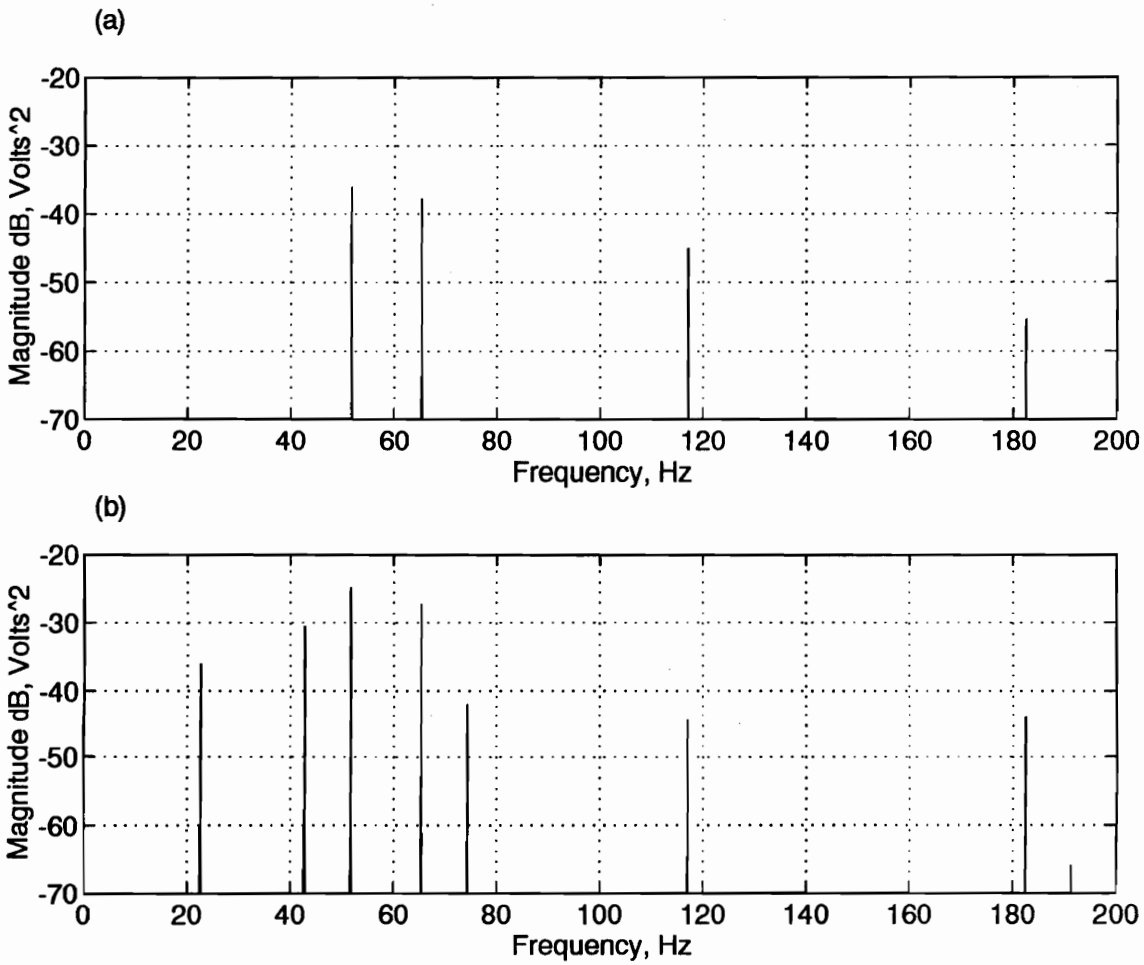

Figure 6.17 Power spectrum of the response at (a) 117.10 Hz and (b) 117.05 Hz.

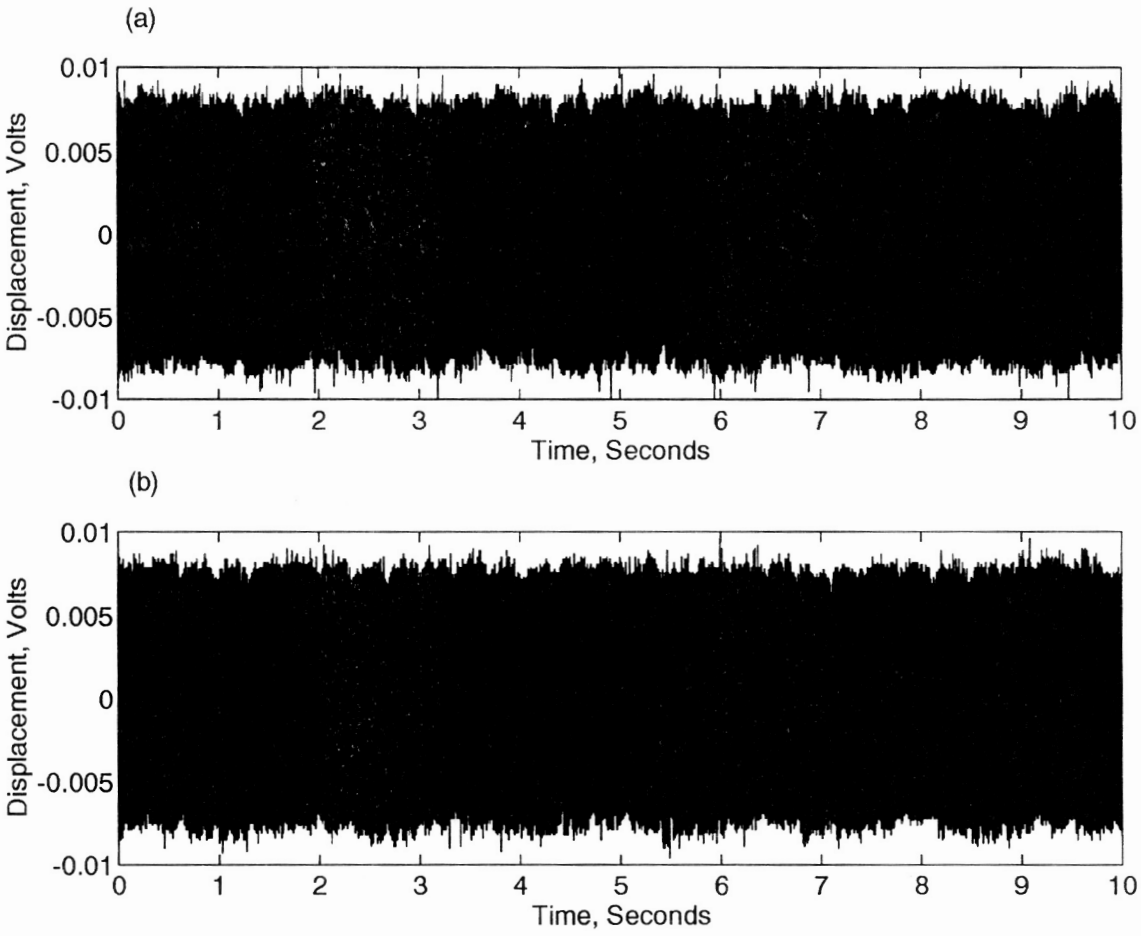

Figure 6.18 Time series of the response at (a) 117.10 Hz and (b) 117.05 Hz.

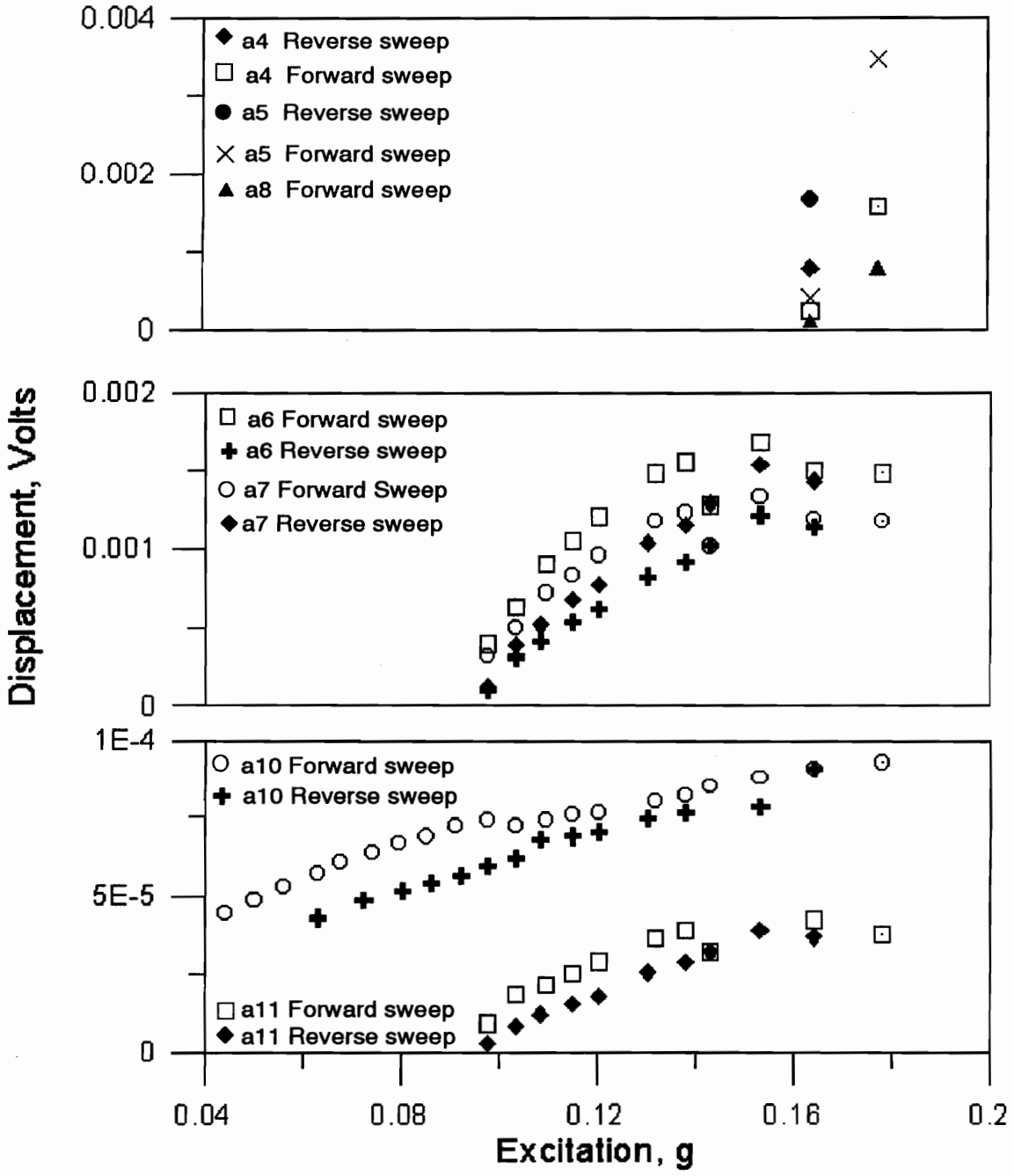

Figure 6.19 Amplitude-response curves at an excitation frequency of 117.19 Hz.

CHAPTER SEVEN

Parameter Identification of Nonlinear Systems

'Prediction is very difficult, especially about the future' Niels Bohr

The previous chapters covered the topic of studying and predicting the nonlinear response of beam and multibeam systems. This final chapter delves into the topic of parameter identification. This is an inverse process, in that, the response of a structure is used to ascertain numerical values of its parameters. The method of multiple scales together with a set of forcing amplitude sweeps allow for an accurate identification of the nonlinear parameters in a mathematical model of a structure. The specific example of a portal frame is used.

7.1 INTRODUCTION

Mathematical models of certain nonlinear phenomena have proven quite powerful in the prediction of nonlinear phenomena observed in experiments. The complexity of nonlinearity, however, requires the joint insights provided by experiment and theory. One area where experimentation coupled with theoretical modeling can improve the quality of data is the parameter identification. Nayfeh (1985) proposed a series of experiments designed to take advantage of the knowledge of certain idiosyncrasies of nonlinear phenomena and the powerful method of multiple scales to identify nonlinear parameters. Specifically, we intend to show that we can identify the parameters for a simplified nonlinear model of a portal frame. In this particular instance, we are also able to provide a measure of linear damping in addition to those

of the half-power point and logarithmic decrement methods.

7.2 EXPERIMENTAL SETUP

Figure 7.1 shows a schematic of the portal frame; it consists of three spring steel beams and two aluminum corner masses. The dimensions of the corner masses are 0.2413 x 0.0191 x 0.00089 *m*. The corner masses have dimensions of 0.0318 x 0.0318 *m* in the plane of the frame. A strain gage located about 0.0254 *m* from the base of one of the vertical beams measured the response of the frame. The experimental setup followed that of the portal frame experiments in Chapter 6 with the laser vibrometer replaced by the strain gage. The linear natural frequencies were found in the manner described in Chapter 5.

7.3 MATHEMATICAL MODEL

The dominant nonlinearity of the portal frame is quadratic for certain control parameter regions. The quadratic nonlinearity points to the possibility of subharmonic-resonance behavior. We intend to take advantage of the nature of the subharmonic resonance coupled with an analytical model to predict the system parameters. The generic mathematical model for a single-degree-of-freedom system with quadratic and cubic nonlinearities (Nayfeh, 1981) is

$$\ddot{u} + \omega_o^2 u + 2\mu\dot{u} + \alpha_2 u^2 + \alpha_3 u^3 = 2f\cos(\Omega t + \tau) \tag{7.1}$$

where u is the single-mode structural response, ω_o is its linear natural frequency, μ is related to the linear viscous damping coefficient, α_2 is the quadratic stiffness coefficient, and α_3 is the cubic stiffness coefficient. The term on the right-hand side represents a harmonic external excitation. Though we mentioned that the primary nonlinearity is quadratic, we must always keep in mind that this is only an approximation. In nonlinear system studies, the nonlinearity is in general expanded in a polynomial form which is the most amenable to mathematical analysis.

The lowest order is quadratic. However, depending upon the values of the control parameters, higher-order nonlinearities may gain in influence. For this reason, we have included the next highest-order nonlinearity, which is cubic, for the purpose of an improved model. Next, conditions for the activation of a subharmonic resonance of order one-half (for the case of weak nonlinearity and light damping) require that the excitation frequency Ω is nearly twice the linear natural frequency. The resulting solution is given by (Nafyeh, 1985)

$$u = a\cos(\omega_o t + \beta) + \{\frac{\alpha_2 a^2}{6\omega_o^2}[\cos(2\omega_o t + 2\beta) - 3] + \frac{2f}{\omega_o^2 - \Omega^2}\cos(\Omega t + \tau)\} + \ldots \qquad (7.2)$$

where the amplitude and phase variations are governed by

$$\dot{a} = -\mu a + \frac{\alpha_2 fa}{3\omega_o^3}\sin\gamma \qquad (7.3a)$$

$$a\dot{\beta} = \frac{9\omega_o^2\alpha_3 - 10\alpha_2^2}{24\omega_o^3}a^3 - \frac{\alpha_2 fa}{3\omega_o^3}\cos\gamma \qquad (7.3b)$$

and

$$\gamma = \tau + \sigma t - 2\beta = \tau + \Omega t - 2(\omega_o + \beta) \qquad (7.4)$$

with σ being a small detuning parameter.

The general procedure is to first determine the fixed points of Eqs. (7.3) which, according to Eq. (7.2), correspond to periodic motions. It is these fixed points, if stable, that are observable in an experiment. The locus of all fixed points can be found from combining Eqs. (7.3) into one equation. This equation, the frequency-response equation, is found to be

$$\left(\frac{3\mu\omega_o^3}{\alpha_2}\right)^2 + \left(\frac{\delta_1 a^2 - \sigma}{\delta_2}\right)^2 = f^2 \qquad (7.5)$$

where

$$\delta_1 = \frac{9\omega_o^2\alpha_3 - 10\alpha_2^2}{12\omega_o^3} \text{ and } \delta_2 = \frac{2\alpha_2}{3\omega_o^3}.$$

To complete our formulation, it is necessary to consider the stability of the fixed points. Only the stable fixed points are observable in an experiment. Now for the subharmonic, the modulation equations have two solutions, a trivial (no subharmonic response) and a nontrivial (subharmonic) response. The polar form is convenient for studying the stability of motions for the subharmonic response. Bypassing the details, for stable subharmonic motions, we find that

$$\left(\frac{9\omega_o^2\alpha_3 - 10\alpha_2^2}{24\omega_o^3}\right)^2 a^2 - \sigma\left(\frac{9\omega_o^2\alpha_3 - 10\alpha_2^2}{24\omega_o^3}\right) > 0 \tag{7.6}$$

where a is the amplitude of the subharmonic response. For the stability of the trivial solution, the Cartesian form of the modulation equations is applicable. Again, skipping the details of the Cartesian transformation, we find that the trivial solution is unstable in a frequency region defined by

$$2\omega_o - \sqrt{\left(\frac{\alpha_2 f}{3\omega_o^3}\right)^2 - \mu^2} < \Omega < 2\omega_o + \sqrt{\left(\frac{\alpha_2 f}{3\omega_o^3}\right)^2 - \mu^2}\,. \tag{7.7}$$

One immediate observation is that the phase of the response is algebraically removed and only a measure of the response amplitude is required. Now, we take advantage of another feature of the subharmonic resonance, namely, the jump points. For excitation frequencies below the linear natural frequency, as the excitation amplitude is varied, the response experiences a sudden disproportionate change in amplitude. We have two such points, one leads to an upward jump and the other leads to a downward jump. Mathematically, we can find these points from the frequency-response equation. For the jump up point, we have

$$f_u = \frac{3\omega_o^2}{|\alpha_2|}\left[\frac{\omega_o^2}{4}\left(\Omega - 2\omega_o\right)^2 + \omega_o^2\mu^2\right]^{\frac{1}{2}} \tag{7.8}$$

and for the jump down point we find that

$$f_d = \frac{3\mu\omega_o^3}{|\alpha_2|} \quad . \tag{7.9}$$

We note that the jump up and down points depend on the coefficient of the quadratic term and the damping term but do not depend on the coefficient of the cubic term. These equations provide the basis for a parameter identification method, which is described in the next section.

7.4 PARAMETER IDENTIFICATION

A series of experiments were designed to estimate the damping and nonlinear coefficients. In this section, we describe two different sets of experiments that allow for the estimation of the nonlinear coefficients.

7.4.1 METHOD 1

The first method relies only on the need to calculate a series of jump up points to determine the quadratic stiffness coefficient. It follows from Eq. (7.8) that two different values of the jump up points can be used to estimate the linear viscous damping coefficient. The linear natural frequency and linear viscous damping are parameters usually found from a linear modal analysis. The linear viscous damping coefficient, in particular, can be found from either the half-power point method or the logarithmic decrement method. Here, we propose an additional method to estimate the linear viscous damping coefficient.

The jump up points can be found by changing the detuning parameter. The following equation allows for the estimation of the linear damping coefficient:

$$\mu^2 = \frac{f_u^{**2} g_2^{*} - f_u^{*2} g_2^{**}}{g_3 (f_u^{*2} - f_u^{**2})} \tag{7.10}$$

where

$g_2 = \frac{1}{4}\omega_o^2(\Omega - 2\omega_0)^2$ and $g_3 = \omega_o^2$. The superscripts * and ** denote two different values of the jump up excitation amplitude corresponding to two different values of Ω. Therefore, an

experiment, where the forcing frequency is fixed and the forcing amplitude is slowly varied is required. Once a jump up point has been determined, the experiment is rerun for a different value of the forcing frequency. With two such values the linear damping coefficient can be found from Eq. (7.10). This is an important point. Once the linear viscous damping coefficient is found, it can then be used to calculate the square of the quadratic coefficient by using the relation

$$\alpha_2^2 = \frac{9\omega_o^4}{f_u^{*2}}(g_2^* + g_3\mu^2). \tag{7.11}$$

Finally, the cubic coefficient can be found from the frequency-response equation, Eq. (7.5), by using the amplitude of the response at only one point after the jump up point. We note that the linear viscous damping coefficient will necessarily be positive and that the sign of the quadratic coefficient is undetermined in Eq. (7.11) but found by examining the sign of the drift term in Eq. (7.2).

7.4.2 METHOD 2

The second method involves conducting an entire forcing amplitude sweep. Again, at a set forcing frequency (nearly twice the natural frequency of interest), the forcing amplitude is slowly increased until the trivial solution loses stability and a jump to a large-amplitude periodic motion occurs. This represents the jump up point. Then from this point, the forcing amplitude is slowly decreased until the response jumps down to the trivial motion. This represents the jump down point. The jump up and down points are sufficient to determine the linear viscous damping coefficient and the quadratic coefficient from Eqs. (7.8) and (7.9) while the cubic stiffness coefficient and the sign of the quadratic stiffness coefficient can again be found through Eqs. (7.5) and (7.2).

7.5 RESULTS

In this section, we present the parameters identified for the portal frame described in Section 7.2. We used the frame to test both methodologies outlined in the previous section. Method 1 is used to identify the parameters of the frame for the first mode. These parameters are then used to predict the occurrence of other jump points for various values of the detuning as a check on the accuracy of these parameter values. Method 2 is used to identify the parameters of the frame for the second mode. For validation, we use the identified parameter values to predict a typical frequency-response curve.

7.5.1 SUBHARMONIC RESONANCE OF THE FIRST MODE

For the frame under consideration, we found the first linear natural frequency to be 3.79 Hz. Following Method 1, we only documented the jump up points. The experimental procedure consisted of several runs. Each run began by setting the forcing frequency at a value slightly below that of twice the first natural frequency. Slowly increasing the forcing amplitude, we allowed for the decay of transients. When a steady state was reached, the forcing amplitude was further increased. The forcing amplitude was increased in this quasi-static manner until a point was reached were a large contribution from the first mode was apparent in the response of the structure. The power spectrum of the response data from the strain gage was the key element in identifying the activation of the subharmonic resonance. Once it was certain that the subharmonic resonance of order one-half was indeed activated, the forcing frequency was adjusted to a slightly smaller value. In this manner, we were able to change the detuning and continue with the experiment until the next jump point. Each run consisted of collecting the jump up forcing amplitudes for four different forcing frequencies. Three runs were performed for a total of 12 jump up points. The forcing amplitude from each run for a particular frequency detuning was then averaged. Table 7.1 lists the average forcing amplitude for four jump up points and their corresponding forcing frequencies. We use the jump up forcing amplitudes for points 1 and 2 to calculate the linear viscous damping coefficient from Eq. (7.10) and the

quadratic coefficient from Eq. (7.11). Solving Eqs. (7.10) and (7.11) yields $\mu = 0.008$ and $\alpha_2^2 \approx 146.89$. We also estimated the linear viscous damping coefficient by using the method of logarithmic decrement. The result is $\mu \approx 0.0086$, which is close to that estimated by applying the subharmonic resonance method.

Table 7.1 Jump up forcing amplitudes (Volts).

Point	Forcing frequency (Hz)	Jump up amplitude (Expt.)	Jump up amplitude (Predicted)
1	7.575	0.112	0.112
2	7.550	0.224	0.224
3	7.525	0.380	0.386
4	7.500	0.544	0.549

Next, we validate the identified parameter values by predicting the jump up forcing amplitudes for points 3 and 4 from Eq. (7.8). Table 7.1 shows that the experimentally identified parameters predict very well the subharmonic response of the frame (calibration constant for the accelerometer is 0.1 V/g).

7.5.2 SUBHARMONIC RESONANCE OF THE SECOND MODE

The second linear natural frequency for the frame was 24.35 Hz. Experiments designed based on Method 2 were used to identify the parameters for the second mode. In this case, one amplitude-response curve was generated (Figure 7.2). The jump up and down points were used to identify the linear viscous damping and quadratic coefficient from Eqs. (7.8) and (7.9). Then the amplitude of the second mode in a region of the subharmonic resonance was used to estimate the cubic coefficient through Eq. (7.5). From this procedure, we found that $\mu = 0.07$, $\alpha_2 = 5196.0$, and $\alpha_3 = 50593.0$. From the half-power point, we found that $\mu = 0.03$ for the second mode. Though the two values for damping are on the same order, the agreement is good (The half-power point is susceptible to measuring errors and the parameter

identification method may require more data points). To validate this procedure, we matched a typical experimentally obtained frequency-response curve with one based on the estimated parameter values. Figure 7.3 shows the observed and predicted frequency-response curves of the frame; the agreement is good. The second approach appears to work well without the need for detailed data gathering. More robust parameter values may be obtained with an increase in the number of data points.

7.6 CHAPTER REMARKS

This final chapter concerned parameter identification of nonlinear systems. We found that, for a structure, a methodology based on the subharmonic resonance can be useful to estimate some of its nonlinear parameters. In addition, we have found an additional tool that complements (and possibly surpasses) the half-power point and logarithmic decrement in estimating the linear viscous damping coefficient. Two different approaches have been presented that take advantage of the characteristics of the subharmonic resonance. In the first approach, one needs to record only a series of jump up points and one amplitude for the subharmonic response. In the second approach, however, one requires an entire amplitude sweep. This requires a very slow variation of the control parameter to insure that a steady state is reached. Furthermore, the activation of the subharmonic response usually implies large amplitudes. This was observed for the second mode. For this reason, not many data points were obtained. An entire frequency sweep exposes the structure to the possibility of early fatigue or damage can be considerable when nonlinear motions are activated. With the need for improved accuracy, experiments must be carried out more than once. These reasons make the first method more appealing and practical from the viewpoint of structural testing. An increase in the number of data points will improve the accuracy of either method. A major limitation on the number of data points (or control parameter increments) is the type of instrumentation used. However, we have shown that a

methodical and careful approach can lead to fairly accurate results in identifying parameters of a nonlinear system.

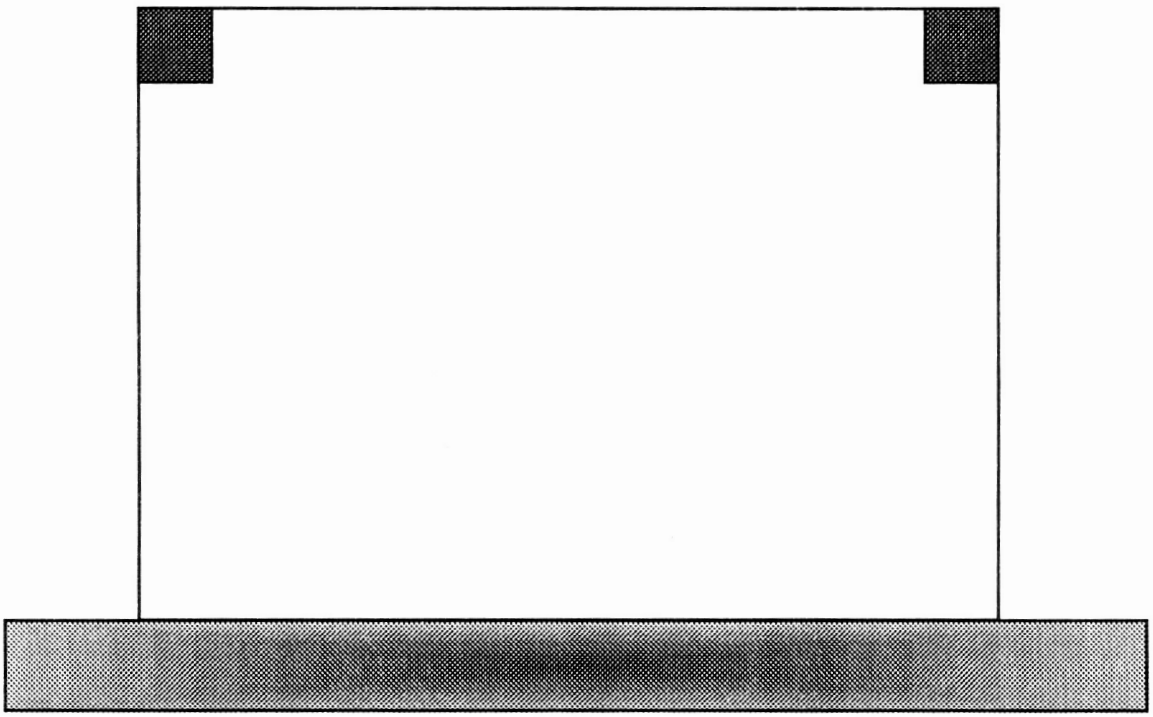

Figure 7.1 A schematic of the portal frame.

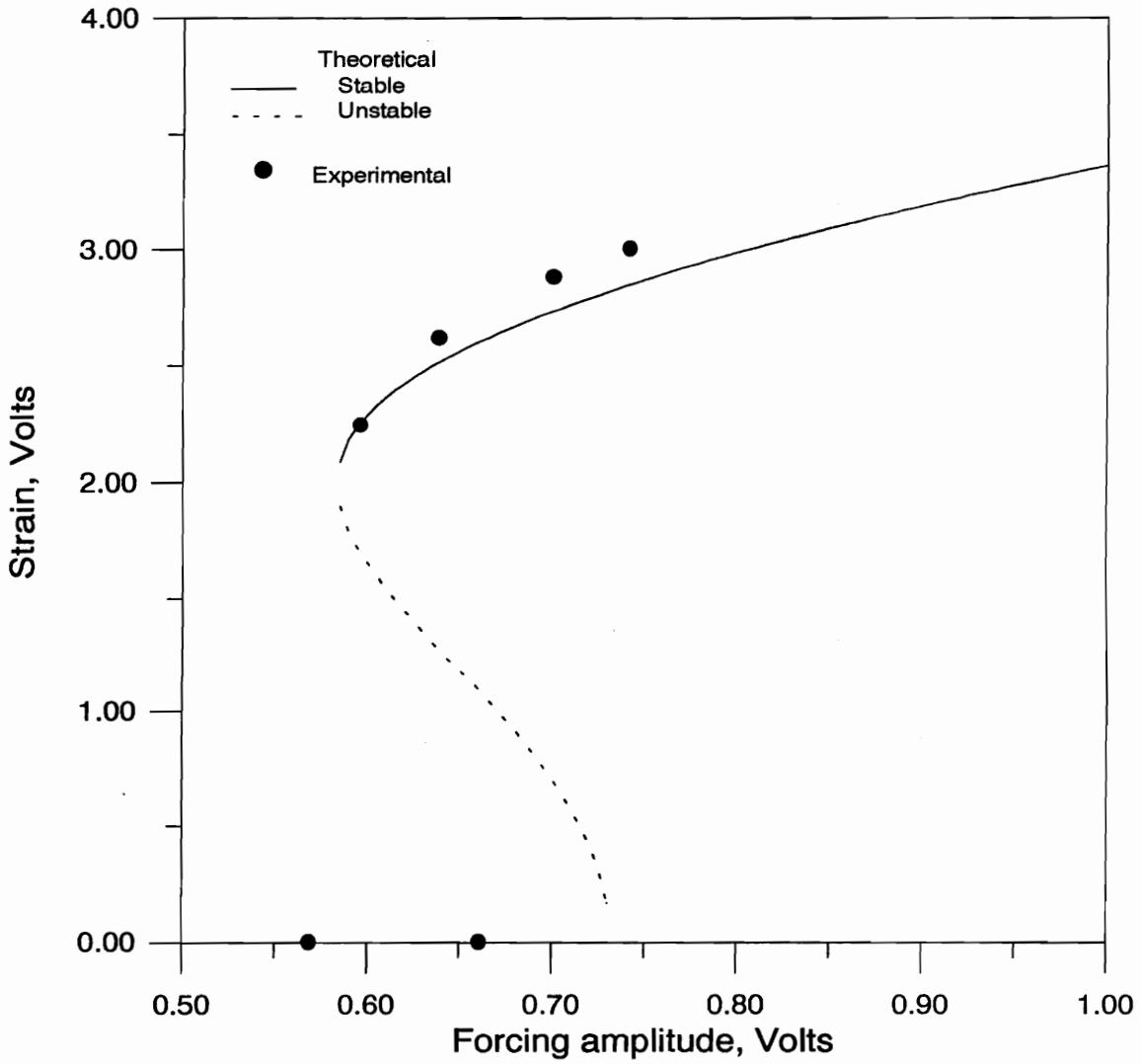

Figure 7.2 Amplitude-response curves for the second mode of the frame.

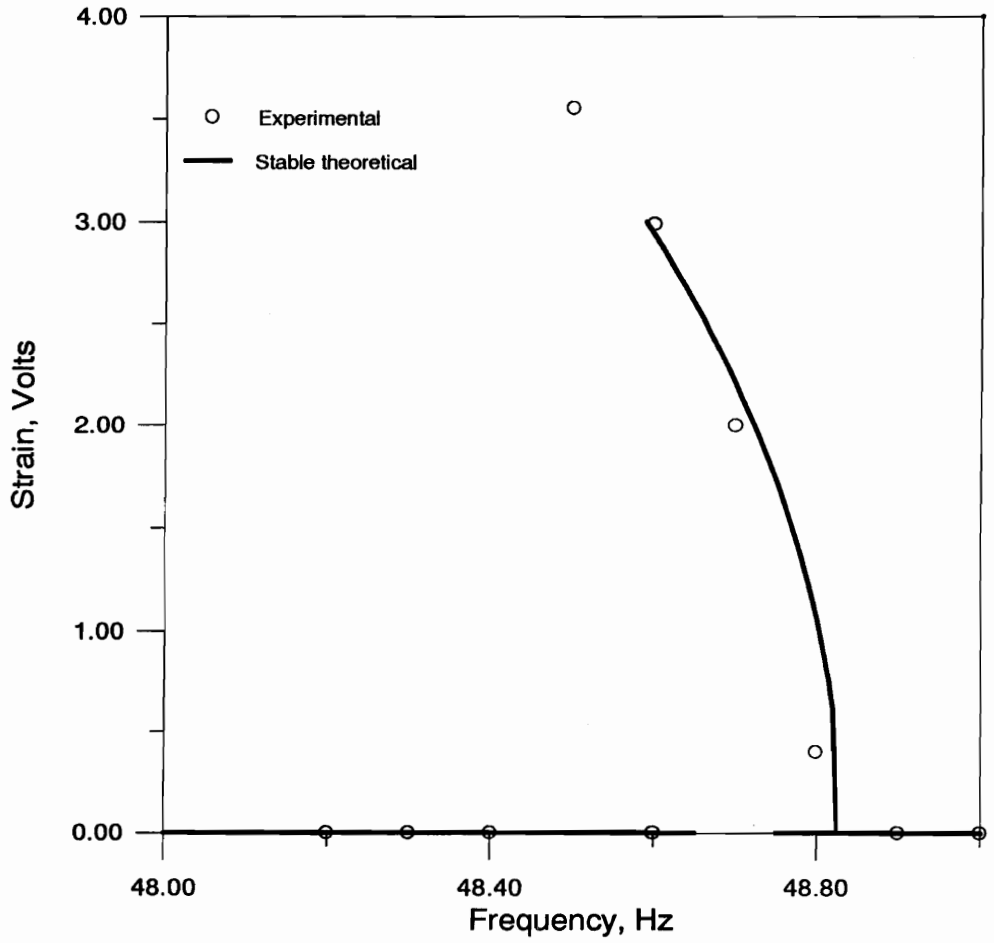

Figure 7.3 Frequency-response curves for the second mode of the frame.

CHAPTER EIGHT

Final Remarks

'To doubt everything and to believe everything are two equally convenient solutions: both dispense with the necessity of reflection' H. Poincare

In this final chapter, we summarize the results presented in the preceding chapters. We finish with a platform of suggestions for future work for those who wish to jump further into the field of nonlinear vibrations.

8.1 DISSERTATION SUMMARY

An experimental and theoretical study of the nonlinear dynamics of beam and multibeam systems has been presented. The subtopics of modal interactions, nonideal boundary conditions, and nonlinear parameter estimation were investigated.

In the study of the dynamics of structures, the presence of nonlinear mechanisms can produce very complicated motions. The ability to understand, model, and predict these phenomena is a key in the study of nonlinear systems. And since systems are by nature nonlinear, only linear under very restricted conditions, it is prudent to know more about the transfer of energy amongst modes.

We studied modal interactions of two systems: a flexible metallic cantilever beam to a transverse harmonic excitation and a flexible metallic portal frame under harmonic support motions. The reason for choosing these two apparently similar structures was that the beam possesses a dominant cubic nonlinearity and the frame possesses a dominant quadratic

nonlinearity for weakly nonlinear motions. This difference dictates the type of modal interaction phenomena that can be observed. For the cantilever beam, we observed the transfer of energy from the directly excited fourth mode to the first mode through a nonresonant modal interaction. The signature of this particular modal energy transfer mechanism is a series of unsymmetric sidebands around the peak (corresponding to the directly excited mode) in the spectrum of the response. The spacing is approximately equal to the frequency of the lower-frequency mode, in this case, the first mode. The presence of the sidebands is indicative of phase and amplitude modulations of the directly excited mode. We also observed a transfer of energy from the directly excited fourth mode to the second and fifth modes. The mechanism responsible for the modal energy transfer was a subcombination internal resonance. For both cases, the amplitudes of the lower frequency modes were the same order (or larger) than that of the directly excited mode. For a structure undergoing motions influenced by nonlinearities, the possibility of an energy transfer to a low-frequency high-amplitude mode exists.

For the frame, the rich modal density allowed for the simultaneous satisfaction of several internal resonance conditions. By exciting a single mode, we observed the activation of a multimode response consisting of contributions from seven different modes, most of which had a lower frequency than that of the directly excited mode. Once again, the contributions from the lower-frequency modes dominated the response such that any analysis that failed to account for modal interactions would severely underestimate the dynamic stresses induced in the frame. We also found that, for nonlinear motions, the type and location of the transducer may be a nontrivial factor in an accurate measurement of the relative contributions of the active modes.

The next subtopic concerned the issue of modeling boundary conditions. We found that for a beam with one end free and the other clamped (with a hardened steel fixture) and excited near the natural frequency of its fourth mode, a model with torsional clamping elasticity was required for accurate prediction of the amplitudes and jump points. The torsional stiffness consisted of

linear and nonlinear (cubic) terms.

The final subtopic, parameter estimation of nonlinear systems, completes the circle. We offered a set of experiments that can provide estimates of some of the nonlinear parameters of a system. This method is based on the subharmonic resonance. Two different approaches were presented. Though both approaches rely on the same theoretical formulation, the main difference is that one approach may be more amenable to experimental procedures. The difficulty in documenting nonlinear motions and the damage that may ensue from such motions was one motivation for this dual approach.

An important byproduct of the above parameter estimation method was the addition of a new way of measuring the linear viscous damping.

The implications for structural design is that an accurate identification of the linear natural frequencies is only the first step. Next, one must insure that the operating environment does not result in a significant shift in the natural frequencies measured in a laboratory setting (i.e., testing of space structures on earth and actual operation in a vacuum); attempt to ascertain the dominant nonlinearity of the system; identify the frequencies that satisfy the relevant resonant modal interactions for the type of nonlinearity in the model; be aware of the possibility of high-to-low energy transfer; understand that moving the forcing frequency to a higher range does not provide immunity from nonlinear motions; and, use all this information to redesign or control the structure as necessary to avoid the undesirable frequency ranges.

For an added touch of sophistication or when the dangerous frequency ranges can not be avoided, a `simple' nonlinear model that contains the dominant source of nonlinearity may be developed. Application of a perturbation method will then allow for a qualitative analysis in which the effect of various parameter changes can be investigated. This is important since the intuitive panaceas of linear systems, such as additional damping, are not always stabilizing.

In the nonlinear testing of structures, the assumptions of ideal boundary conditions may need

to be examined. For design purposes, the actual boundary conditions may well depend upon the motion of the structure. The identification of the boundary conditions is a difficult task and sometimes the effect of different sources can not be separated. Nevertheless, a model that captures the effect of nonideal boundary conditions is very useful and realistic.

8.2 FURTHER RESEARCH TOPICS

We make several suggestions for further research mainly as an extension of the work done here. Other advanced topics were briefly cited in Chapter 1.

With the study of modal interactions, the natural question that arises is how to prevent or control the energy transfer to low-frequency modes. This issue may point to the need to incorporate 'smart' materials as actuators in a control algorithm that is itself nonlinear. However, nonlinear motions may not always be a plague to be contained. Rather there may be designs that can take advantage of modal interactions where such behavior is desirable. This may help reduce the need for additional outside energy sources.

The need for more improved modeling of boundaries, joints, and connections in mechanical structures is obvious. Nonlinear modeling of boundary conditions is rare and, even then, is restricted to nonlinear stiffness terms. There is a need for more data on and improved modeling of boundary conditions. The inclusion and study of boundary damping is one major direction for such research.

More work needs to be done in comparing the accuracy of determining the linear viscous damping through a subharmonic resonance with the accuracy of the conventional linear methods of the logarithmic decrement and half-power point.

Finally, most research for parameter estimation has gone into improving linear modal analysis with some recent moves into the nonlinear arena. The key stumbling block may be an adequate experimental procedure that can have general application. It is believed that no one approach

can gain universality and so efforts must be made in many disciplines. The major thrust of improvement in this area may more likely come from technological advances in instrumentation and signal processing. Aside from the parameters, the estimation methods need to be able to measure nonlinear normal modes.

to be examined. For design purposes, the actual boundary conditions may well depend upon the motion of the structure. The identification of the boundary conditions is a difficult task and sometimes the effect of different sources can not be separated. Nevertheless, a model that captures the effect of nonideal boundary conditions is very useful and realistic.

8.2 FURTHER RESEARCH TOPICS

We make several suggestions for further research mainly as an extension of the work done here. Other advanced topics were briefly cited in Chapter 1.

With the study of modal interactions, the natural question that arises is how to prevent or control the energy transfer to low-frequency modes. This issue may point to the need to incorporate 'smart' materials as actuators in a control algorithm that is itself nonlinear. However, nonlinear motions may not always be a plague to be contained. Rather there may be designs that can take advantage of modal interactions where such behavior is desirable. This may help reduce the need for additional outside energy sources.

The need for more improved modeling of boundaries, joints, and connections in mechanical structures is obvious. Nonlinear modeling of boundary conditions is rare and, even then, is restricted to nonlinear stiffness terms. There is a need for more data on and improved modeling of boundary conditions. The inclusion and study of boundary damping is one major direction for such research.

More work needs to be done in comparing the accuracy of determining the linear viscous damping through a subharmonic resonance with the accuracy of the conventional linear methods of the logarithmic decrement and half-power point.

Finally, most research for parameter estimation has gone into improving linear modal analysis with some recent moves into the nonlinear arena. The key stumbling block may be an adequate experimental procedure that can have general application. It is believed that no one approach

BIBLIOGRAPHY

ABAQUS, 1989, User's Manual, Version 4.8, Hibbit, Karlsson & Sorensen.

Abramovich, H., and Hamburger, O., 1991, 'Vibration of a Cantilever Timoshenko Beam with Tip Mass', *Journal of Sound and Vibration*, Vol. 148, pp. 162-170.

Anderson, T.J., Balachandran, B., and Nayfeh, A.H., 1992, 'Observations of Nonlinear Interactions in a Flexible Cantilever Beam', In *Proceedings of the 33rd AIAA Structures, Structural Dynamics, and Materials Conference*, Dallas, TX.

Anderson, T.J., Balachandran, B., and Nayfeh, A.H., 1994, 'Nonlinear Resonances in a Flexible Cantilever Beam', *Journal of Vibration and Acoustics*, Vol. 116, pp. 480-484.

Anderson, T.J., Nayfeh, A.H., and Balachandran, B., 1996a, 'Coupling Between High-Frequency Modes and a Low-Frequency Mode: Theory and Experiment', *Nonlinear Dynamics*, in press.

Anderson, T.J., Nayfeh, A.H., and Balachandran, B., 1996b, 'Experimental Verification of the Importance of the Nonlinear Curvature in the Response of a Cantilever Beam', *Journal of Vibration and Acoustics*, Vol. 118, pp. 21-27.

Andre, J.C., 1996, 'Nonlinear Vibrations in Beams and Frames: The Effect of the Deformed Equilibrium State', *Nonlinear Dynamics*, submitted.

Ashworth, R.P., and Barr, A.D.S., 1987, 'The Resonances of Structures with Quadratic Inertial Non-Linearity under Direct and Parametric Harmonic Excitation', *Journal of Sound and Vibration*, Vol. 118, pp. 47-68.

Baker, W.E., Woolam, W.E., and Young, D., 1967, 'Air and Internal Damping of Thin Cantilever Beams', *International Journal of Mechanical Sciences*, Vol. 9, pp. 743-766.

Balachandran, B., 1990, *A Theoretical and Experimental Study of Modal Interactions in Resonantly Forced Structures*, Ph.D. Dissertation, Virginia Polytechnic Institute and State University, Blacksburg, VA.

Balachandran, B., and Khan, K.A., 1995, 'Spectral Analyses of Nonlinear Interactions', In *ASME 15th Biennial Mechanical Vibration and Noise Conference*, Boston, MA, DE-Vol. 84-1, pp. 633-640.

Balachandran, B., and Nayfeh, A.H., 1990a, 'Nonlinear Motions of Beam-Mass Structure', *Nonlinear Dynamics*, Vol. 1, pp. 39-61.

Balachandran, B. and Nayfeh, A.H., 1990b, 'Nonlinear Oscillations of a Harmonically Excited Composite Structure', *Composite Structures*, Vol. 16, pp. 323-339.

Balthazar, J.M., and Brasil, R.M.L.R.F., 1995, 'On Non-Linear Normal Modes of a 2-DOF Model of a Structure with Quadratic Non-Linearities', *Journal of Sound and Vibration*, Vol. 182, pp. 659-664.

Barr, A.D.S., and McWhannell, D.C., 1971, 'Parametric Instability in Structure under Support Motion', *Journal of Sound and Vibration*, Vol. 14, pp. 491-509.

Benharsi, Y., Penny, J.E.T., and Friswell, M.I., 1995, 'Identification of Damping Parameters of Vibrating Systems with Cubic Stiffness Nonlinearity', In *Proceedings of the 13th International Modal Analysis Conference*, Nashville, TN, pp. 623-629.

Bert, C.W., 1973, 'Material Damping: An Introductory Review of Mathematical Models, Measures and Experimental Techniques', *Journal of Sound and Vibration*, Vol. 29, pp. 129-153.

Bhat, B.R., and Wagner, H., 1976, 'Natural Frequencies of a Uniform Cantilever with a Tip Mass Slender in the Axial Direction', *Journal of Sound and Vibration*, Vol. 45, pp. 304-307.

Blevins, R.D., 1979, *Formulas for Natural Frequency and Mode Shape*, Van Nostrand, New York.

Bolotin, V.V., 1964, *The Dynamic Stability of Elastic Systems*, Holden-Day, San Francisco.

Boutaghou, Z.E., and Erdman, A.G., 'On the Dynamics of Timoshenko/Euler-Bernoulli Beams: A Unified Approach', *ASME Design Engineering*, Vol. 18-3, pp. 69-76.

Burton, T.D., and Kolowith, M.. 1988, 'Nonlinear Resonances and Chaotic Motion in a Flexible Parametically Excited Beam', In *Proceedings of the Second Conference on Non-Linear Vibrations, Stability, and Dynamics of Structures and Mechanisms*, Blacksburg, VA.

Busby, H.R., Nopporn, C., and Singh, R, 1986, 'Experimental Modal Analysis of Non-Linear Systems: A Feasibility Study', *Journal of Sound and Vibration*, Vol. 180, pp. 415-427.

Bux, S.L., and Roberts, J.W., 1986, 'Non-Linear Vibratory Interactions in Systems of Coupled Beams', *Journal of Sound and Vibration*, Vol. 104, pp. 497-520.

Cartmell, M.P., 1990, *Introduction to Linear, Parametric and Nonlinear Vibrations*, Chapman and Hall, New York.

Cartmell, M.P., and Roberts, J.W., 1988, 'Simultaneous Combination Resonances in an Autoparametrically Resonant System', *Journal of Sound and Vibration*, Vol. 123, pp. 81-101.

Chun, K.R., 1972, 'Free Vibration of a Beam with One End Spring-Hinged and the Other Free', *Journal of Applied Mechanics*, Vol. 39, pp. 1154-1155.

Crandall, S.H., 1970, 'The Role of Damping in Vibration Theory', *Journal of Sound and Vibration*, Vol. 11, pp. 3-18.

Crespo da Silva, M.R.M., 1991, 'Equations for Nonlinear Analysis of 3D Motions of Beams', *Applied Mechanics Review*, Vol. 44, pp. S51-S59.

Crespo da Silva, M.R.M., and Glynn, C.C., 1978a, 'Nonlinear Flexural-Flexural-Torsional Dynamics of Inextensional Beams. I. Equations of Motion', *Journal of Structural Mechanics*, Vol. 6, pp. 437-448.

Crespo da Silva, M.R.M., and Glynn, C.C., 1978b, 'Nonlinear Flexural-Flexural-Torsional Dynamics of Inextensional Beams. II Forced Motions', *Journal of Structural Mechanics*, Vol. 6, pp. 449-461.

Crespo da Silva, M.R.M., and Zaretzky, C.L., 1990, 'Non-Linear Modal Coupling in Planar and Non-Planar Responses of Inextensional Beams', *International Journal of Non-Linear Mechanics*, Vol. 25, pp. 227-239.

Cusumano, J.P., and Moon, F.C., 1989, 'Low Dimensional Behavior in Chaotic Nonplanar Motions of a Forced Elastic Rod: Experiment and Theory', In *Nonlinear Dynamics in Engineering Systems*, IUTAM Symposium, Germany, pp. 59-66.

Cusumano, J.P., and Moon, F.C., 1995a, 'Chaotic Non-Planar Vibrations of the Thin Elastica, Part I: Experimental Observation of Planar Instability', *Journal of Sound and Vibration*, Vol. 179, pp. 185-208.

Cusumano, J.P., and Moon, F.C., 1995b, 'Chaotic Non-Planar Vibrations of the Thin Elastica, Part I: Experimental Observation of Planar Instability', *Journal of Sound and Vibration*, Vol. 179, pp. 209-226.

Dally, J.W., Riley, W.F., and McConnell, K.G., 1993, *Instrumentation for Engineering Measurements*, Wiley, New York.

Dippery, K.D. and Smith, S.W., 1995, 'Applications of Time-Frequency Analysis to Structures with Internal Resonance', In *Proceedings of the 15th Biennial Mechanical Vibration and Noise Conference*, Boston, MA, DE-Vol. 84-1, pp. 663-670.

Ditto, W.L., and Pecora, L.M., 1993, 'Mastering Chaos', *Scientific American*, Vol. 269, pp. 78-84.

Donnell, L.H., 1976, *Beams, Plates and Shells*, McGraw-Hill, New York.

Dowell, E.H., and Traybar, J., and Hodges, D.H., 1977, 'An Experimental-Theoretical Correlation Study of Nonlinear Bending and Torsion Deformations of a Cantilever Beam', *Journal of Sound and Vibration*, Vol. 50, pp. 533-544.

Dugundji, J. and Mukhopadhyay, V., 1973, 'Lateral Bending-Torsion Vibrations of a Thin Beam under Parametic Excitation', *Journal of Applied Mechanics*, Vol. 44, pp. 693-698.

Dym, C.L., and Shames, I.H., 1973, *Solid Mechanics: A Variational Approach*, McGraw-Hill, New York.

Evan-Iwanowski, R.M., 1976, *Resonance Oscillations in Mechanical Systems*, Elsevier, New York.

Ewins, D.J., 1991, *Modal Testing: Theory and Practice*, Wiley, New York.

Fackerell, J.W.A., White, P.R., and Pinnington, R.J., 1993. 'Higher Order Spectra to Characterize Acoustic and Vibrational Signals', In *Proceedings of the Institute of Acoustics*. Vol. 15, Part 3, pp. 799-802.

Farghaly, S.H., and Shebl, M.G., 1995, 'Exact Frequency and Mode Shape Formulae for Studying Vibration and Stability of Timoshenko Beam System', *Journal of Sound and Vibration*. Vol. 180, pp. 205-227.

Feldman, M. and Braun, S., 1995, 'Identification of Nonlinear System Parameters Via the Instantaneous Frequency: Application of the Hilbert Transform and Wigner-Ville Techniques', In *Proceedings of the 13th International Modal Analysis Conference*, Nashville, TN, Vol. I, pp. 637-642.

Forys, A., and Niziol, J., 1984, 'Internal Resonance in a Plane System of Rods', *Journal of Sound and Vibration*, Vol. 95, pp. 361-374.

Genta, G., 1993, *Vibration of Structure and Machines*, Springer-Verlag, New York.

Goldstein, H., 1981, *Classical Mechanics*, Addison-Welsey, Massachusetts.

Gorman, D.J., 1975, *Free Vibration Analysis of Beams and Shafts*, Wiley, New York.

Guckenheimer, J., and Holmes, P. J., 1983, *Nonlinear Oscillations, Dynamical Systems, and Bifurcations of Vector Fields*, Springer-Verlag, New York.

Haddow, A.G., Barr, A.D.S., and Mook, D.T., 1984, 'Theoretical and Experimental Study of Modal Interaction in a Two-Degree-of-Freedom Structure', *Journal of Sound and Vibration*, Vol. 97, pp. 451-473.

Haddow, A.G., and Hasan, S.M., 1988, 'Nonlinear Oscillations of a Flexible Cantilever: Experimental Results', In *Proceedings of the Second Conference on Nonlinear Vibrations, Stability, and Dynamics of Structures and Mechanisms*, Blacksburg, VA.

Haering, W.J., Ryan, R.R., and Scott, R.A., 1992, 'A New Flexible Body Dynamic Formulation for Beam Structures Undergoing Large Overall Motions', In *Proceedings of the 33rd Structures, Structural Dynamics, and Materials Conference*, Dallas, TX.

Haight, E.C., and King, W.W., 1971, 'Stability of Nonlinear Oscillations of an Elastic Rod', *The Journal of the Acoustical Society of America*, Vol. 52, pp. 899-911.

Hajj, M.R., Miksad, R.W., and Powers, E.J., 1993, 'Fundamental-Subharmonic Interaction: Effect of Phase Relation', *Journal of Fluid Mechanics*, Vol. 256, pp. 403-426.

Hajj, M.R., Nayfeh, A.H., and Popovic, P., 1995, 'Identification of Nonlinear Systems Parameters Using Polyspectral Measurements and Analysis', In *ASME 15th Biennial Mechanical Vibration and Noise Conference*, Boston, MA, DE-Vol. 84-1, pp. 651-661.

Harris, C.M., 1998, *Shock and Vibration Handbook*, McGraw-Hill, New York.

He, J. and Ewins, D.J., 1987, 'A Simple Method of Interpretation for the Modal Analysis of Nonlinear Systems', In *Proceedings of the 5th International Modal Analysis Conference*, Vol. I, pp. 626-634.

Hodges, D.H., 1984, 'Proper Definition of Curvature in Nonlinear Beam Kinematics', *AIAA Journal*, Vol. 22, pp.1825-1827.

Hodges, D.H., 1987a, 'Finite Rotation and Nonlinear Beam Kinematics', *Vertica*, Vol. 11, pp. 297-307.

Hodges, D.H., 1987b, 'Nonlinear Beam Kinematics for Small Strains and Finite Rotations', *Vertica*, Vol. 11, pp. 573-589.

Hodges, D.W., Crespo da Silva, M.R.M., and Peters, D.A., 1988, 'Nonlinear Effects in the Static and Dynamic Behavior of Beams and Rotor Blades', *Vertica*, Vol. 12, pp. 243-256.

Hsieh, S.-R., Shaw, S.W., and Pierre, C., 1994, 'Normal Modes for Large Amplitude Vibration of a Cantilever Beam', *International Journal of Solids and Structures*, Vol. 31, pp. 1981- 2014.

Hyer, M.W., 1979, 'Whirling of a Base-Excited Cantilever Beam', *Journal of Acoustical Society of America*, Vol. 65, pp. 931-939.

Ibrahim, R.A., 1991, 'Nonlinear Random Vibrations: Experimental Results', *Applied Mechanics Review*, Vol. 44, pp. 423-446.

Jeronimidis, G., and Atkins, A.G., 1995, 'Mechanics of Biological Materials and Structures: Nature's Lesson for the Engineer', *Part C: Journal of Mechanical Engineering Science*, Vol. 209, pp. 221-235.

Kapania, R.K., and Raciti, S., 1989, 'Recent Advances in Analysis of Laminated Beams and Plates, Part II: Vibrations and Wave Propagation', *AIAA Journal*, Vol. 27, pp. 935-946.

Kapania, R.K., and Raciti, S., 1989a, 'Nonlinear Vibrations of Unsymmetically Laminated Beams', *AIAA Journal*, Vol. 27, pp. 201-201.

Kim, T., and Dugundji, J., 1993, ' Nonlinear Large Amplitude Vibration of Composite Helicopter Blade at Large Static Deflection', *AIAA Journal*, Vol. 31, pp. 938-946.

Kobayashi, A.S. (Ed.), 1993, *Handbook on Experimental Mechanics*, VCH Publishers, New York.

Komerath, N.M., Liou, S.G., Schwartz, R.J., and Kim, J.M., 1992b, 'Flow over a Twin-Tailed Aircraft at Angle of Attack Part II: Temporal Characteristics', *Journal of Aircraft*, Vol. 29, pp. 553-558.

Laura, P.A.A, Maurizi, M.J., and Rossi, R.E., 1989, 'A Survey of Studies Dealing with Timoshenko Beams', *The Shock and Vibration Digest*, Vol. 22, pp. 3-10.

Laura, P.A.A., Pombo, J.L., and Susemihl, E.A., 1974, 'A Note on the Vibrations of a Clamped-Free Beam with a Mass at the Free End', *Journal of Sound and Vibration*, Vol. 37, pp. 161-168.

Leissa, A.W., and Sonalla, M.I., 1991, 'Vibrations of Cantilever Beams with Various Initial Conditions', *Journal of Sound and Vibration*, Vol. 150, pp. 83-99.

Lin, R.M. and Ewins, D.J., 1990, 'On the Location of Structural Nonlinearity from Modal Testing-A Feasibility Study', In *Proceedings of the 8th International Modal Analysis Conference*, Kissimmee, FL, pp. 358-364.

Lin, R.M. and Lim, M.K., 1993, 'Identification of Nonlinearity from Analysis of Complex Modes', *Modal Analysis*, Vol. 8, pp. 285-299.

Liu, W.H., and Huang, C.-C., 1988, 'Free Vibration of Restrained Beam Carrying Concentrated Masses', *Journal of Sound and Vibration*, Vol. 123, pp. 31-42.

Love, A.E.H., 1944, *A Treatise on the Mathematical Theory of Elasticity*, Dover, New York.

Low, K.H., and Ng, C.K., 1992, 'An Analysis Program for Vibration Modes of a Link Carrying Solid Mass', *Computers & Structures*, Vol. 43, pp. 775-785.

Marlowe, J.M., and Buehrle, R.D., 1993, 'SEDS EMP Modal Survey: Test Results and Model Correlations of a Non-Linear Space Structure', In *Proceedings of the 11th International Modal Analysis Conference*, Kissimmee, FL, Vol. 1, pp. 51-61.

Mazzilli, C.E.N., and Brasil, R.M.L.R.F., 1995, 'Effect of Static Loading on the Nonlinear Vibrations of a Three-Time Redundant Portal Frame: Analytical and Numerical Studies', Nonlinear Dynamics, Vol. 8, pp. 347-366.

Meirovitch, L., 1967, *Analytical Methods in Vibrations*, Macmillan, New York.

Meirovitch, L., 1975, *Elements of Vibration Analysis*, McGraw-Hill, New York.

Mitchell, L.D., and Neumann, M.L., 1995, 'The Investigation of the Structural Response Stability of Lightly Damped Structures over Long Testing Periods', In *Proceedings of the 13th Modal Analysis Conference*, Nashville, TN, pp. 749-755.

Moon, F.C., 1987, *Chaotic Vibrations*, Wiley, New York.

Moon, F.C., and Holmes, P.J., 1985, 'Double-Poincare Sections of a Quasi-Periodically Forced Chaotic Attractor', *Physical Letters A*, Vol. 111, pp. 157-160.

Narita, Y. and Leissa, A.W., 1992, 'Frequencies and Mode Shapes of Cantilevered Laminated Composite Plates', *Journal of Sound and Vibration*, Vol. 154, pp. 161-172.

Nashif, A.D., Jones, D.I.G., and Henderson, J.P., 1985, *Vibration Damping*, Wiley, New York.

Nayfeh, A.H., 1973, *Perturbation Methods*, Wiley, New York.

Nayfeh, A.H., 1981, *Introduction to Perturbation Techniques*, Wiley, New York.

Nayfeh, A.H., 1985, 'Parametric Identification of Nonlinear Dynamic Systems', *Computers & Structures*, Vol. 20, pp. 487-493.

Nayfeh, A.H., and Balachandran, B., 1989, 'Modal Interactions in Dynamical and Structural Systems', *Applied Mechanics Review*, Vol. 42, pp. S175-S201.

Nayfeh, A.H., and Balachandran, B., 1995, *Applied Nonlinear Dynamics*, Wiley, New York.

Nayfeh, A.H., Balachandran, B., Colbert, M.A., and Nayfeh, M.A., 1989, 'An Experimental Investigation of Complicated Responses of a Two-Degree-of-Freedom Structure', *Journal of Applied Mechanics*, Vol. 55, pp. 960-967.

Nayfeh, A.H., Chin, C., and Nayfeh, S.A., 1994, 'Nonlinear Normal Modes of a Cantilever Beam', In *Proceedings of the Fifth Conference on Nonlinear Vibrations, Stability, and Dynamics of Structures and Mechanisms*, Blacksburg, VA.

Nayfeh, A.H., and Mook, D.T., 1979, *Nonlinear Oscillations*, Wiley, New York.

Nayfeh, A.H., and Mook, D.T., 1995, 'Energy Transfer from High-Frequency to Low-Frequency Modes in Structures', *Special 50th Anniversary Design Issue* (ASME), Vol. 117, pp. 186-195.

Nayfeh, A.H., Mook, D.T., and Lobitz, D.W., 1974, 'Numerical-Perturbation method for the Nonlinear Analysis of Structural Vibrations', *AIAA Journal*, Vol. 12, pp. 1222-1228.

Nayfeh, A.H., and Pai, P.F., 1989, 'Non-Linear Non-Planar Parametric Responses of an Inextensional Beam', *International Journal of Non-Linear Mechanics*, Vol. 24, pp. 139-158.

Nayfeh, A.H., and Pai, P.F., 1996, *Linear and Nonlinear Structural Mechanics*, Wiley, New York, in press.

Nayfeh, S.A., and Nayfeh, A.H., 1993, 'Nonlinear Interactions Between Two Widely Space Modes-External Excitation', *International Journal of Bifurcation and Chaos*, Vol. 3, pp. 417-427.

Nayfeh, S.A., and Nayfeh, A.H., 1994, 'Energy Transfer from High- to Low-Frequency Modes in a Flexible Structure via Modulation', *Journal of Vibration and Acoustics*, Vol. 116, pp. 203-207.

Nayfeh, T.A., Nayfeh, A.H., and Mook, D.T., 1994, `A Theoretical and Experimental Investigation of a Three-Degree-of-Freedom Structure', *Nonlinear Dynamics*, Vol. 3. pp. 353-374.

Noltingk, B.E. (Ed.), 1995, *Instrumentaion Reference Book*. Butterworth-Heinemann. Boston.

Oden, J.T., and Bathe, K.J., 1978. `A Commentary on Computational Mechanics'. *Applied Mechanics Review*. Vol. 31, pp. 1053-1058.

Ostachowicz, W.M., and Krawczuk, M., 1991, `Analysis of the Effect of Cracks on the Natural Frequencies of a Cantilever Beam", *Journal of Sound and Vibration*, Vol. 150. pp. 191-201.

Ozguven, H.N. and Imregun, M., 1993, `Complex Modes arising from Linear Identification of Nonlinear Systems', *Modal Analysis*, Vol. 8, pp. 151-164.

Pai, P.F., 1990, *Nonlinear Flexural-Flexural-Torsional Dynamics of Metallic and Composite Beams*, Ph.D. Dissertation, Virginia Polytechnic Institute and State University, Blacksburg, VA.

Pai, P.F., and Nayfeh, A.H., 1990, `Three-Dimensional Nonlinear Vibrations of Composite Beams-I. Equations of Motion', *Nonlinear Dynamics*, Vol.1, pp. 477-502.

Pai, P.F., and Nayfeh, A.H., 1990a, `Non-Linear Non-Planar Oscillations of a Cantilever Beam Under Lateral Base Excitations', *International Journal of Non-Linear Mechanics*. Vol. 25. pp. 455-474.

Pai, P.F., and Nayfeh, A.H., 1992, `A Nonlinear Composite Beam Theory', *Nonlinear Dynamics*, Vol. 3, pp. 273-303.

Popovic, P., Nayfeh, A.H., Oh, K., and Nayfeh, S.A., 1995, `An Experimental Investigation of Energy Transfer from a High-Frequency Mode to a Low-Frequency Mode in a Flexible Structure', *Journal of Vibration and Control*, Vol. 1, pp. 115-128.

Pezeshki, C., Elgar, S., Krishna, R., and Burton, T.D., 1992, `Auto and Cross-Bispectral Analysis of a System of Two Coupled Oscillators with Quadratic Nonlinearities possessing Chaotic Motion', *Journal of Applied Mechanics*, Vol. 59, pp. 657-663.

Randall, R.B., 1987, *Frequency Analysis*, Bruel & Kjaer, Denmark.

Rayleigh (Lord), 1877, *Theory of Sound*, Macmillan, New York.

Roberts, J.W., 1980, 'Random Excitation of a Vibratory System with Autoparametric Interaction', *Journal of Sound and Vibration*, Vol. 69, pp. 101-116.

Sathyamoorthy, M., 1982, 'Nonlinear Analysis of Beams, Part I: A Survey of Recent Advances', *Shock and Vibration Digest*, Vol. 14, pp. 19-35.

Sathyamoorthy, M., 1985, 'Recent Research in Nonlinear Analysis of Beams', *Shock and Vibration Digest*, Vol. 17, pp. 27.

Schmidt, G., and Tondl, A., 1986, *Nonlinear Vibration*, Cambridge University Press. Cambridge. England.

Seydel, R., 1994, *Practical Bifurcation and Stability Analysis*, Springer-Verlag, New York.

Shames, I.H., and Dym, C.L., 1985, *Energy and Finite Element Methods in Structural Mechanics*. McGraw-Hill, New York.

Shyu, I.M.K.,1991, *Forced, NonLinear, Planar, and Nonplanar Oscillations of a Cantilevered Beam Including Static Deflection*, Ph.D Dissertation, Virginia Polytechnic Institute and State University, Blacksburg, VA.

Shyu, R.J., 1994, 'A Spectral Method for Identifying Nonlinear Structures', *Modal Analysis*, Vol. 9, pp. 255-268.

Simon, M. and Tomlinson. G.R., 1984, 'Use of Hilbert Tranform in Modal Analysis of Linear and Non-Linear Structures', *Journal of Sound and Vibration*, Vol. 96, pp. 421-436.

Skowronski, J.M, 1991, *Control of Nonlinear Mechanical Systems*, Plenum Press. New York.

Slater, J.C., and Inman, D.J., 1994, 'Extension of Modal Analysis to Nonlinear Systems', In *Proceedings of 12th International Modal Analysis Conference*, Honolulu. HI. Vol. II, pp. 1684-1691.

Stanbridge, A.B., and Ewins, D.J., 1996, 'Using a Continuously-Scanning Laser Doppler Vibrometer for Modal Testing', In *Proceedings of the 14th International Modal Analysis Conference*, Dearborn, MI, pp. 816-822.

Suleman, A., Modi, V.J., and Venkayya, V.B., 1995, 'Structural Modeling Issues in Flexible Systems', *AIAA Journal*, Vol. 33, pp. 919-923.

Szemplinska-Stupnicka, W., 1990, *The Behavior of Nonlinear Vibrating Systems*, Kluwer, Dordrecht, the Netherlands.

Tabaddor, M., and Nayfeh, A.H., 1995, 'Nonlinear Dynamics of a Transversely Excited Cantilever Beam", In *ASME 15th Biennial Mechanical Vibration and Noise Conference*, Boston, MA, DE-Vol. 84-1, pp. 21-29.

Tailor, D., Kirkman, C., Hershfeld, D., and Wojnar, S., 1994, 'An Approach to Real World Nonlinear Behavior of Space Structures', In *Proceedings of the 12th International Modal Analysis Conference*, Honolulu, Hawaii, Vol. II, pp. 1705-1712,

Thompson, J.M.T., and Bishop, S.R. (Ed.), 1994, *Nonlinearity and Chaos in Engineering Dynamics*, Wiley, New York.

Thomson, W.T., 1981, *Theory of Vibrations with Applications*, Prentice-Hall, New Jersey.

Timoshenko, S., 1921, 'On the Correction for Shear of the Differential Equation for Transverse Vibration of Prismatic Bars', *Philosophical Magazine*, Series 6, pp. 744-746.

To, C.W.S., 1982, 'Vibration of a Cantilever Beam with a Base Excitation and Tip Mass', *Journal of Sound and Vibration*, Vol. 83, pp. 445-460.

Tomlinson, G.R., 1985, 'Using the Hilbert Transform with Linear and Non-Linear Mulit-Mode Systems', In *Proceedings of the 3rd International Modal Analysis Conference*, Vol. I, pp. 255-263.

Washizu, K., 1982, *Variational Methods in Elasticity and Plasticity*, Pergamon Press, Oxford, England.

Wagner, H., and Ramamurti, V., 1977, 'Beam Vibrations -- A Review', *Shock and Vibration Digest*, Vol. 9, pp. 17-24.

Wilson, J., 1996, 'A Bit More (or Less) Accuracy?', *Test Engineering & Management*, April\May, pp. 12-13.

Wilson, H.B., and Gupta, S., 1992, 'Math Software Package Simplifies Structural Analysis', *Sound and Vibration*, August.

Worden, K. and Wright, J.R., 1994, 'Experimental Identification of Multi Degree-of-Freedom Nonlinear Systems using Restoring Force Methods', *Modal Analysis*, Vol. 9, pp. 35-55.

Yang, Y. and Ibrahim, S.R., 1985, 'A Nonparametric Identification Technique for a Variety of Discrete Nonlinear Vibrating Systems', *Journal of Vibration, Acoustics, Stress, and Reliability in Design*, Vol. 107, pp. 60-66.

Zaretzky, C.L., and Crespo da Silva, M.R.M., 1994, 'Experimental Correlation of Non-Linear Modal Coupling in the Response of Cantilever Beams', *Journal of Sound and Vibration*, Vol. 174, pp. 145-167.

Zavodney, L.D., 1991, 'Identification of Nonlinearity in Structural Systems: Theory, Simulation and Experiment', *Applied Mechanics Review*, Vol. 44, Part 2, pp. S295-S303.

Zavodney, L.D., and Nayfeh, A.H., 1989, 'The Non-Linear Response of a Slender Beam Carrying a Lumped Mass to a Principal Parametric Excitation: Theory and Experiment', *International Journal of Non-Linear Mechanics*, Vol. 24, pp. 105-125.

VITA

Mahmood M. Tabaddor took his first gasps of air in E. Lansing, Michigan. His parents graciously accepted the difficult task of training him in the human skills. At the time of his arrival his father was studying in the Engineering Mechanics Department. This together with the position of all the stars, planets, and black holes set forth a chain of events leading from Michigan to Ohio to Iran to Ohio (University of Akron) to Michigan (University of Michigan) to Virginia (Virginia Tech) in pursuit of the same destiny. The slightest perturbation could have set him in an entirely different course. During his years in the academic arena, he has learned that the university is not the noble abode he thought but more like a business. This was very disappointing to him. He developed several personalities to deal with the difficulties of life and for now seems to have settled for one of them. Having enough of the world kicking his butt around, he briefly trained in the martial arts only to really have his butt kicked. On a happier note, he met his soulmate from an ancient world (India) and together they vowed to live and love. But now he must chart new territory in Georgia (Bell Labs) and make his contribution to the march of evolution and the expansion of the universe.